

N73 18528

IFSM -72-32



LEHIGH UNIVERSITY

HYDROGEN ADSORPTION AND DIFFUSION, AND
SUBCRITICAL-CRACK GROWTH IN HIGH-STRENGTH
STEELS AND NICKEL BASE ALLOYS

First Annual Report

November 1, 1971 to October 31, 1972

by

**CASE FILE
COPY**

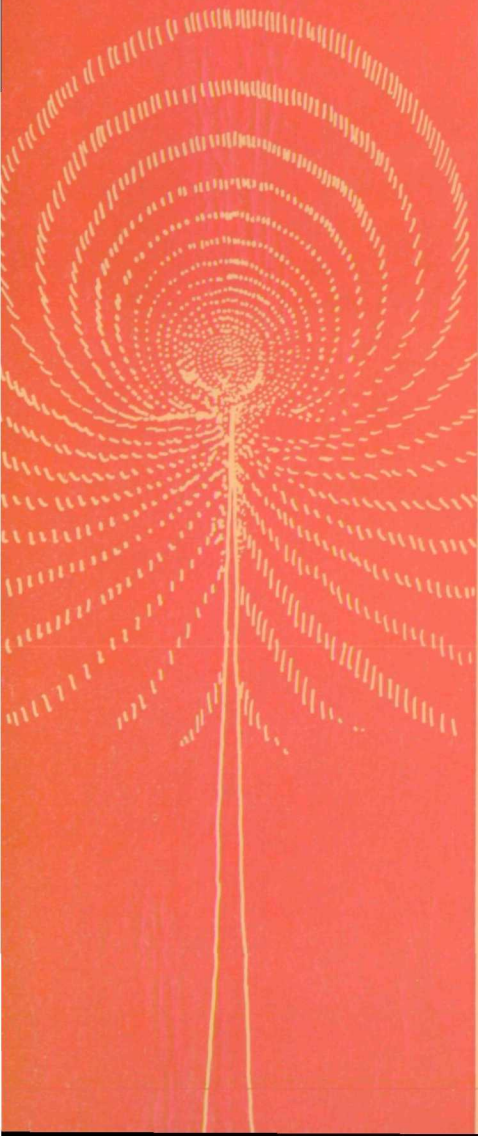
R. P. Wei
K. Klier
G. W. Simmons
E. Chornet

January 1973

National Aeronautics and Space Administration

Grant NGR 39-007-067

TO EFFECTIVE
FRACATURE AND SOLID
MECHANICS



FIRST ANNUAL REPORT

SUBJECT: NASA Grant NGR 39-007-067
"Hydrogen Adsorption and Diffusion, and Subcritical-
Crack Growth in High-Strength Steels and Nickel
Base Alloys"
First Annual Report - November 1, 1971 to
October 31, 1972

ATTENTION: Mr. John Misencik

NASA Lewis Research Center
21000 Brookpark Road
Cleveland, Ohio 44135

PREPARED BY: Drs. R. P. Wei, K. Klier,
G. W. Simmons, and E. Chornet
LEHIGH UNIVERSITY
Bethlehem, Pennsylvania 18015

FIRST ANNUAL REPORT
NASA GRANT NGR 39-007-067

HYDROGEN ADSORPTION AND DIFFUSION, AND SUBCRITICAL-CRACK
GROWTH IN HIGH-STRENGTH STEELS AND NICKEL BASE ALLOYS

by

R. P. Wei, K. Klier, G. W. Simmons and E. Chornet
LEHIGH UNIVERSITY
Bethlehem, Pennsylvania

ABSTRACT

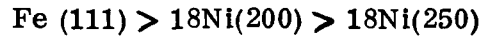
Embrittlement, or the enhancement of crack growth by gaseous hydrogen in high-strength alloys, is of primary interest in selecting alloys for various components in the Space Shuttle. Embrittlement is known to occur at hydrogen gas pressures ranging from fractions to several hundred atmospheres, and is most severe in the case of martensitic high-strength steels. Kinetic information on subcritical-crack growth in gaseous hydrogen is sparse at this time. Corroborative information on hydrogen adsorption and diffusion is inadequate to permit a clear determination of the rate controlling process and possible mechanism in hydrogen enhanced crack growth, and for estimating behavior over a range of temperatures and pressures. Therefore, coordinated studies of the kinetics of crack growth, and adsorption and diffusion of hydrogen, using identical materials, have been initiated. Comparable conditions of temperature and pressure will be used in the chemical and mechanical experiments. Inconel 718 alloy and 18Ni(200) maraging steel have been selected for these studies. Results from these studies are expected to provide not only a better understanding of the gaseous hydrogen embrittlement phenomenon itself, but also fundamental information on hydrogen adsorption and diffusion, and crack growth information that can be used directly for design.

No sustained-load crack growth was observed for the Inconel 718 alloy in gaseous hydrogen (~ 1000 torr) at about -50°C , 25°C and $+300^{\circ}\text{C}$ for stress intensities up to $90 \text{ ksi } \sqrt{\text{in}}$. The rate of fatigue crack growth at room temperature, with $R = K_{\text{min}}/K_{\text{max}} = 0.5$ and $f = 5.0 \text{ Hz}$, was also unaffected by gaseous hydrogen (at ~ 1000 torr).

Preliminary results on the 18Ni(200) maraging steel indicate that sustained-load crack growth was unaffected by hydrogen (~ 1000 torr) at room temperature, but was affected by hydrogen at about -30°C . The rate limiting speed was about $1.5 \times 10^{-4} \text{ in./sec}$ at -30°C , and was about $1/5$ of that for the 18Ni(250) maraging steel. These very preliminary results suggest that the rate and temperature dependence for hydrogen enhanced crack growth is a function of alloy composition and/or of strength level. Additional experiments are in progress.

The surface activity toward hydrogen exchange reactions of the 18Ni(250) maraging steel, 18Ni(200) maraging steel, and of iron single crystal of (111) orientation was investigated. The 18Ni(250) maraging steel was studied as an

additional material not included in the original proposal. The rates of hydrogen atomization by the three types of materials are high and probably sufficient to sustain the crack growth through a mechanism limited by hydrogen atom formation. The order of activities for the formation of surface hydrogen atoms from the gas molecules has been found to be:



Aged specimens were found to be more active than non-aged specimens, and highly perturbed surfaces were more active than annealed surfaces. It appears that the prevention of hydrogen embrittlement in maraging steels should be sought in adding alloying elements which would poison the catalytic activity of the surface for hydrogen atomization, or which would act as traps for hydrogen atoms preventing their surface diffusion. No significant bulk diffusion was observed in the range of temperatures between -190 and 300°C in any of the materials studied. The testing of the Inconel 718 alloy and an austenitic (316) stainless steel for surface reactivity toward hydrogen is planned for the second year of the project.

FIRST ANNUAL REPORT
NASA GRANT NGR 39-007-067

HYDROGEN ADSORPTION AND DIFFUSION, AND SUBCRITICAL-CRACK
GROWTH IN HIGH-STRENGTH STEELS AND NICKEL BASE ALLOYS

I. INTRODUCTION

The embrittling effect of hydrogen on the fracture behavior of steels and certain nickel-base alloys is well known and is of great technological importance. In general, hydrogen embrittlement problems may be broadly separated into those that are caused by dissolved hydrogen* (introduced by prior treatments or chemical reactions) and those that result from the exposure to gaseous hydrogen environment during service, at pressures ranging from tens of torrs to several hundred atmospheres. The problems of embrittlement by hydrogen in solution have been investigated extensively and several mechanisms have been proposed to explain the observed behavior. The first mechanism, the pressure mechanism, suggests that embrittlement is caused by the development of high pressures within internal voids. The pressure build-up results from the accumulation of molecular hydrogen formed from hydrogen that diffuses into these voids [1-4]. The second, the lattice-interaction mechanism, suggests that hydrogen would diffuse to regions of high hydrostatic tension within the lattice, under the influence of a strong stress gradient near the crack tip, and interact with the metal and reduce its cohesive strength [5-8]. The precise nature of the hydrogen-metal interaction is not clearly defined. The third proposed mechanism is the stress-sorption mechanism which suggests the reduction in fracture stress, vis a vis, embrittlement, arises from a reduction in surface energy caused by the adsorption of hydrogen on the surfaces of

* Dissolved hydrogen includes hydrogen dissolved in the crystal lattice, as well as, hydrogen trapped at dislocations, intergranular space and voids.

internal voids [9].

These proposed mechanisms vary widely in rigor and acceptability. The pressure mechanism has been well documented and is generally accepted for explaining phenomena such as quench cracking of steel ingots and forgings, and embrittlement under hydrogen charging conditions [2-4]. Its applicability to cracking of high-strength steels in mildly corrosive environments, such as distilled water, has been seriously questioned [4, 10] (although it appears to be the most plausible mechanism for moisture-enhanced fatigue-crack growth in aluminum and aluminum alloys [11-14].) The other two mechanisms are less established and still need to be tested critically.

Embrittlement by gaseous hydrogen has begun to receive serious attention only in the past few years [15-20]. The effect of gaseous hydrogen at 1 atmosphere on subcritical-crack growth in high-strength steels at room temperature was studied by Hancock and Johnson [15] and Wei and Landes [16] for static loading, and by Spitzig, et al. [17] and Wei and Landes [16] for fatigue. Crack growth studies at low hydrogen pressures and in partially dissociated hydrogen were carried out by Williams and Nelson [18] and Nelson, et al [19] on an AISI 4130 steel over a range of test temperatures. Hydrogen embrittlement caused by gaseous hydrogen at pressures up to 10,000 psi on smooth and notched bars for a variety of materials was investigated by Walter [20]. These investigations indicated that the high-strength martensitic steels are severely embrittled by gaseous hydrogen at pressures ranging from ~ 100 torr to several hundred atmospheres [15-20]. Nickel-base alloys such as Inconel 718 are also embrittled [20]. Austenitic steels, on the other hand, experienced little or no embrittlement [20]. On the basis of their experimental data, Williams and Nelson suggested that the rate controlling process in hydrogen enhanced crack growth is that of adsorption of hydrogen

onto the crack surface, and that hydrogen transport within the lattice cannot be involved [18,19]. Adequate adsorption and diffusion data, however, are not available to critically assess the suggested model. Since chemical composition and microstructure can affect hydrogen enhanced crack growth [20,21] and hydrogen adsorption and diffusion [22], coordinated crack growth and surface chemistry studies utilizing identical materials are needed to develop quantitative information on the mechanism for gaseous hydrogen embrittlement. Such coordinated studies of the kinetics of crack growth in gaseous hydrogen and studies of hydrogen adsorption and diffusion under conditions comparable to those used in the crack growth studies have been initiated under this grant. Inconel 718 alloy and 18Ni(200) maraging steel have been selected for these studies. Principal attention is directed to the 18Ni maraging steel in the chemical studies during the initial phase of the program. Iron and nickel single crystals of selected orientations will also be examined to provide additional information in later studies. These studies are expected to provide not only a better understanding of the gaseous hydrogen embrittlement phenomenon, but also fundamental information on adsorption and diffusion, and crack growth information directly useful for design.

Crack growth experiments are being carried out within the framework of linear elastic fracture mechanics, using the crack-tip stress intensity factor K to characterize the mechanical crack driving force. Experiments are being conducted over a range of temperatures from about -60°C to $+300^{\circ}\text{C}$, at a hydrogen gas pressure of one atmosphere. A hydrogen-deuterium exchange technique is used in the surface chemistry studies. By following the exchange kinetics between adsorbed and absorbed hydrogen and gaseous deuterium, the mechanism of adsorption and the

magnitude of the diffusion coefficients in the test material will be determined. The deuterium labelling method was selected after careful consideration of tritium labelling, X-ray absorption and electron probe methods.

Progress during the first year of this grant is summarized herein. The crack growth and the chemical experiments are discussed separately.

II. KINETICS OF SUBCRITICAL CRACK GROWTH

A. Materials

An 1/8-inch-thick Inconel 718 alloy sheet and an 1/4-inch-thick 18Ni(200) maraging steel plate are used in these studies. Both of these alloys were vacuum melted.

The Inconel 718 alloy sheet was obtained from the Huntington Alloy Products Division of INCO in the cold rolled and pickle annealed condition, and was heat treated. Chemical composition and heat treatment for this alloy are given in Table 1. Longitudinal and transverse tensile properties are given in Table 2. These results show that this material generally conforms to AMS 5596C specifications and is acceptable. Crack growth resistance curves for this alloy (for monotonically increasing loads) in the longitudinal (LT) and transverse (TL) directions were determined using 3-inch-wide SEN specimens, Figure 1. These crack growth resistance curves are shown in Figure 2.

The 18Ni(200) maraging steel was obtained as 1/2-inch-thick plate from the United States Steel Corporation. It was hot rolled straight-away into 1/4-inch-thick plate and heat treated. Chemical composition and heat treatment for this steel are given in Table 3. A 16-hour aging treatment was used in an attempt to develop

yield strength of approximately 200 ksi in this alloy. Longitudinal tensile properties of this steel are given in Table 4. Because of the considerable warpage of this steel from heat treatment, crack growth resistance curves were not determined. This steel, however, had been tested by Dabkowski et al [23] and is representative of this grade of maraging steel.

B. Procedures

The kinetics of subcritical crack growth under sustained-load in dehumidified hydrogen is being examined over a range of temperatures from -60 to +300°C. 3-inch-wide center-cracked specimens, Figure 3, oriented in the longitudinal (LT) direction are used for the Inconel 718 alloy sheet in this investigation. Because of the warpage problem, modified wedge-opening-load (WOL) specimens, Figure 4, oriented in the longitudinal (LT) direction are used for the 18Ni(200) maraging steel plate.* All specimens contain starter notches introduced by electro-discharge machining (EDM) and are precracked in fatigue in dehumidified argon before testing. The precrack is extended from the end of the starter notch by approximately 0.1 inch. Fatigue precracking and testing are carried out in an 100,000-lb. capacity MTS closed-loop electrohydraulic testing operated in load control. Load control was estimated to be better than ± 1 percent. The stress intensity factor K for the center-cracked specimens is computed from Equation 1; where P = applied load, B = specimen thickness, W = specimen width, and a = half-crack length.

$$K = \frac{P}{BW} \sqrt{\pi a \sec(\pi a/W)} \quad (1)$$

* Preliminary data were obtained on 3-inch-wide center-cracked specimens of this material.

A secant correction for finite specimen width was used [24]. This correction closely approximates the series correction given by Isida [24, 25]. The stress intensity factor K for the WOL specimens is computed from Equation 2 [26]:

$$K = \frac{P\sqrt{a}}{BW} \left[30.96 - 195.8 \left(\frac{a}{W}\right) + 730.6 \left(\frac{a}{W}\right)^2 - 1186.3 \left(\frac{a}{W}\right)^3 + 754.6 \left(\frac{a}{W}\right)^4 \right] \quad (2)$$

Equation 2 was developed for a specimen with height to width ratio (H/W), Figure 4, of 0.486, and is valid for a/W from about 0.3 to 0.7.

A continuous recording electrical potential system is used for monitoring crack growth [27]. This system monitors crack growth by measuring changes in electrical potential (vis-a-vis, resistance) across the crack and gives a measure of the change in average (through-thickness average) crack length. The detailed experimental procedure for this method has been described elsewhere [27]. For the center-cracked specimens, an analytical calibration curve developed by Johnson is used [27, 28]. For the WOL specimens, an experimental calibration curve, Figure 5, is used. Resolution at room temperature for the center-cracked Inconel 718 alloy specimens is better than 0.001 inch in half-crack length (a). Resolution for 18Ni(200) maraging steel (WOL) specimens at room temperature is also better than 0.001 inch in crack length (a). Based on overall system stability and sensitivity, the lower limit for rate measurement is estimated to be about 10^{-7} inch per second.

Dehumidified high purity hydrogen is used as the test environment. The dehumidified hydrogen environment is maintained around the crack by clamping aluminum chambers to the faces of the center-cracked test specimen, or by enclosing the entire WOL specimen in an environment chamber, Figure 6. Dehumidification and additional purification are accomplished by passing hydrogen (99.999% purity) through

a gas purifier (Matheson Model 460 purifier with Model 461-R cartridge for moisture), through a series of cold traps at -196°C , then through a heated palladium membrane purifier at P before admission to the test chambers. To reduce back diffusion of impurities, an additional cold trap and a silicone fluid back-diffusion trap are used on the discharge side. Schematic diagram of the overall environment control system is shown in Figure 7. A rigorous purging procedure is followed. The gas system is purged for about two hours before each test using 99.999% purity argon. During this initial purging operation, the various components of the gas system up-stream from the back-diffusion trap (Figure 7) were heated to at least 100°C . The cold traps were then filled with liquid nitrogen, and the environment-specimen assembly was again heated to a minimum of 100°C while maintaining argon flow. The system is then evacuated with a mechanical pump and back-filled with hydrogen. Hydrogen is then allowed to flow through the palladium purifier and the system for at least 15 minutes prior to the start of the experiment. Continuous flow at a chamber pressure of about 5 psig is maintained throughout the experiment for experiments at ~ 1000 torr. Experiment at other hydrogen pressures can be carried out readily by using hydrogen-helium mixtures. With the procedure, the impurity level in the environment is estimated to be less than 5 p.p.m. (on the basis of mass spectroscopic analysis of argon purified in a similar manner in the system.) Electrical resistance heating tapes are used to heat the specimens for tests above room temperature. Cooling with chilled dry nitrogen is used for the low temperature tests. Temperature stability of better than $\pm 2^{\circ}\text{C}$ can be maintained during each test.

C. Results and Discussions

As a part of the planned first-year research, 1/8-inch-thick Inconel 718 alloy

and 1/4-inch-thick 18Ni(200) maraging steel plate specimens are being tested in dehumidified gaseous hydrogen under a slightly positive pressure of about 5 psig (or, about 1000 torr) over a range of temperatures from about -60°C to +300°C. Available results on the two materials will be discussed separately below.

1. Inconel 718 Alloy

Crack growth experiments have been carried out on the Inconel 718 alloy at about -50, +25 and +300°C. Increasing K levels for the sustained-load crack growth tests were obtained by increases in the applied load, or by further extension of the crack by fatigue. By the latter procedure some fatigue crack growth data in gaseous hydrogen were obtained. The results showed that there was no detectable crack growth under sustained loading at these temperatures for K levels up to about 90 ksi-in.^{1/2} (the lower limit of detectability for crack growth being about 10⁻⁷ in/sec.). Fatigue crack growth data obtained during these tests also show the absence of hydrogen effect at room temperature for K_{max} up to 90 ksi-in.^{1/2}, at R = K_{min}/K_{max} = 0.5 and a test frequency of 5.0 Hz. (Figure 8). These results are consistent with fatigue test results obtained previously on a 0.06-inch-thick Inconel 718 alloy sheet [29]. These results suggest that there is little effect of hydrogen under these conditions of temperature and pressure (~ 1000 torr). The absence of gaseous hydrogen embrittlement under these conditions, however, does not preclude the possibility of embrittlement at other temperatures and pressures. Embrittlement of this alloy in high pressure hydrogen has been observed by Walter and Chandler [20] using smooth and notched round tensile specimens. Evaluation of the crack growth characteristics, coupled with surface chemistry studies, at other conditions would be desirable. Fatigue crack growth has been shown to be a function of temperature

(see Figure 8) decreasing by about a factor of 3 from +300°C to -50°C. This temperature dependence is of importance to service performance and needs to be considered in design.

2. 18Ni(200) Maraging Steel

Because of delays and technical difficulties in the procurement and preparation of the 18Ni(200) maraging steel, experimental work on this material has just begun. Modified WOL specimens (Figure 4) are being used in place of the 3-inch-wide center-cracked specimen (Figure 3) as planned in the original program. Some preliminary results were obtained on the 3-inch-wide center-cracked specimens. The results indicate that no detectable crack growth occurred in gaseous hydrogen (≈ 1000 torr) at room temperature for K levels up to about $70 \text{ ksi-in.}^{\frac{1}{2}}$. Crack growth, however, was observed at about -30°C and exhibited a rate limiting speed of about 1.5×10^{-4} in./sec. This speed is about 1/5 of that for the 18Ni(250) maraging steel tested at the same temperature, Figure 9. These very preliminary results suggest that the temperature dependence for hydrogen enhanced crack growth is a function of alloy composition and/or of strength level, Figure 10 [30]. Additional experiments to fully characterize the temperature and pressure dependence of crack growth in hydrogen for this alloy are in progress.

III. HYDROGEN ADSORPTION AND DIFFUSION

A. Experimental Arrangement and Procedure

Hydrogen adsorption and diffusion in metals and alloys are being studied using a hydrogen-deuterium exchange technique. Based on a statistical treatment of the exchange reactions in which diatomic molecules react with solids containing

the same kind of atoms [31], the mechanism of adsorption and the diffusion coefficients can be determined by following two derived quantities K and W during the exchange experiment:

$$K = \frac{[\text{HD}]_{(g)}^2}{[\text{D}_2]_{(g)} [\text{H}_2]_{(g)}} \quad (3)$$

$$W = 2[\text{D}_2]_{(g)} + [\text{HD}]_{(g)} \quad (4)$$

$[\text{D}_2]_{(g)}$, $[\text{H}_2]_{(g)}$, and $[\text{HD}]_{(g)}$ are the molecular fractions of the D_2 , H_2 and HD molecules, respectively, in the gaseous phase at a given time. At equilibrium, the quantity K assumes the value of 4, and becomes equal to the equilibrium constant. Deviation of K from this equilibrium value provides a direct measure of the proportion of different possible mechanisms of the exchange, and identification of the likely process associated with gaseous hydrogen embrittlement [31]. Measurements of the change in atomic deuterium concentration (W) in the gaseous phase give information regarding the extent of hydrogen diffusion into the bulk material and the relative contribution of this process to crack growth.

An ultrahigh vacuum (UHV) apparatus for the hydrogen deuterium exchange experiment has been constructed. A schematic diagram of this apparatus is shown in Figure 11. Ultrahigh vacuum is obtained by cryostatic roughing, followed by pumping with a titanium sublimation pump and a titanium sputter ion pump. The total pressures in the apparatus are measured by an ionization gage (low pressures) and by a Pirani gage (intermediate and high pressures). A quadrupole residual gas analyzer is used to monitor the D_2 , H_2 and HD components in the gaseous phase during the exchange experiments through a calibrated capillary. To provide a

reaction cell that is free of metal deposits, a separate cleaning cell is provided. (Details of the cleaning cell and of the reaction cell are given in Figures 12 and 13 respectively). The cleaning cell is isolated from the reaction cell by a ground glass valve during the exchange experiments, so that the specimen is the only metal in contact with the experimental gases. For exchange experiments at high temperatures, the specimen is heated by an external, 1 kilowatt, 300 kHz R. F. generator. Experiments at low temperatures are carried out by cooling the reaction cell with a stream of chilled nitrogen regulated by a variable temperature controller.

Specimens (0.65 x 7 x 10 mm) are cut from materials used in the crack growth studies. These specimens are polished mechanically, and then chemically. After rinsing in distilled water and in methanol, they are dried and transferred to the cleaning cell, Figure 12, in the UHV apparatus. The specimens are heated by electron bombardment and sputter cleaned by argon ($\sim 10^{-4}$ torr) ion bombardment in this cell by applying the proper potentials to the electrodes as shown in Figure 12. After a number of ion bombardment and heating cycles, reproducible surface conditions can be obtained. Chemical cleaning may be appropriate in some cases, and can be accomplished by heating the specimens in hydrogen at low pressures.

Following cleaning, the specimen is transferred into the reaction cell. Hydrogen (or deuterium) at selected pressure is admitted and allowed to react with the clean specimen for a predetermined length of time. Hydrogen (or deuterium) is then pumped out rapidly, and is replaced by deuterium (or hydrogen). Valves 1 and 2, Figure 13, are then closed so that the exchange reactions can be carried out in a small volume, isolated from the rest of the vacuum apparatus. To permit continuous sampling of the reaction mixture at relatively high pressures ($\sim 10^{-3}$ torr)

with the quadrupole analyzer, and to prevent contact with the metal walls of the analyzer, a small amount of the reaction mixture is admitted directly into the ionization chamber of the analyzer through a calibrated capillary leak, C, Figure 13. The amounts of deuterium (D_2), hydrogen (H_2) and the mixed molecules (HD) are monitored as functions of time to determine the time variation of K and W.

In the apparatus described above, the activity of a metal surface can be investigated in three ways:

1. By mass spectrometric monitoring of an exchange reaction between hydrogen (H_2) and deuterium (D_2) molecules catalyzed by the metal surface. This rate is a measure of the ability of the metal to atomize hydrogen in its surface.

2. By mass-spectrometric monitoring of a replacement reaction in which hydrogen is placed in the material first and then isothermally replaced by deuterium from the gas phase. The total rate of production of hydrogen in the gaseous phase is a measure of the extent of adsorption and diffusion. The rates of appearance of the individual molecules H_2 and HD and of disappearance of D_2 from the gas phase are measures of the mechanism by which hydrogen enters the surface layer.

3. By flash desorption of hydrogen from the metal surfaces. This technique enables the determination of the total adsorbed amounts and approximate binding strength of hydrogen to the surface.

B. Materials

The materials studied in the first year were the 18Ni(250) maraging steel, 18Ni(200) maraging steel, and a single crystal of iron cut and polished to expose the (111) plane. The 18Ni(250) maraging steel was investigated as an additional material not included in the original proposal. The samples were 0.6 mm thick rectangular slabs of total surface area of about 1.5 cm².

The following pretreatments were employed:

1. The metal surface was cleaned by argon ion bombardment (denoted as AB) under the conditions specified in section III-A. According to the results of Auger spectroscopic analyses, the surface composition of the ion bombarded material was the same as the nominal bulk composition (within the limits of accuracy of Auger spectroscopy). This cleaning procedure was employed prior to any of the subsequent treatments.

2. Some specimens were then surface-annealed at 400°C by electron bombardment for 5-10 minutes. This treatment is denoted A (annealed sample); absence of this treatment is denoted NA (non-annealed sample).

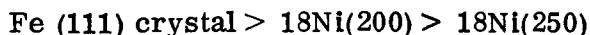
3. Prior to any cleaning procedure, the steel specimens were always heated to 850°C in vacuo and subsequently cooled to room temperature without aging at 500°C. Experiments on these annealed, non-aged specimens are marked by the symbol NAG. However, some specimens were aged at 500°C for 3 hrs. after the first argon ion bombardment, and subsequently ion bombarded again. These specimens are denoted AG (aged).

C. Results and Discussion

The replacement reactions (process #2, page 14) were attempted by loading the specimens with deuterium (D_2) at 10^{-2} torr and 25°C and replacing the gas phase by hydrogen (H_2) at 10^{-4} torr from a volume of 1.5 liter. No replacement reactions were observed at temperatures between -190°C and 200°C. This result indicates that not much hydrogen was picked up by the materials studied, at least not in excess of 10-20 layers. Further experiments are in progress at lower pressures of hydrogen to pursue the replacement reaction with a greater sensitivity.

The exchange reactions (process #1, page 14) were then investigated to provide a measure of the activity of the steel and iron crystal surfaces towards atomization of hydrogen. The ranges of pressures 10^{-3} to 10^{-2} torr and temperatures between -190°C and $+300^{\circ}\text{C}$ were investigated. Measurable rates of the exchange $\text{H}_2(\text{g}) + \text{D}_2(\text{g}) \rightleftharpoons 2\text{HD}(\text{g})$ were obtained at temperatures between 0°C and 300°C . The results of the measurements of the total homomolecular rate of exchange ($R + R' + R''$) for the different materials and treatments are summarized in Table 5. The experimental material substantiating these data is presented in Appendix I.

The rates ($R + R' + R''$) are those of overall adsorption, atomization, and recombination of hydrogen molecules on the given surface, irrespective of the mechanism by which the surface atomization takes place. These rates are therefore representative of the ability of the given material to atomize and recombine hydrogen. The data in Table 5 demonstrate the following order of chemical activities:



The effect of pretreatments is such that non-annealed surfaces are more active than annealed surfaces and that aged specimens are more active than non-aged specimens. The activation energies for all samples are between 0.5 and 4.0 kcal/mole and are higher on 18Ni(250) specimens than on 18Ni(200) specimens. The kinetic data presented in Table 5 are based on the initial rates. The rates themselves are not constant with time as shown in the last column of Table 5, and indicate some decay of the surface activity with time. This phenomenon is most likely caused by hydrogen self-poisoning of the surface.

The initial rates ($R + R' + R''$) on the iron crystal ($\approx 10^{17}$ molecules/cm.² sec at 25°C and 10^{-2} torr) are quite comparable to the adsorption rates of hydrogen

on polycrystalline iron, obtained by extrapolation of data reported by Chornet and Coughlin [32]. These authors also determined the activation energy for adsorption to be 0.5 kcal/mole which is at the lower end of the range of activation energies for the H_2/D_2 exchange observed in this work. We can thus tentatively conclude that the exchange rates are kinetically limited by and coincide with the adsorption rates, and conversely, that the adsorption rates are determined by the rates of surface atomization of the impinging hydrogen molecules. The dissociation of the hydrogen molecules into atoms is the most common mechanism for activation of hydrogen for chemical reactions, and may be suggested as one possible reason for hydrogen embrittlement. The hydrogen atoms adsorbed in the vicinity of a crack tip may weaken the metal-metal bond and cause an enhancement of the crack growth rate (stress sorption cracking), or may diffuse ahead of the crack tip and form a composite zone whose mechanical cohesion is weaker than that of the hydrogen-free material. In order to test these possibilities, it is desirable to compare the rates of hydrogen atom production with the crack growth rates under comparable temperature and pressure conditions. So far the chemical rates and the crack growth rates have been obtained at different pressures but the pressure dependence of the crack growth rates permits tentative comparison to be made. Taking the crack growth rate of the 18Ni(250) maraging steel to be 10^{-3} cm/sec in 86 torr hydrogen [30] and assuming the rate to be proportional to the square root of pressure [30], we obtain a linear rate of 1000 Å/sec at 10^{-2} torr. If the crack growth rate is determined by the supply of hydrogen atoms, the rate of formation of the new surface will be given by the rate of production of hydrogen atoms that can reach the crack tip. Calculations based on the observed rates of atomization show that hydrogen atoms from the

region extending to 50 Å on both sides of the crack tip would be sufficient to sustain the crack growth rate of 1000 Å/sec. The rate of transport of the hydrogen atoms within the 50 Å distance would have to be sufficiently high for this mechanism to operate. On the surface of pure iron, the lateral mobility of hydrogen atoms is indeed high since the entropy of the adsorbed hydrogen has been found to be close to the entropy of a two-dimensional monatomic gas [32].

The situation on alloy surfaces which are our main concern may or may not be different from that on pure iron. The differences may stem from different chemical composition, structure and texture of the iron and steel surfaces, and may affect both the reactivity of the surface and the lateral mobility of the hydrogen atoms. From the comparison of the activities in Table 5, the steel surfaces do not appear to have components more active than iron itself. In fact, their activities are so close to that of pure iron that it would seem that the iron alone may be responsible for their reactivity toward hydrogen. The effects of chemical composition will be further investigated on steel specimens aged at 400-500°C for 3 hrs. at which temperatures and times Auger spectroscopy revealed a substantial enrichment of the surface by titanium and molybdenum.

The effects of texture and surface roughness can be crudely estimated from the comparison of argon bombarded, non-annealed surfaces with argon bombarded and annealed surfaces. There is a distinct difference in the reactivities of the non-annealed and annealed surfaces, although their chemical composition is approximately the same. The non-annealed surfaces have in average about half order of magnitude higher activity than the non-annealed surfaces (Table 5). This effect is easily understood in terms of higher activity of atoms displaced from their regular positions,

increased concentration of vacancies, and generally higher energy content of the non-annealed, highly perturbed surfaces. The difference in the activity of the annealed and non-annealed surfaces is not great, however, and one can expect that slightly perturbed surfaces will have their activity close to that of the annealed surface. It would of course be desirable to know what kind of surface perturbations occur at the crack surface, and therefore it is planned to carry out the hydrogen adsorption and exchange experiments on the actual crack surface which will yield additional kinetic information for comparison with that presently obtained for pure iron and steel surfaces cleaned by argon bombardment.

The effects of structure are perhaps reflected in the differences in the activities of the aged and non-aged specimens of the 18Ni(250) maraging steel (Table 5, rows 6 and 7). The aged specimens exhibit about one order greater activity than the non-aged specimens indicating a higher reactivity of the aged martensitic structure over the annealed structure. These results should be compared with crack growth data on the aged and the annealed maraging steels.

IV. SUMMARY

1. No sustained-load crack growth was observed for the Inconel 718 alloy in gaseous hydrogen (~ 1000 torr) at about -50°C , 25°C and $+300^{\circ}\text{C}$ for stress intensities up to $90 \text{ ksi } \sqrt{\text{in}}$. The rate of fatigue crack growth at room temperature, with $R = K_{\text{min}}/K_{\text{max}} = 0.5$ and $f = 5.0 \text{ Hz}$, was also unaffected by gaseous hydrogen (at ~ 1000 torr).

2. Preliminary results on the 18Ni(200) maraging steel indicated that sustained-load crack growth was unaffected by hydrogen (~ 1000 torr) at room

temperature, but was affected by hydrogen at about -30°C . The rate limiting speed was about 1.5×10^{-4} in./sec. at -30°C , and was about 1.5 of that for the 18Ni(250) maraging steel. These very preliminary results suggest that the rate and temperature dependence for hydrogen enhanced crack growth is a function of alloy composition and/or of strength level. Additional experiments are in progress.

3. The rates of hydrogen atomization by the three types of materials investigated are high and probably sufficient to sustain the crack growth through a mechanism limited by hydrogen atom formation.

4. The differences between the activities of the 18Ni(250), 18Ni(200) and iron (111) surfaces are small, indicating that either the alloying elements (mainly nickel) exhibit activity close to that of iron or that iron may be the principal carrier of the hydrogen activation.

5. Aged specimens are more active for hydrogen atomization than non-aged specimens.

6. Surface roughness induced by ion bombardment increases the activity of all materials studied.

7. It appears that prevention of hydrogen embrittlement in maraging steels should be sought in adding alloying elements which would poison the catalytic activity of the surface for hydrogen atomization, or which would act as traps for hydrogen atoms preventing their surface diffusion. The effects of gaseous poisons such as O_2 , N_2O , CS , and CS_2 should also be considered if the presence of these gases can be accepted on technological grounds. The experiments on poisoning of the steel surfaces by these gases with respect to hydrogen adsorption and exchange can be carried out in our present system without modification.

REFERENCES

1. C. Zapffe and C. Sims, AIME Trans. 145, 225 (1941).
2. F. Garofalo, Y. T. Chou, and V. Ambegaokar, Acta Met., 8, 504 (1960).
3. B. A. Bilby and J. Hewitt, Acta Met., 10, 587 (1962).
4. A. S. Tetelman, Proceedings - Fundamental Aspects of Stress Corrosion Cracking, Natl. Assoc. Corr. Engrs., Houston, 446 (1969).
5. R. P. Frohberg, W. J. Barnett, and A. R. Troiano, Trans. ASM, 47, 892 (1955).
6. H. H. Johnson, J. G. Morlet, and A. R. Troiano, Trans. TMS-AIME, 212, 528 (1958).
7. E. A. Steigerwald, F. W. Schaller, and A. R. Troiano, Trans. TMS-AIME, 215, 1048 (1959).
8. A. R. Troiano, Trans. ASM, 52, 54 (1960).
9. N. O. Petch and P. Stables, Nature, 169, 842 (1952).
10. H. H. Johnson, Proceedings - Fundamental Aspects of Stress Corrosion Cracking, Natl. Assoc. Corrosion Engrs., Houston, 439 (1969).
11. R. P. Wei, Intl. J. Fract. Mech., 4, 159 (1968).
12. R. P. Wei, J. Eng'g. Fract. Mech., 1, 633 (1970).
13. F. J. Bradshaw and C. Wheeler, RAE Tech. Memo. No. MAT 26 (1968).
14. T. Bloom and A. J. Nicholson, J. Inst. Metals, 89, 183 (1960).
15. G. G. Hancock and H. H. Johnson, Trans. TMS-AIME (1966).
16. R. P. Wei and J. D. Landes, Matl. Res. & Std., ASTM, Vol. 9, No. 7, 25 (1969).
17. W. A. Spitzig, P. M. Talda, and R. P. Wei, J. Eng'g. Fract. Mech., 1, 155 (1968).
18. D. P. Williams and H. G. Nelson, Metallurgical Trans., 1, 63 (1970).
19. H. G. Nelson, D. P. Williams, and A. S. Tetelman, "Embrittlement of a Ferrous Alloy in a Partially Dissociated Hydrogen Environment," preprint of a paper submitted for publication in the Metallurgical Trans. (1970).

20. R. J. Walter and W. T. Chandler, "Effect of High-Pressure Hydrogen on Metals," paper presented at the Symposium on Effects of Gaseous Hydrogen on Metals, 1968, Materials Eng'g. Congress, Detroit, Mich., 13-17 October 1968.
21. R. P. Wei, "The Effects of Temperature and Environment on Subcritical Crack Growth," presented at the WESTEC Conference (1972); Rept. IFSM-72-14, Lehigh University (April 1972).
22. R. A. Oriani, Proceedings - Fundamental Aspects of Stress Corrosion Cracking, Natl. Assoc. Corr. Engrs., Houston, 32 (1969).
23. D. S. Dabkowski, L. F. Porter, and G. E. Loveday, "Evaluation of Vacuum Induction Melted 18Ni(180) and 18Ni(250) Maraging Steels," Rept. 39.018-007(3), Applied Research Laboratory, U. S. Steel Corporation, January 1, 1967.
24. W. F. Brown, Jr. and J. E. Srawley, ASTM STP 410 (1966).
25. M. Isida, "Crack Tip Stress Intensity Factors for the Tension of an Eccentrically Cracked Strip," Lehigh University, Dept. of Mechanics Report (1965).
26. W. G. Clark, Jr., private communication.
27. J. D. Landes, "Kinetics of Subcritical-Crack Growth and Deformation in a High-Strength Steel," Ph. D. Dissertation, Lehigh University, (1970).
28. Che-Yu Li and R. P. Wei, Mat'l. Res. and Stds., ASTM, 6, 392 (1966).
29. R. P. Wei, unpublished results.
30. S. J. Hudak, Jr. and R. P. Wei, "The Kinetics of Hydrogen Enhanced Crack Growth in High Strength Steels," to be published.
31. K. Klier, J. Novakova, and P. Jiru, J. Catalysis 2, 479 (1963).
32. E. Chornet and R. W. Coughlin, J. Catalysis 27, 246 (1972).

APPENDIX I

The data on the time dependences of the concentrations of gaseous H₂, D₂, and HD molecules over various metal specimens investigated are given herein.

The relative concentrations of the individual molecules at any given time are represented as molecular fractions, for example

$\frac{[HD]}{[H_2] + [HD] + [D_2]}$ is the relative concentration of the HD molecules. The reduced concentrations are $\frac{[H_2] - [H_2]_{\infty}}{[H_2]_0 - [H_2]_{\infty}}$, $\frac{[HD] - [HD]_{\infty}}{[HD]_0 - [HD]_{\infty}}$, and $\frac{[D_2] - [D_2]_{\infty}}{[D_2]_0 - [D_2]_{\infty}}$, respectively. The derived quantity

$K = \frac{[HD]^2}{[H_2][D_2]}$ is a measure of the mixing entropy in the gaseous phase, and is also plotted in some of the graphs. Its time dependence is a measure of the approach of the system metal-hydrogen to the equilibrium where K has a maximum value of 4.

The data are presented in three separate sets, one for each material studied.

A. 18Ni(250) Maraging Steel

1. NAG-AB-NA (non-aged, argon bombarded, non-annealed) specimen.

The time dependences of the relative concentrations of H₂, HD, and D₂ at pressures around 10⁻² torr are given for the individual temperature runs in Figures 14-18. The variations in the pressure from one experiment to another were slight and did not significantly affect the measured rates. Also plotted in Figures 14-18 is the function $K = [HD]^2/[H_2] \cdot [D_2]$. The rates of exchange are quantitatively evaluated by plotting the logarithms of the reduced concentrations of the D₂ and HD molecules against time. The slopes of the lines drawn through the experimental points in these coordinates give the rates of homomolecular exchange, $\frac{1}{a} (R + R' + R'')$, where $a = [H_2] + [HD] + [D_2]$. An experimental check for the validity of this treatment is that the slopes for the reduced concentrations

of H_2 , HD, and D_2 coincide. Figures 19-23 show the replotted data of Figures 14-18 for the reduced concentrations of the D_2 and HD molecules. The concentrations of D_2 and HD follow roughly the same lines, demonstrating that the true rates ($R + R' + R''$) are measured. The temperature dependence of the rates ($R + R' + R''$) is shown in Figure 24. The maximum exhibited on this temperature dependence was not found with other preparations of the 18Ni(250) maraging steel and is not understood at the present moment.

2. AG-AB-NA (aged, argon bombarded, non-annealed) specimen.

The rates of the H_2/D_2 exchange are represented as the time variations of the logarithms of the reduced concentrations of HD and D_2 in Figures 25-32. The temperatures and pressures at which these experiments were carried out are given in the figure captions.

The temperature dependence of the rates is presented in Figure 33, together with the temperature dependence on the AG-AB-A 18Ni(250) maraging steel.

3. AG-AB-A (aged, argon bombarded, non-annealed) specimen.

The rates of the H_2/D_2 exchange are represented as the variations of the logarithms of the reduced concentrations of HD and D_2 in Figures 34-40. The temperatures and pressures at which these experiments were carried out are again given in the figure captions.

The temperature dependence of the rates is presented in Figure 33, together with the temperature dependence on the AG-AB-NA 18Ni(250) maraging steel.

B. 18Ni(200) Maraging Steel

1. AG-AB-NA (aged, argon bombarded, non-annealed) specimen.

The rates of the H_2/D_2 exchange are again represented as the time

dependences of the logarithm of the reduced concentrations of HD and D₂ in Figures 41-45, with temperatures and pressures given in the figure captions.

The temperature dependence of the rates is represented in Figure 46, together with the temperature dependence of the exchange rates on the AG-AB-A 18Ni(200) maraging steel.

2. AG-AB-A (aged, argon bombarded, non-annealed) specimen.

The rates of the H₂/D₂ exchange are again represented as the time dependences of the logarithms of the reduced concentrations of HD and D₂ in Figures 47-51, with temperatures and pressures given in the figure captions.

The temperature dependence of the rates is represented in Figure 46, along with the temperature dependence of the rates on the AG-AB-NA 18Ni(200) maraging steel.

Fe (111) Single Crystal

The iron single crystal was cut along the (111) plane, mechanically and chemically polished, and cleaned in the ultrahigh vacuum system by repeated argon ion and electron bombardments. The final treatment was electron bombardment annealing at 750-800°C. By this procedure, the (111) crystallographic orientation of iron crystal is restored. The data on iron crystal serve as a reference for comparison of the various ferrous alloys. The rates of the H₂/D₂ exchange on Fe (111) were the highest observed. The time dependence of the logarithm of the reduced concentrations of HD and D₂ are represented in Figures 52-54. The data on activation energies are not available since time limits permitted the experiments to be done only at room temperatures.

The Time Dependence of the Rates

All rates measured in this work decayed with time by varying factors of 2-5 in 10 minutes (Table 5). The time dependence will certainly affect the slopes of the logarithms of the reduced concentrations vs. time, and therefore the calculated rates ($R + R' + R''$) are time averages over the duration of the experiment. It is unlikely that the time dependence is caused by poisoning of the surface by residual gases other than hydrogen since the clean surfaces retain their activity when kept in vacuum without the presence of hydrogen. The poisoning of the surface by the diffusion of impurities from the bulk is also unlikely since the time effects are little temperature dependent and since no time changes in surface chemical composition were observed by Auger spectroscopy at the temperatures of these experiments. A physical relaxation of the surface is ruled out on the annealed specimens which still show a similar time dependence as the non-annealed specimens. The remaining possibility is self-poisoning of the surface by hydrogen. At the present time this seems to be the best explanation of the time decay of the activity. Hydrogen may exist in the surface in various forms, one or more of which may be formed by a slow reaction. The question of time dependence of the reaction rates will be given further attention in the next year of the project.

TABLE 1
 CHEMICAL COMPOSITION AND HEAT TREATMENT
 FOR INCONEL 718 ALLOY SHEET

Chemical Composition, Weight Percent
 (INCO Huntington Alloy Products Div. Heat No. HT94B1ES)

	AMS 5596 C		Supplier's Analysis	Check Analysis
	<u>min.</u>	<u>max.</u>		
C	---	0.10	0.05	0.03
Mn	---	0.35	0.07	0.40
Si	---	0.35	0.19	0.17
P	---	0.015	0.009	0.007
S	---	0.015	0.007	0.004
Ni	50.0	55.0	53.81	54.2
Cr	17.0	21.0	18.40	17.9
Mo	2.8	3.3	2.96	2.94
Cu	---	0.1	0.04	0.05
Cb + Ta	5.0	5.5	5.19	3.68
Ti	0.65	1.15	1.00	1.00
Al	0.4	0.8	0.58	0.43
Co	---	1.0	0.03	0.12
B	---	---	0.0028	ND*
Fe	Balance		17.65	ND*(~19.1)

*ND - Not Determined

Heat Treatment

Solution Anneal - 1800°F, 1 hour + Air Cool

Age - 1325°F, 8 hours + Furnace Cool to 1150°F + Hold
 at 1150°F for total aging time of 18 hours + Air Cool

TABLE 2

Tensile Properties of Inconel 718 Sheet
(Heat No. HT94B1ES)

<u>Source</u>	<u>Orientation</u>	<u>Tensile Strength ksi</u>	<u>Yield Strength ksi</u>	<u>Elongation in 2 in. percent</u>
Lehigh University	Longitudinal	203.4	166.8	18.0
		205.1	168.5	18.0
		<u>202.8</u>	<u>166.2</u>	<u>17.5</u>
	(Average)	203.8	167.2	17.8
	Transverse	200.5	167.4	17.0
		201.9	168.4	17.0
		<u>201.7</u>	<u>168.5</u>	<u>17.0</u>
201.4		168.1	17.0	
Huntington Alloy (Supplier)	Transverse	202.0	177.0	18.0
AMS 5596C	Transverse	180.0 (min.)	150.0 (min.)	12 (min.)

TABLE 3

CHEMICAL COMPOSITION AND HEAT TREATMENT
FOR 18Ni(200) MARAGING STEEL PLATE

Chemical Composition, Weight Percent
(U.S. Steel Corporation Heat No. L-50446)

	<u>Supplier's</u> <u>Analysis []</u>	<u>Check</u> <u>Analysis</u>
C	0.002	ND*
Mn	<0.02	ND
Si	0.003	ND
P	0.003	ND
S	0.007	ND
Ni	17.50	17.89
Co	7.60	7.50
Mo	2.93	2.75
Ti	0.20	0.18
Al (sol.)	0.007	ND
N	0.004	ND
O	0.0011	ND
Fe	Balance	Balance

* ND - Not Determined

Heat Treatment

Solution Anneal - 1650°F, 1/2 hour + Air Cool

Re-solution Anneal - 1500°F, 1/2 hour + Water Quench

Age - 900°F, 16 hours + Water Quench

TABLE 4

Tensile Properties of 18Ni(200) Maraging Steel Plate
(U. S. Steel Heat No. L-50446)

<u>Orientation</u>	<u>Tensile Strength</u> ksi	<u>Yield Strength</u> ksi	<u>Elongation</u> in 2 in. percent
Longitudinal	193.1	185.7	13.0
	192.8	185.5	13.0
	<u>193.2</u>	<u>185.0</u>	<u>12.5</u>
(Average)	193.0	185.4	12.8

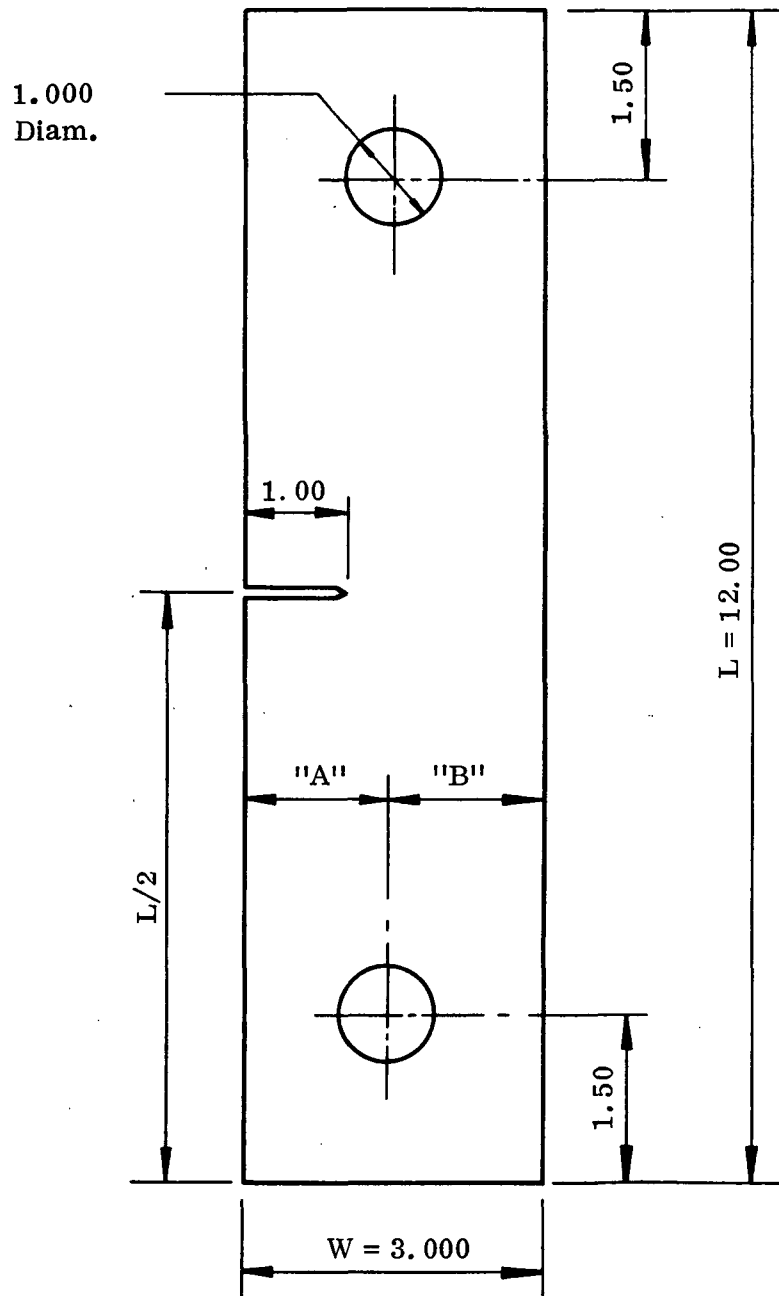
TABLE 5

Summary of the Rates, Activation Energies, and Time Dependences
of the H₂/D₂ Exchange on 18 Ni (250) Maraging Steel,
18 Ni (200) Maraging Steel, and Iron Crystal of (111) Orientation

Material	Treatment ^a	Rate of homomolecular exchange R + R' + R'' at 25°C ^b	E _A (kcal/mole)	Time Dependence
Iron single crystal, (111) plane	AB-A (750°C)	1 × 10 ¹⁷		10 ¹⁷ → 4 × 10 ¹⁶ in 10 min
18 Ni 200 maraging steel	AG-AB-A	5 × 10 ¹⁶	0.55	5 × 10 ¹⁶ → 1 × 10 ¹⁶ in 10 min
	AG-AB-NA	1 × 10 ¹⁷	1.0	
18 Ni 250 maraging steel	AG-AB-A	1 × 10 ¹⁶	2.25	3 × 10 ¹⁶ → 10 ¹⁶ in 10 min (200°C) 1.5 × 10 ¹⁶ → 6 × 10 ¹⁵ in 10 min (100°C)
	AG-AB-NA	4 × 10 ¹⁶	1.2	
	NAG-AB-NA	4.5 × 10 ¹⁵	1.0-4.0	

^a AG = aged, NAG = non-aged, AB = argon bombarded, A = annealed at 700 - 800°C after argon bombardment, NA = non-annealed.

^b Rates are in molecules/cm² sec. Homomolecular exchange is the reaction H_{2(g)} + D_{2(g)} ⇌ 2HD_(g) catalyzed by the surface.



Note: "A" = "B" + 0.001

Figure 1: SEN Fracture Toughness Test Specimen

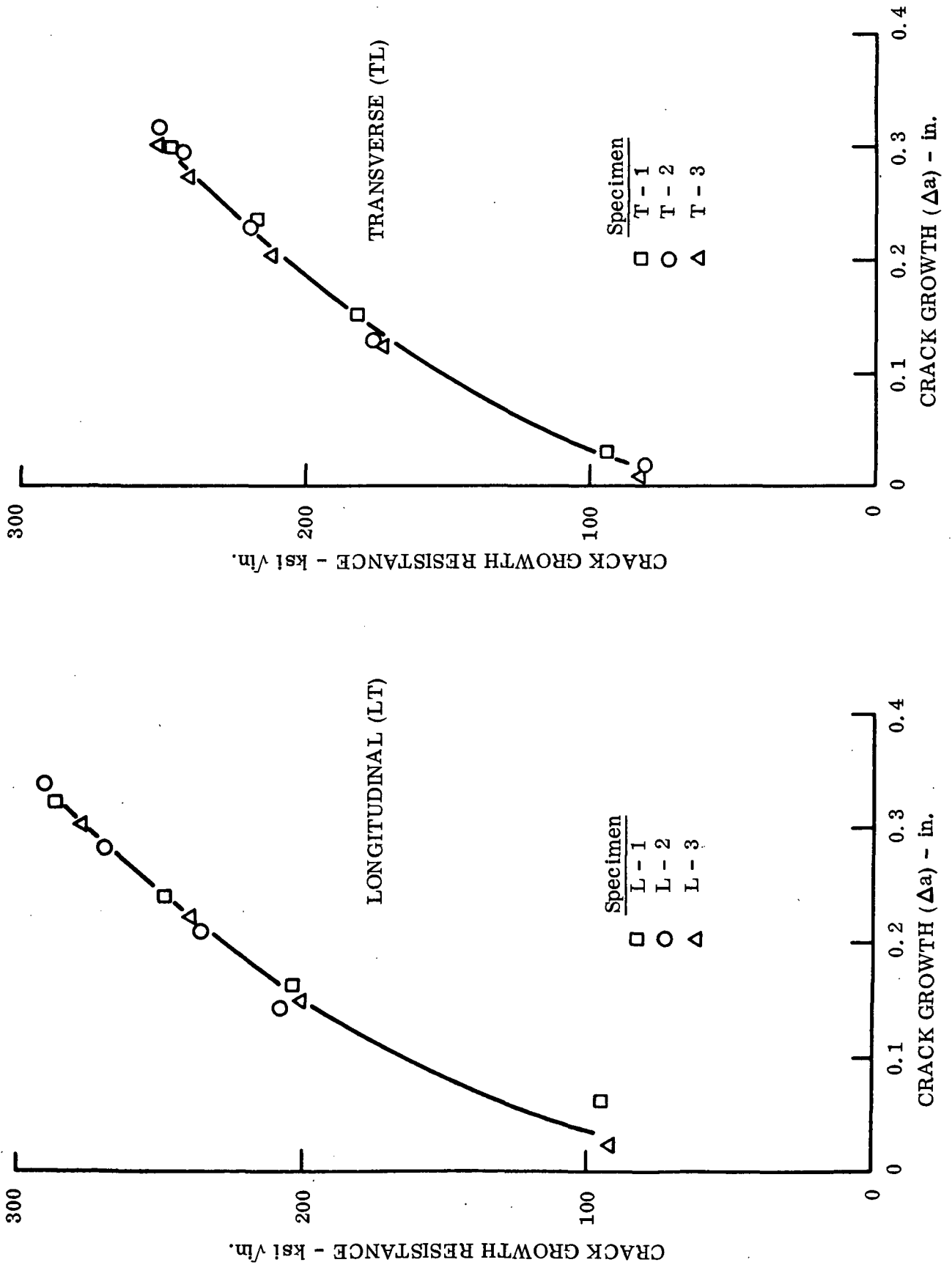


Figure 2: Crack growth resistance curves for 1/8-inch-thick Inconel 718 alloy sheet (solution annealed and aged)

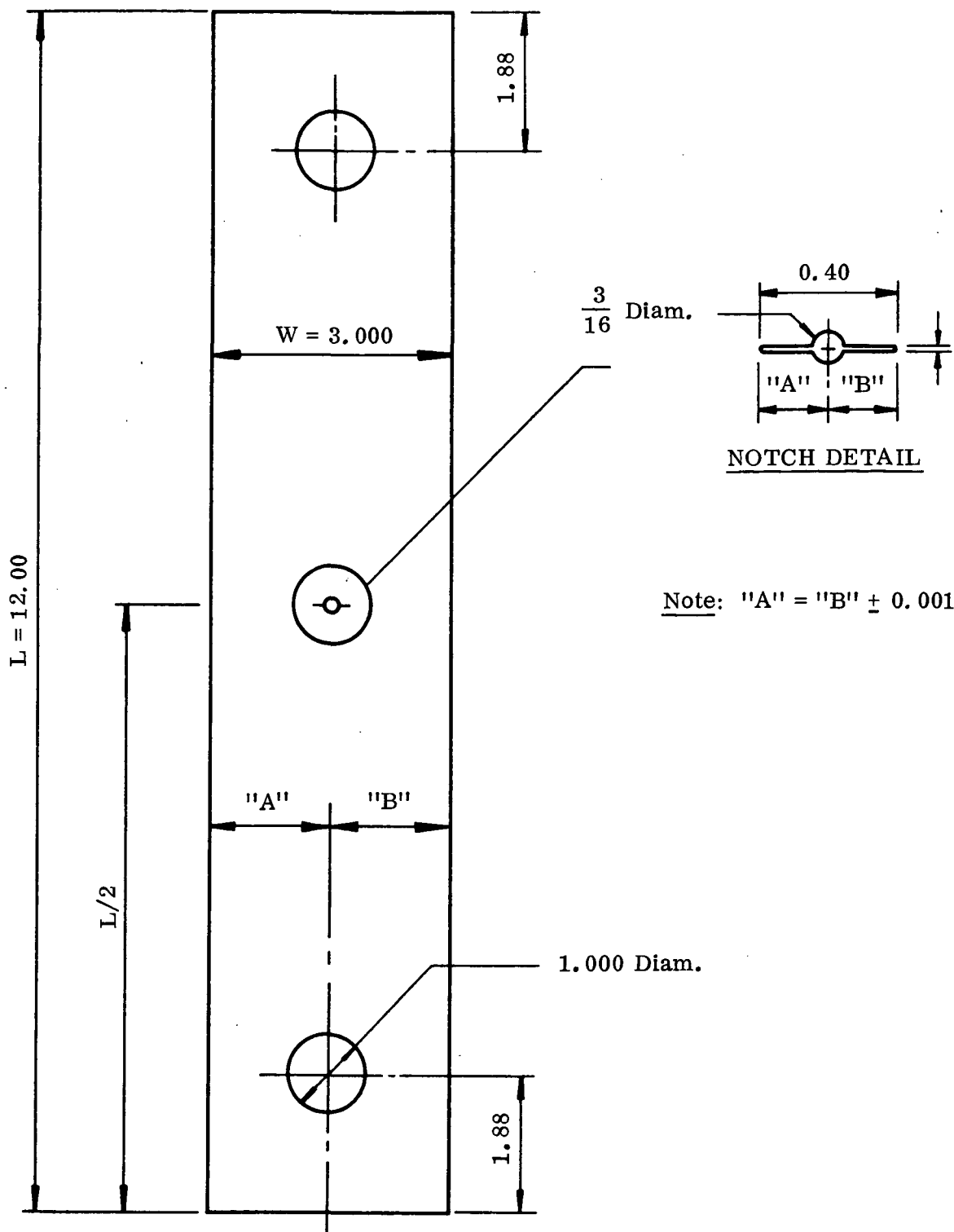


Figure 3: Center-Cracked Crack Growth Test Specimen

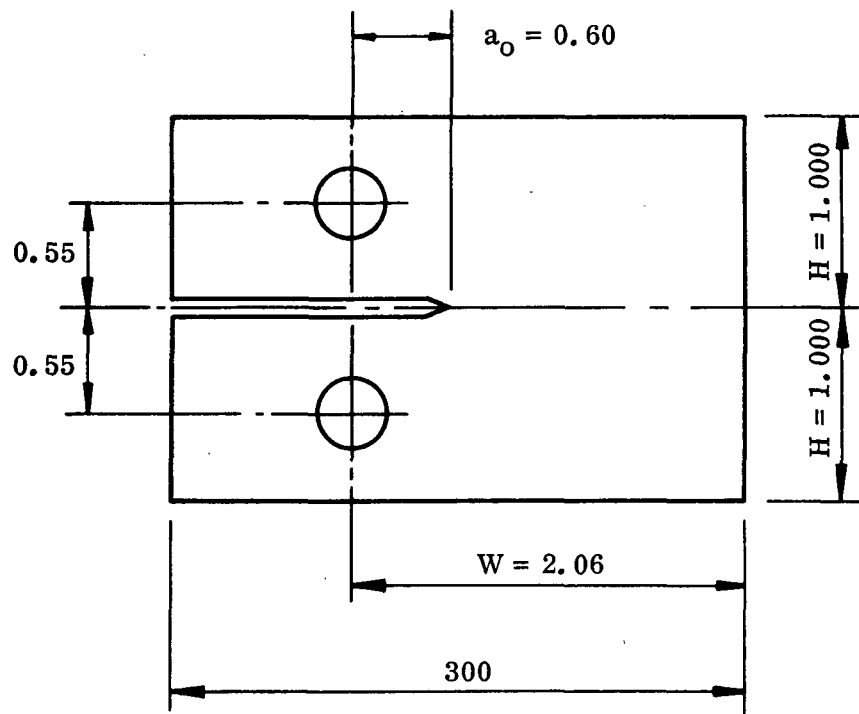


Figure 4: Modified Wedge-Opening-Load (WOL) Specimen

○ Specimen S3-CAL [$I = 2.1$ amp., $V_r = 443.2 \mu\text{v}$ at $a = 0.602$ in.]

△ Specimen S4-CAL [$I = 3.3$ amp., $V_r = 708.2 \mu\text{v}$ at $a = 0.602$ in.]

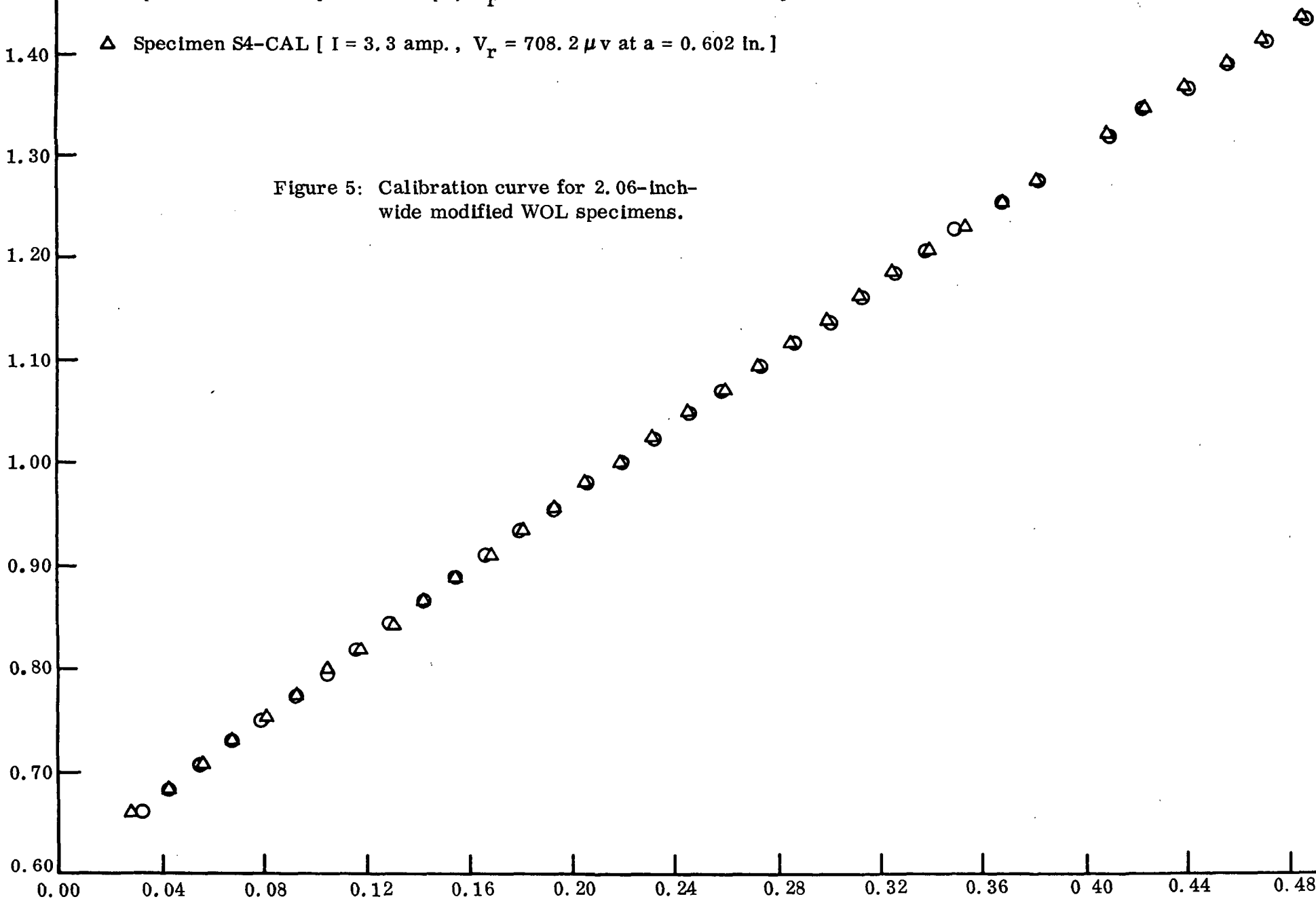
Figure 5: Calibration curve for 2.06-inch-wide modified WOL specimens.

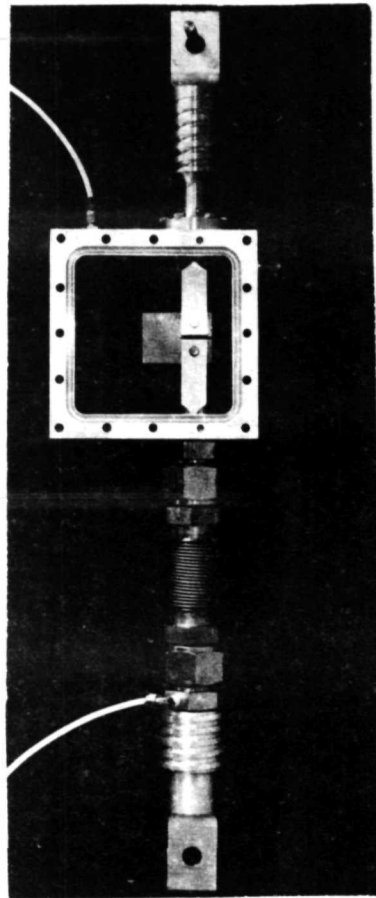
a_{visual} (Corrected) - Inches

1.40
1.30
1.20
1.10
1.00
0.90
0.80
0.70
0.60

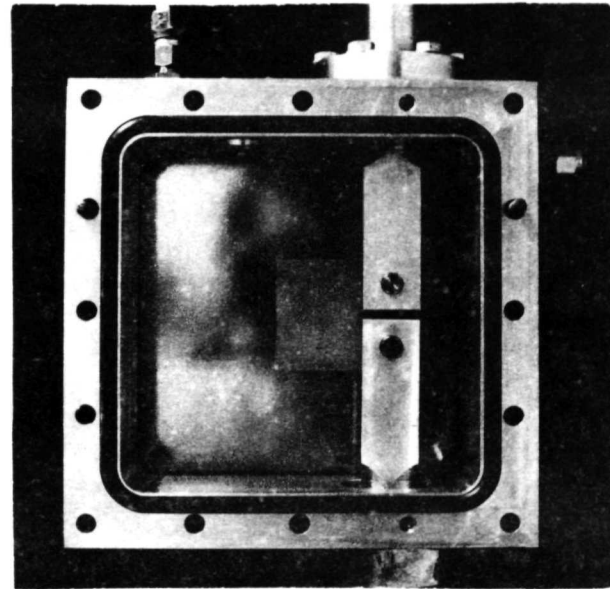
0.00 0.04 0.08 0.12 0.16 0.20 0.24 0.28 0.32 0.36 0.40 0.44 0.48

$V - V_r / V_r$





(a)



(b)

Figure 6: (a) Environment chamber and load train for modified WOL specimens (both covers removed); (b) close-up of environment chamber and specimen.

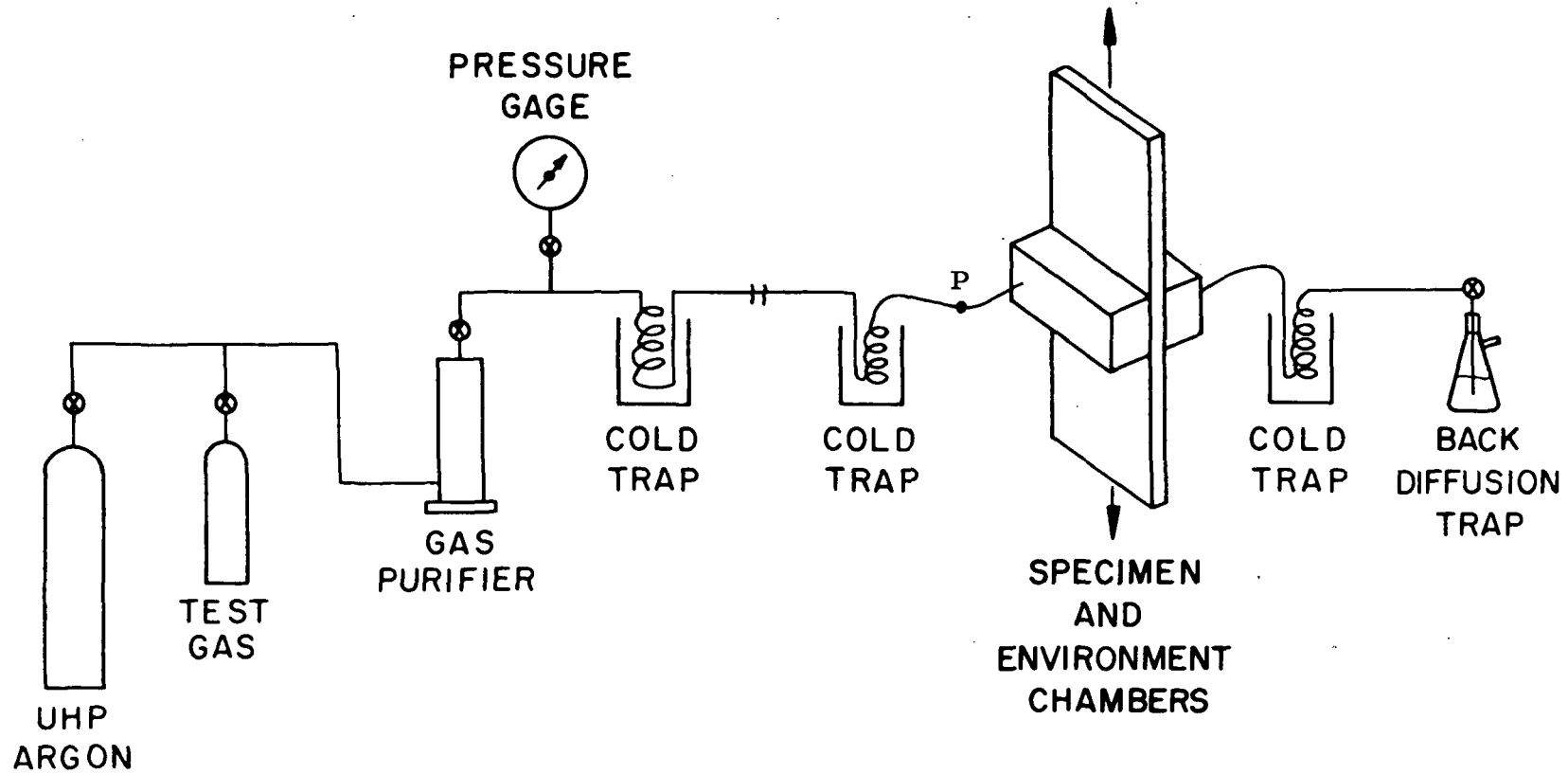


Figure 7: Schematic Diagram of Environmental Control System.

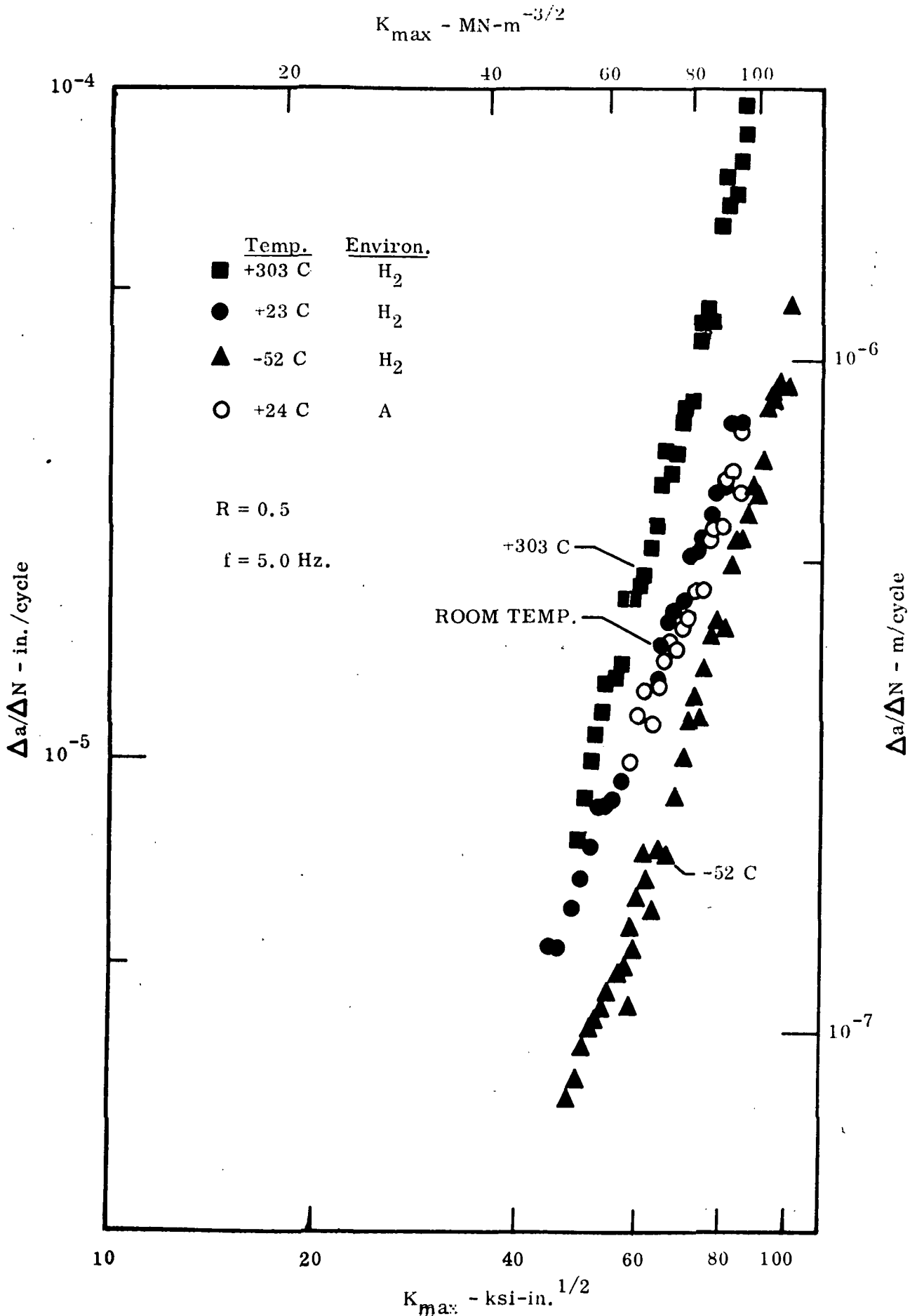


Figure 8: Fatigue crack growth in Inconel 718 alloy sheet in dehumidified hydrogen and argon at ~ 1000 torr.

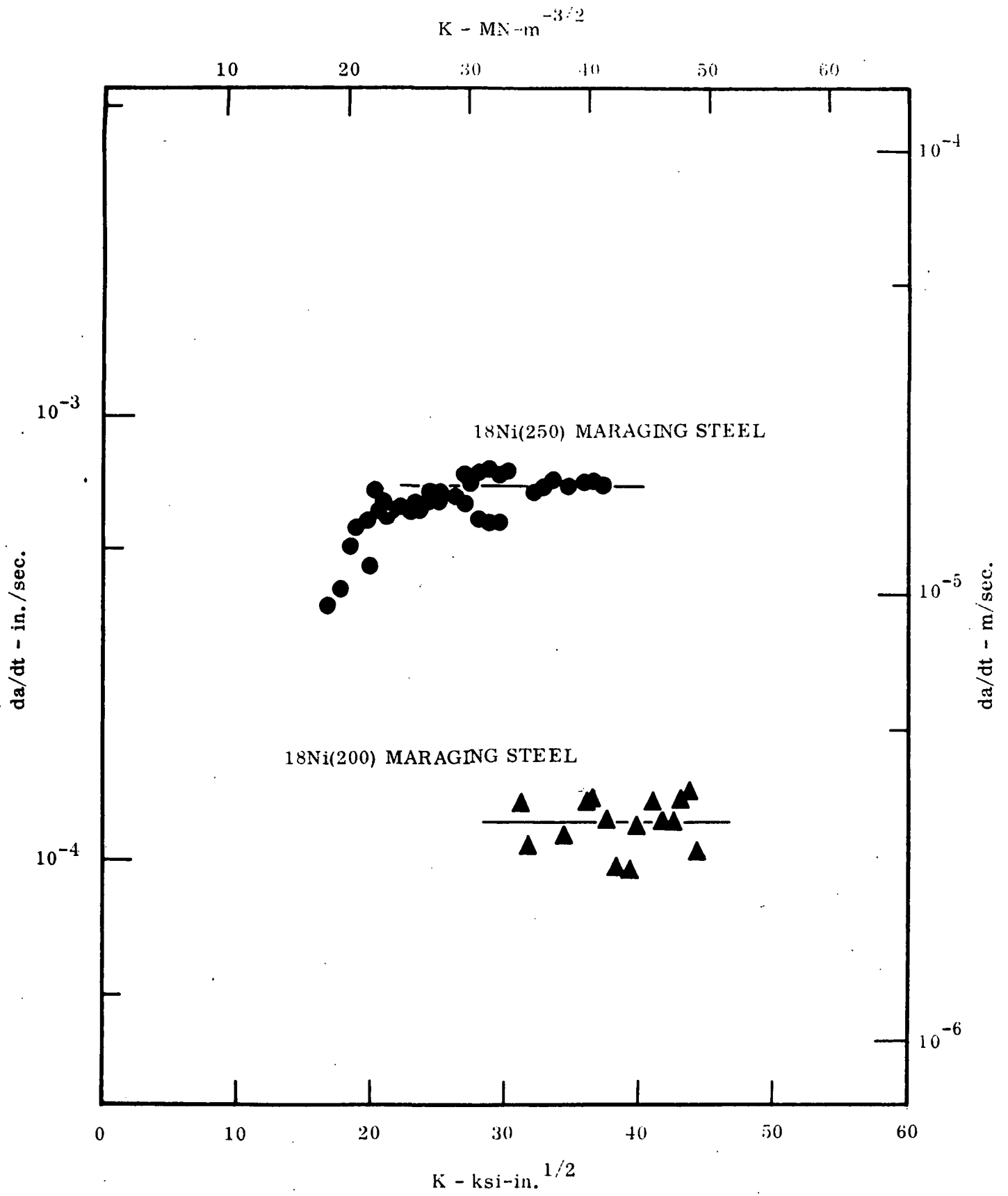


Figure 9: Hydrogen-enhanced subcritical crack growth at about -30°C .

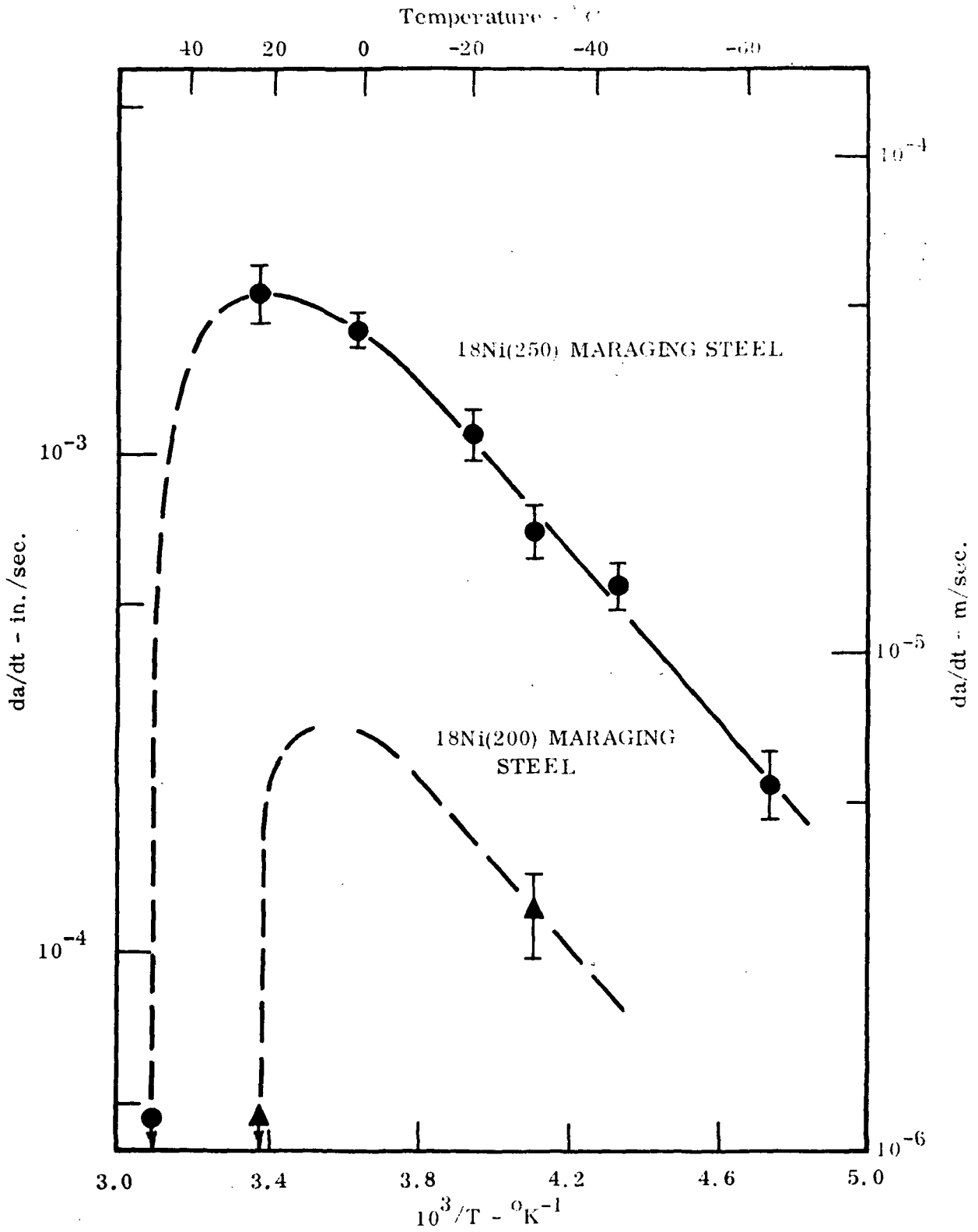


Figure 10: Effect of temperature on stage II crack growth at ~ 1000 torr.

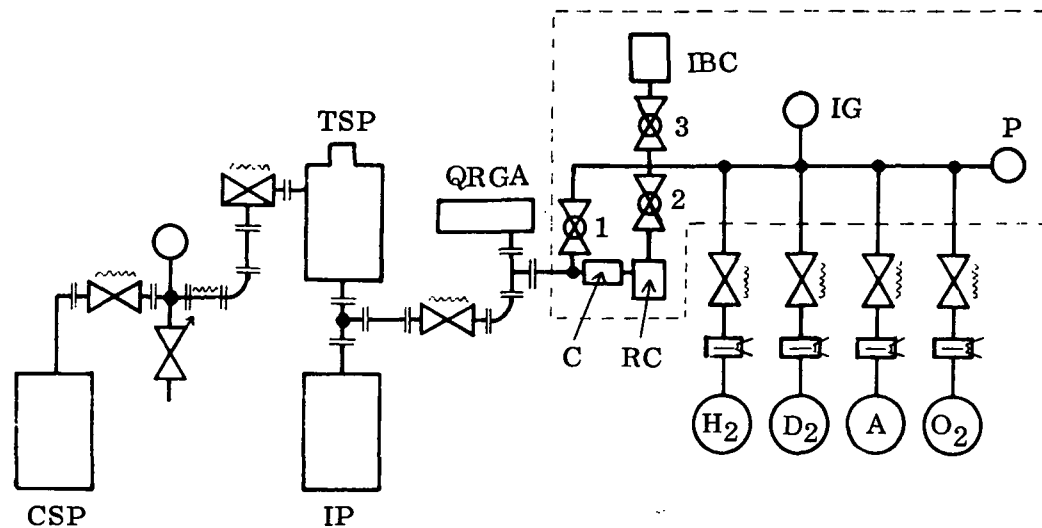


Figure 11: Block diagram of the UHV system for exchange measurements. Framed part is an all-glass apparatus with magnetically operated glass ball-to-socket valves 1, 2 and 3; ion and electron bombardment cell IBC; ionization gauge IG and Pirani gauge P as pressure sensors; reaction cell RC; and calibrated leak C. The sputter ion pump IP is a Varian 50 ls^{-1} model, used conjointly with an air cooled 50 ls^{-1} Varian titanium sublimation pump TSP; the cryosorbent, CSP, uses Linde Molecular Sieve 13X; the bellow valves are Granville-Phillips Type C metal valves; and a Varian quadrupole residual gas analyzer (QRGA) is used to monitor the exchange experiments.

Bombardment
electron
ion

Cathode
+25
+25

Grid
+500
+500

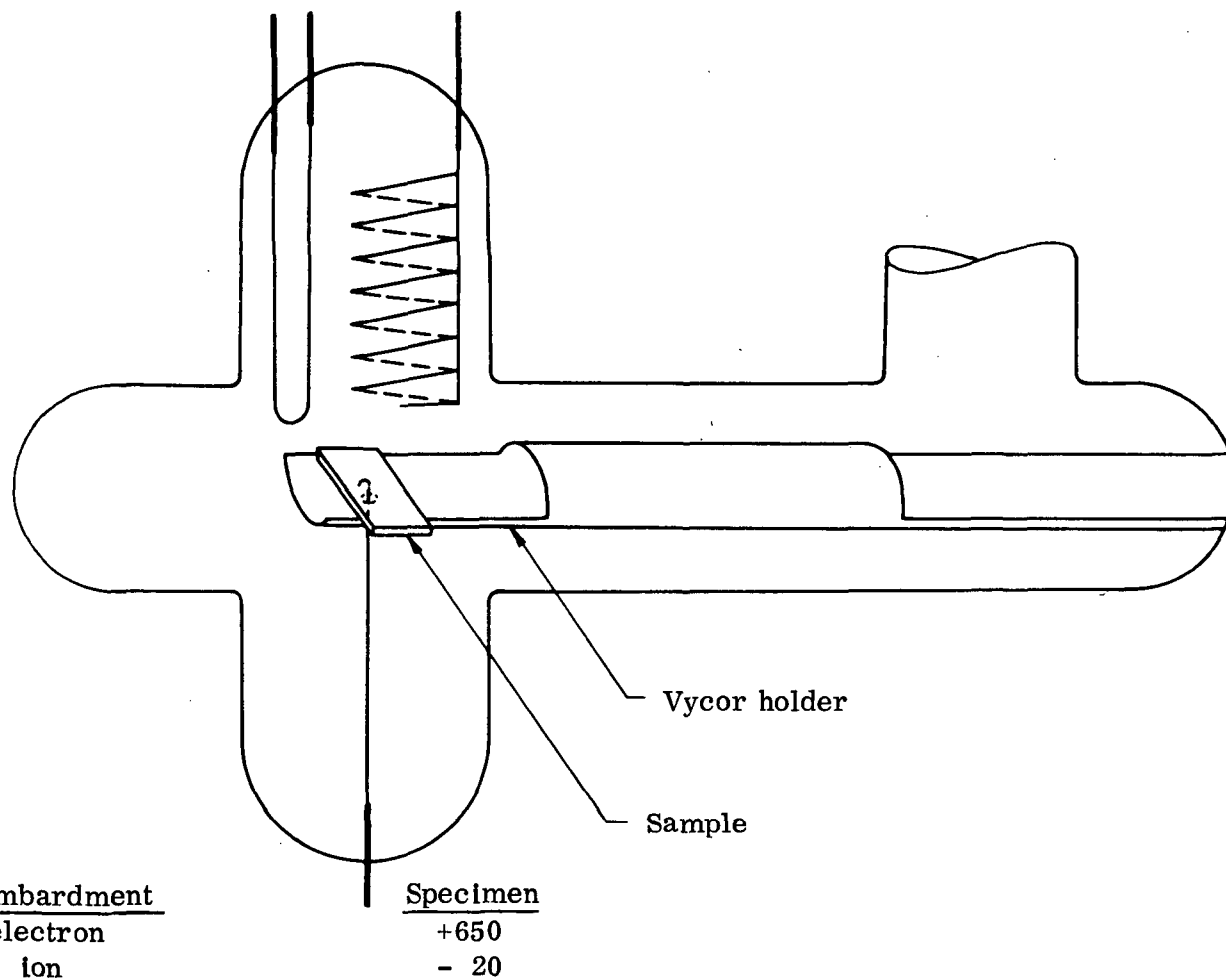


Figure 12: Schematic representation of the electron and ion bombardment cell IBC. The sample rests on a tungsten lead connected via a feedthrough to the potentials required for electron and ion bombardment. The specimen is placed in and removed from the bombarding position by an external magnet.

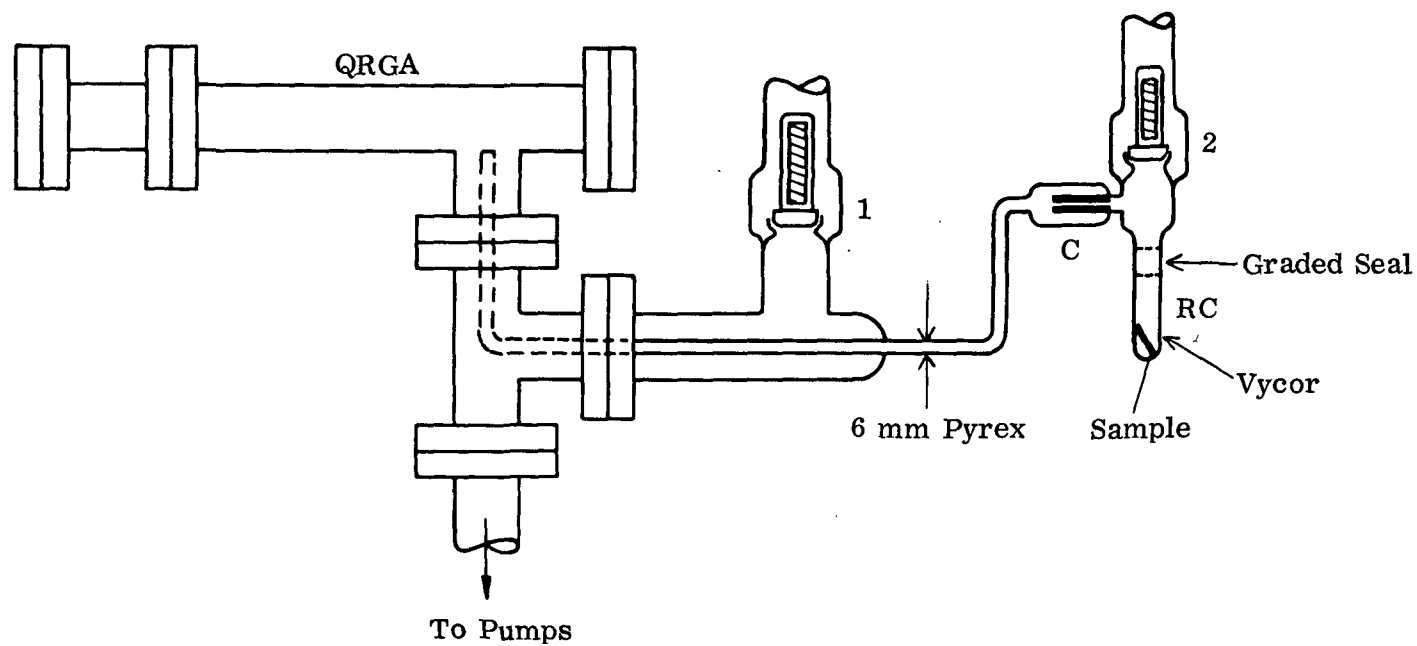
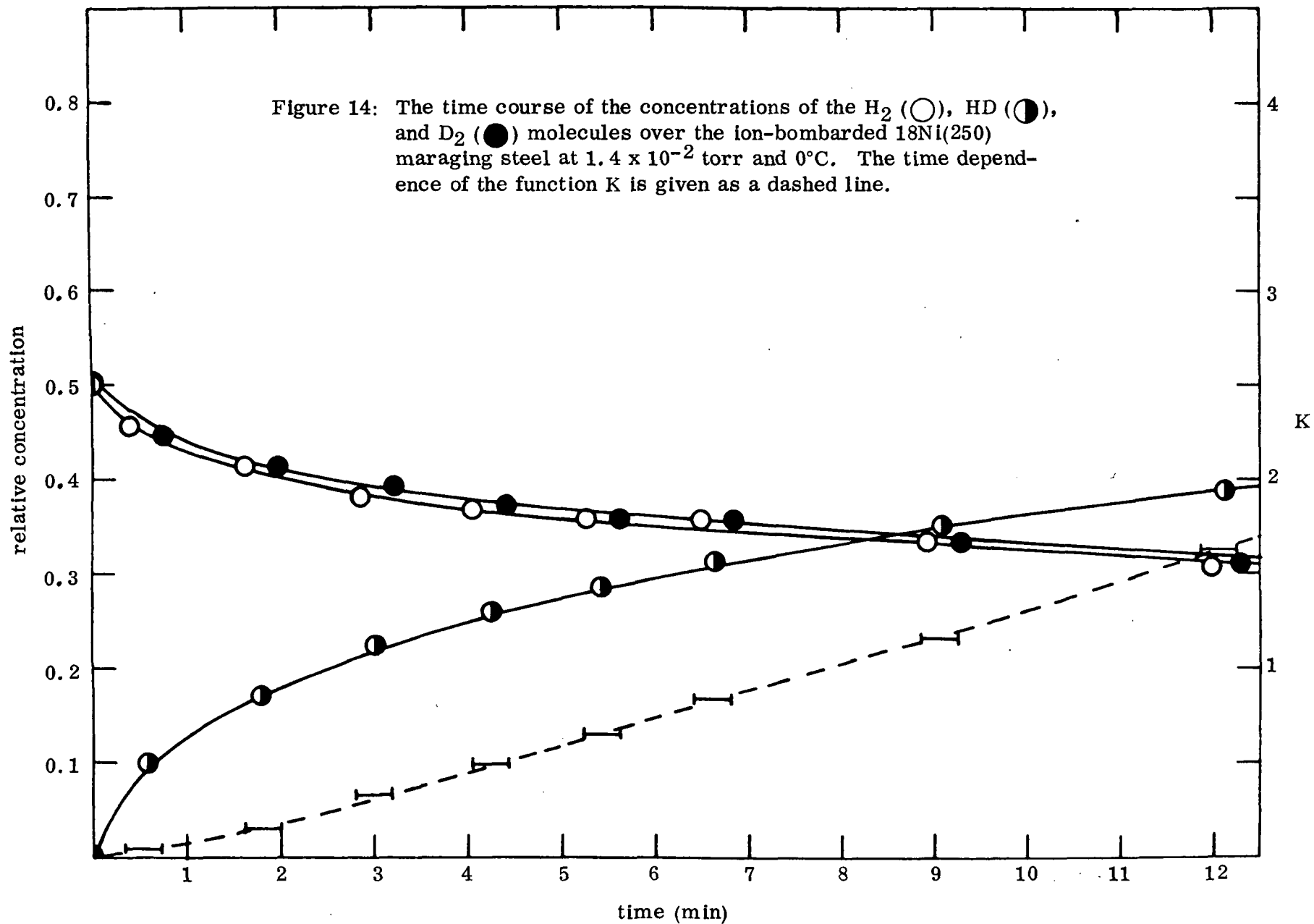
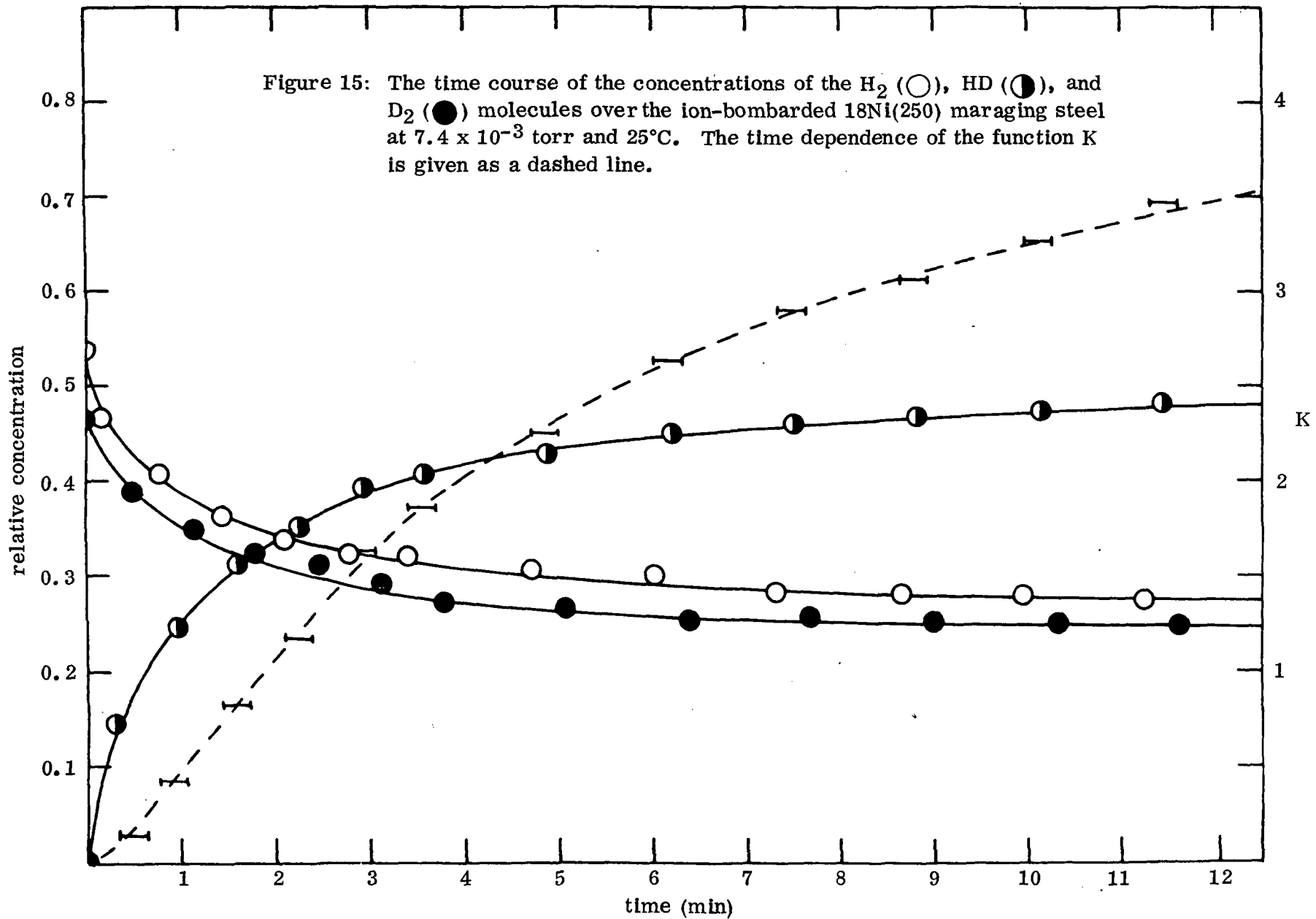
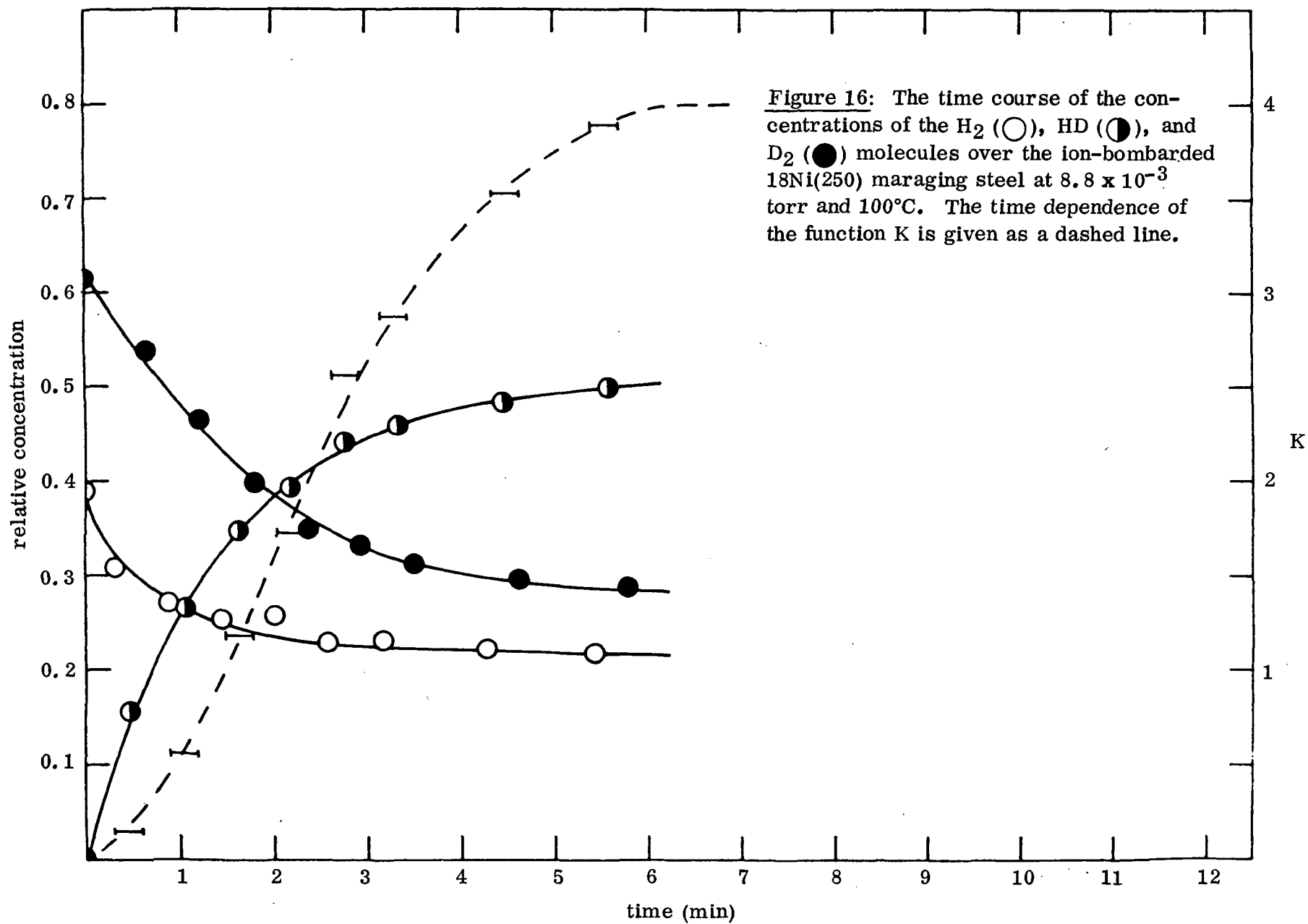
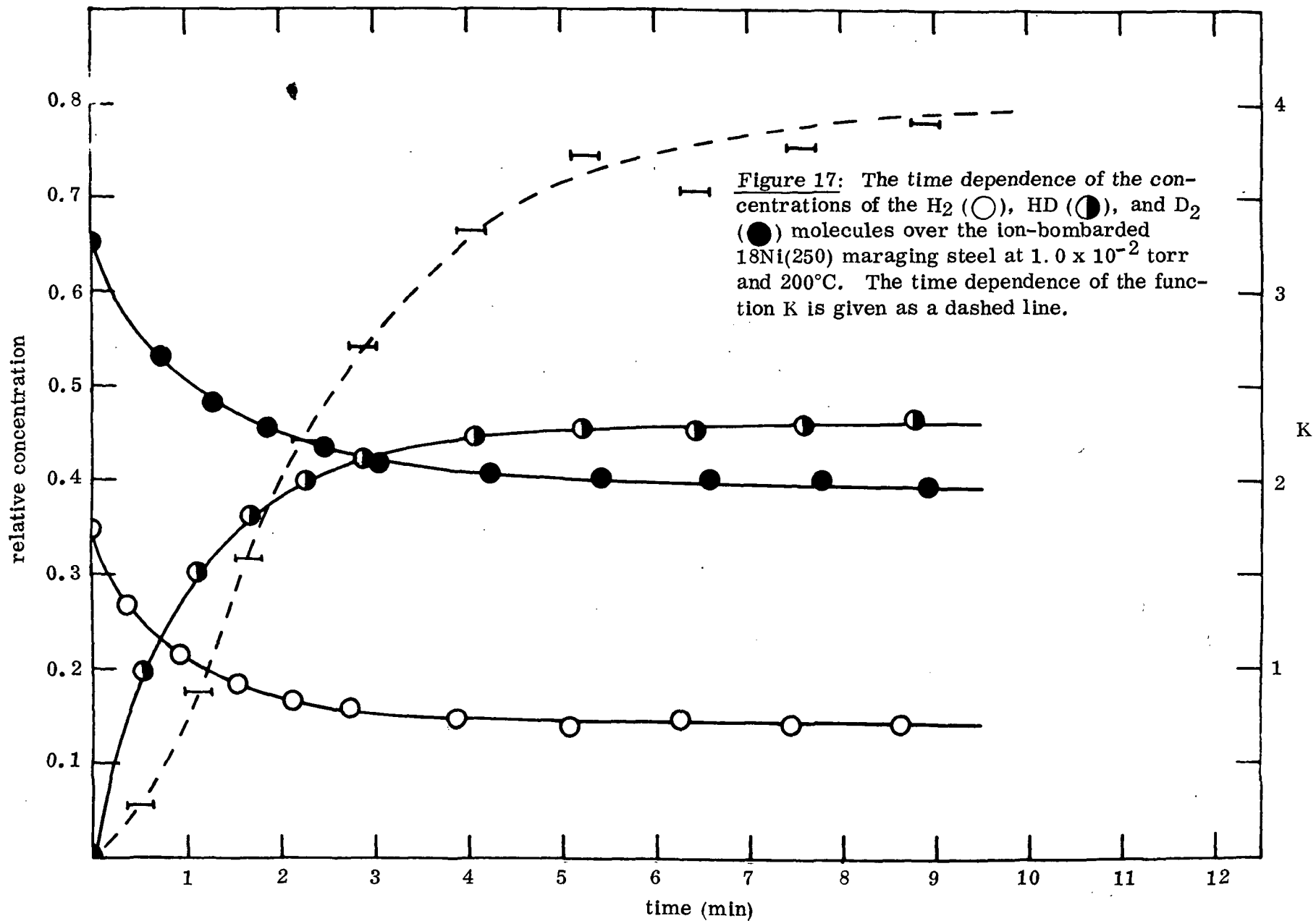


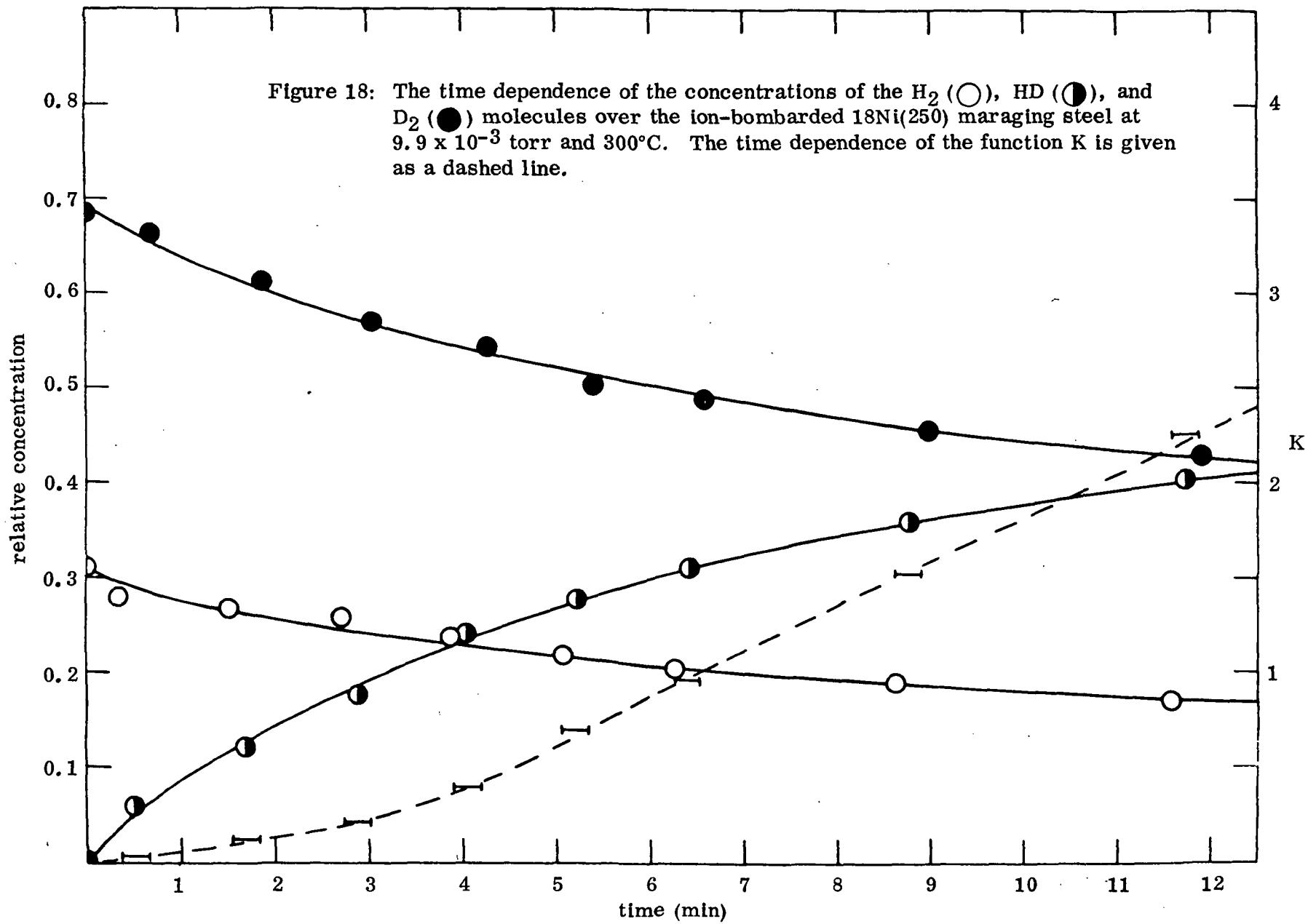
Figure 13: Arrangement between the reaction cell and the quadrupole. The calibrated conductance is a 0.002 inch capillary mounted on a Pyrex envelope. The reaction products reach the ionization chamber of the quadrupole via a 6 mm o.d. Pyrex tubing.

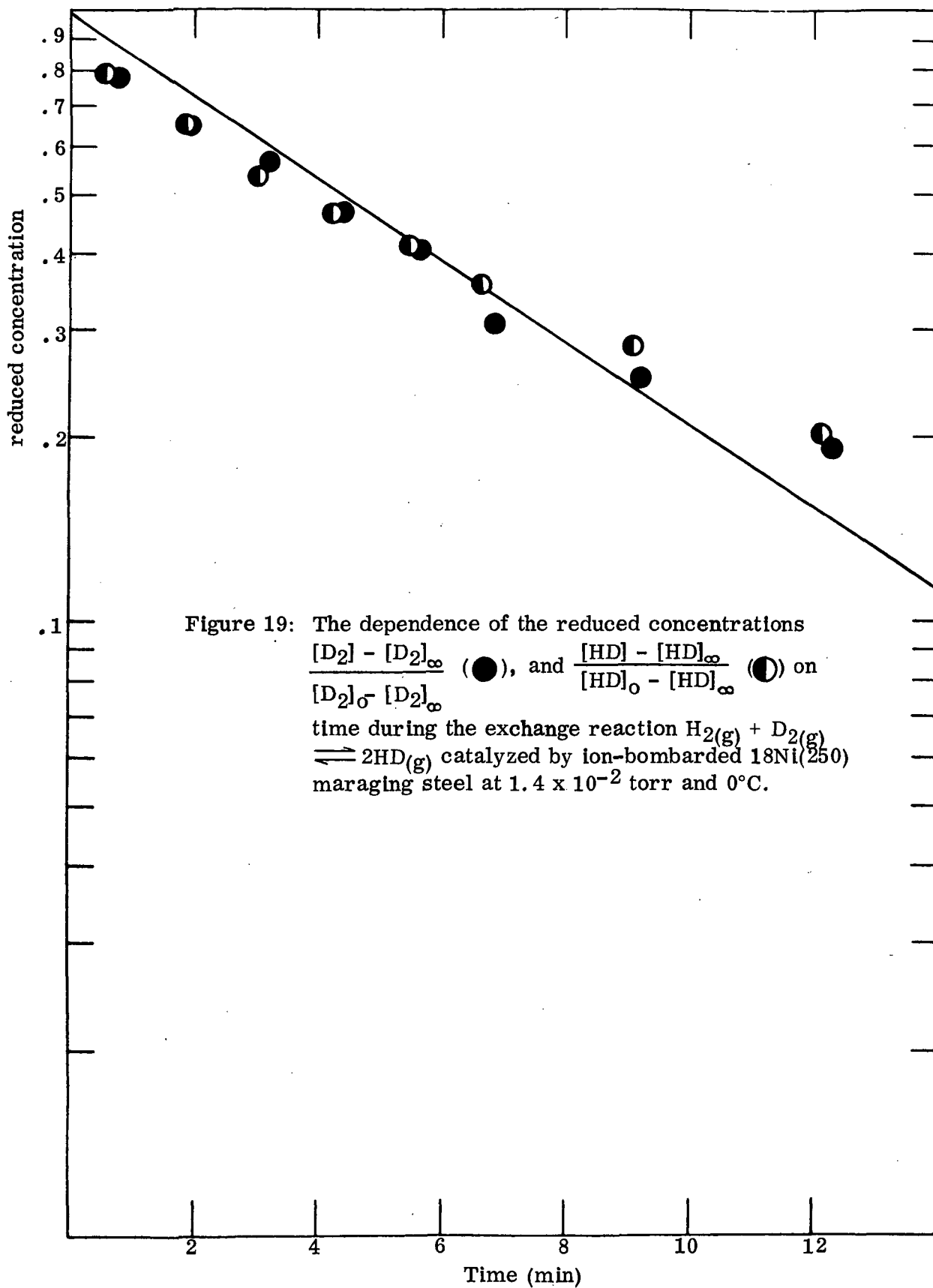


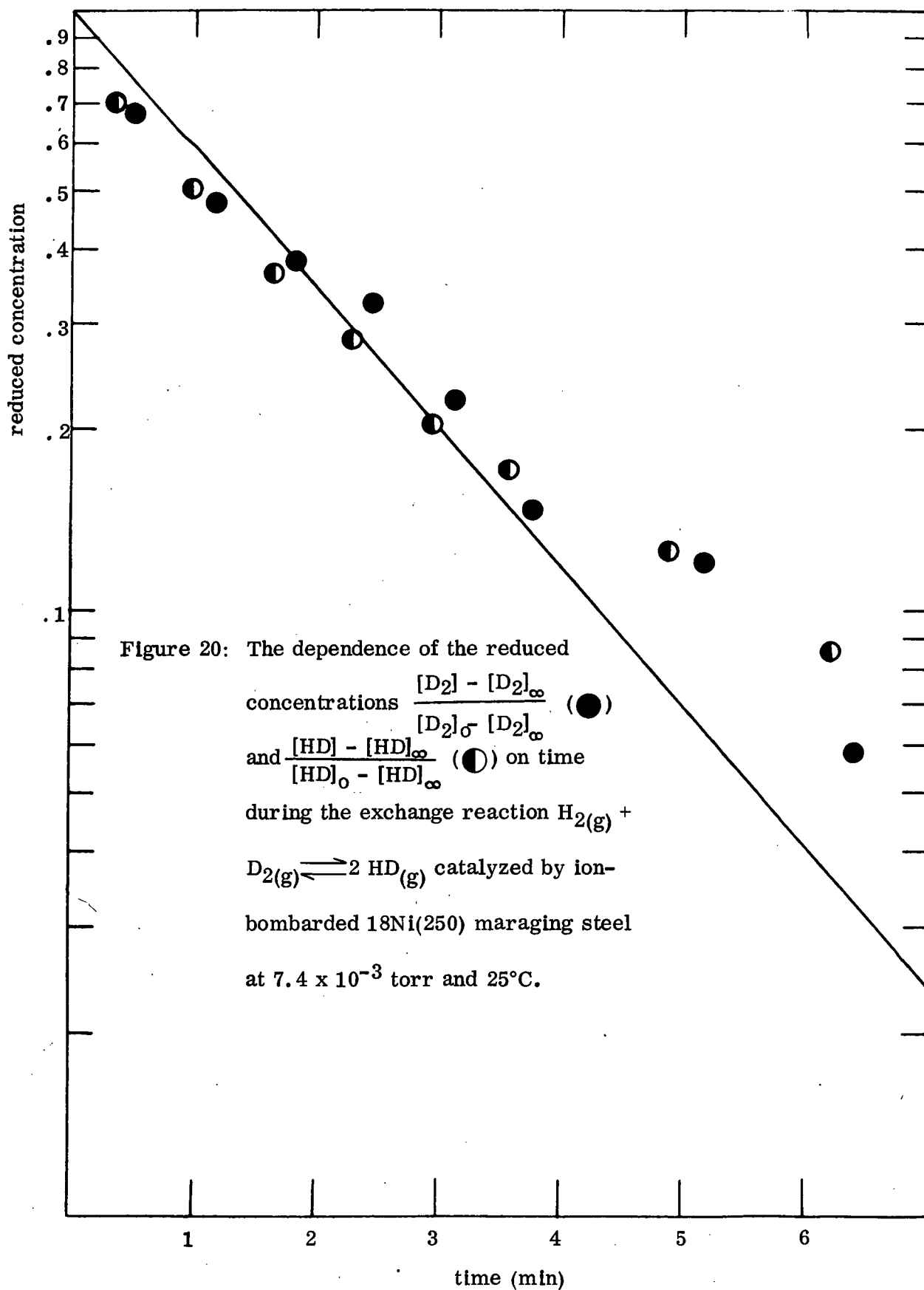


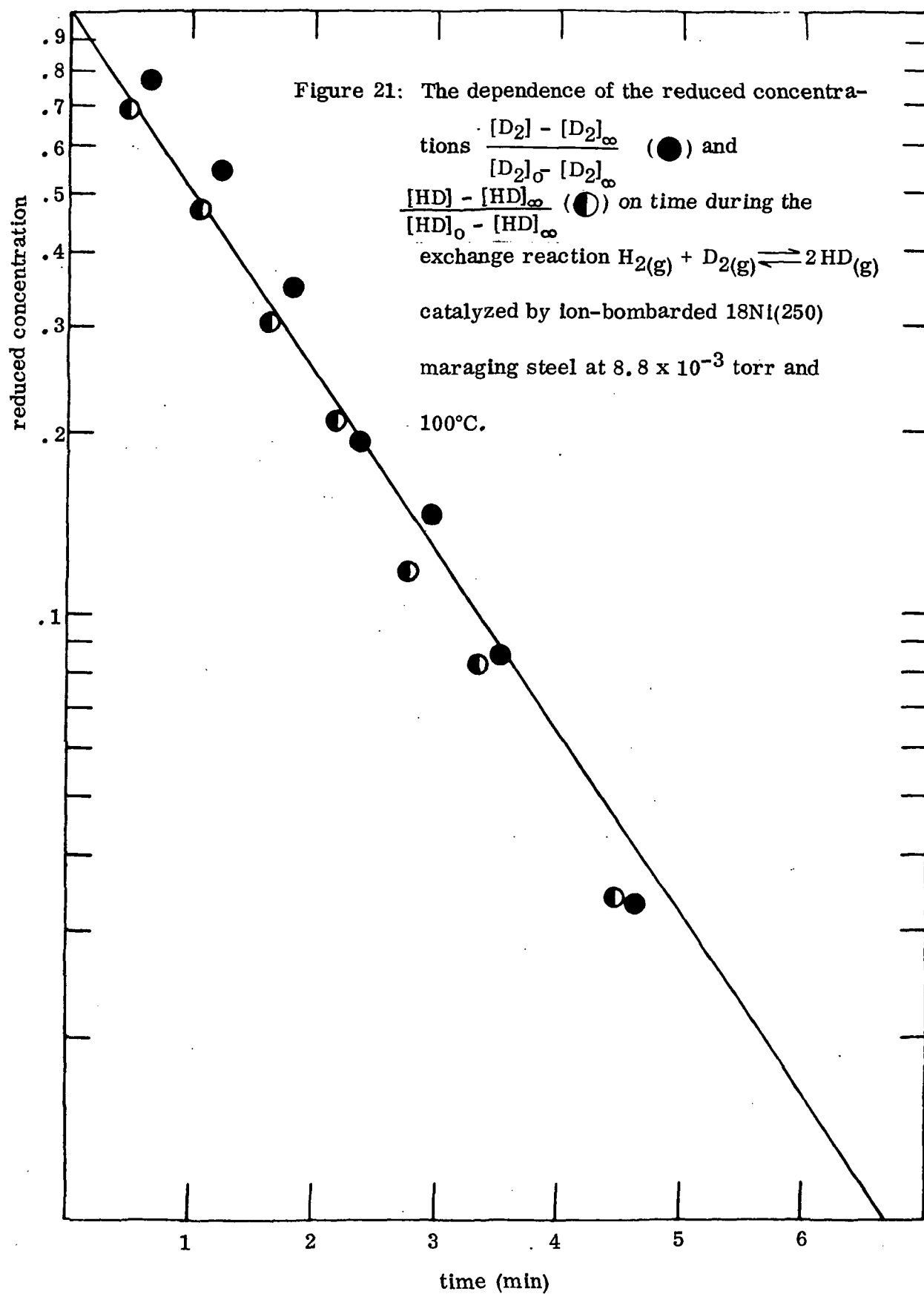


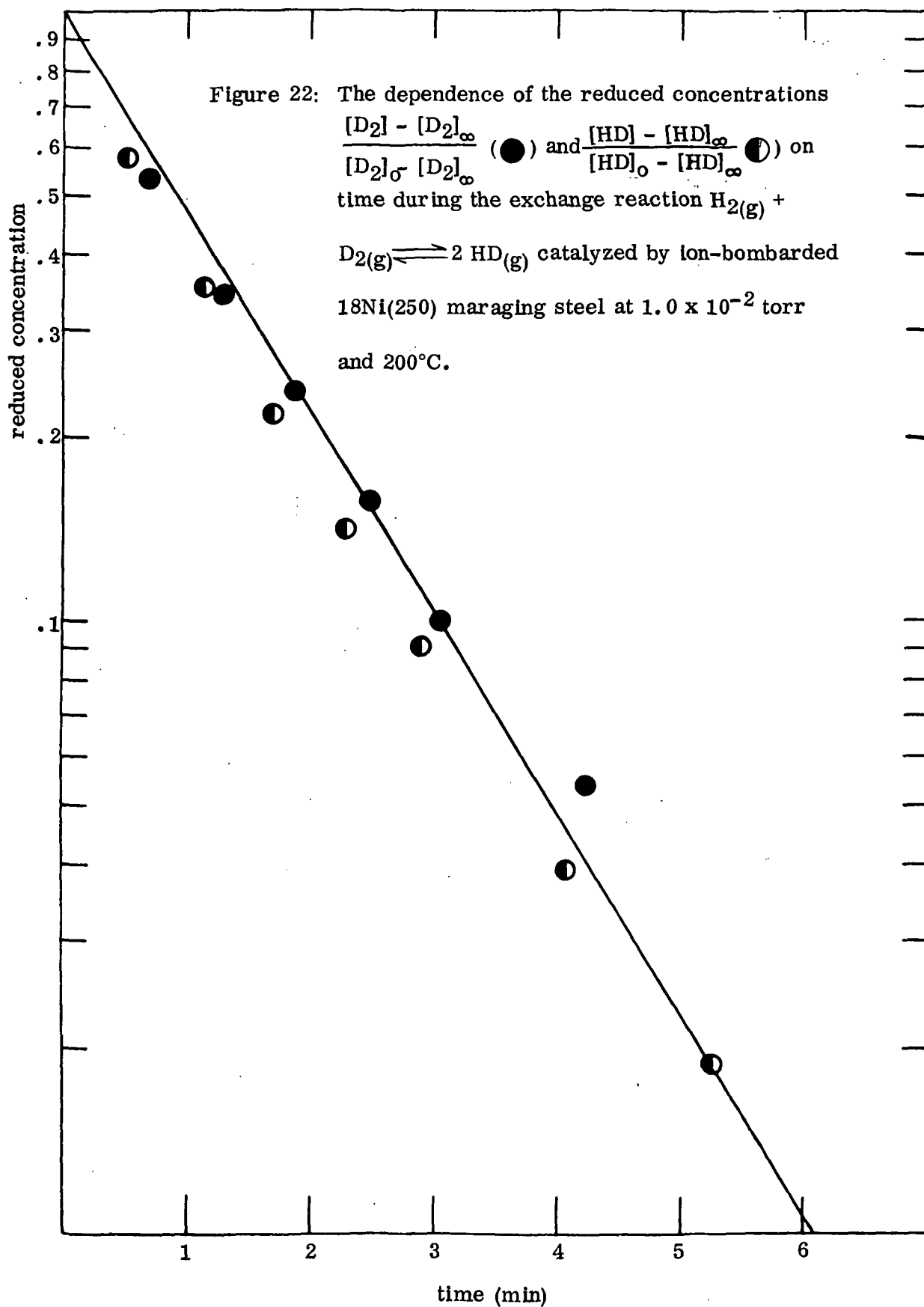


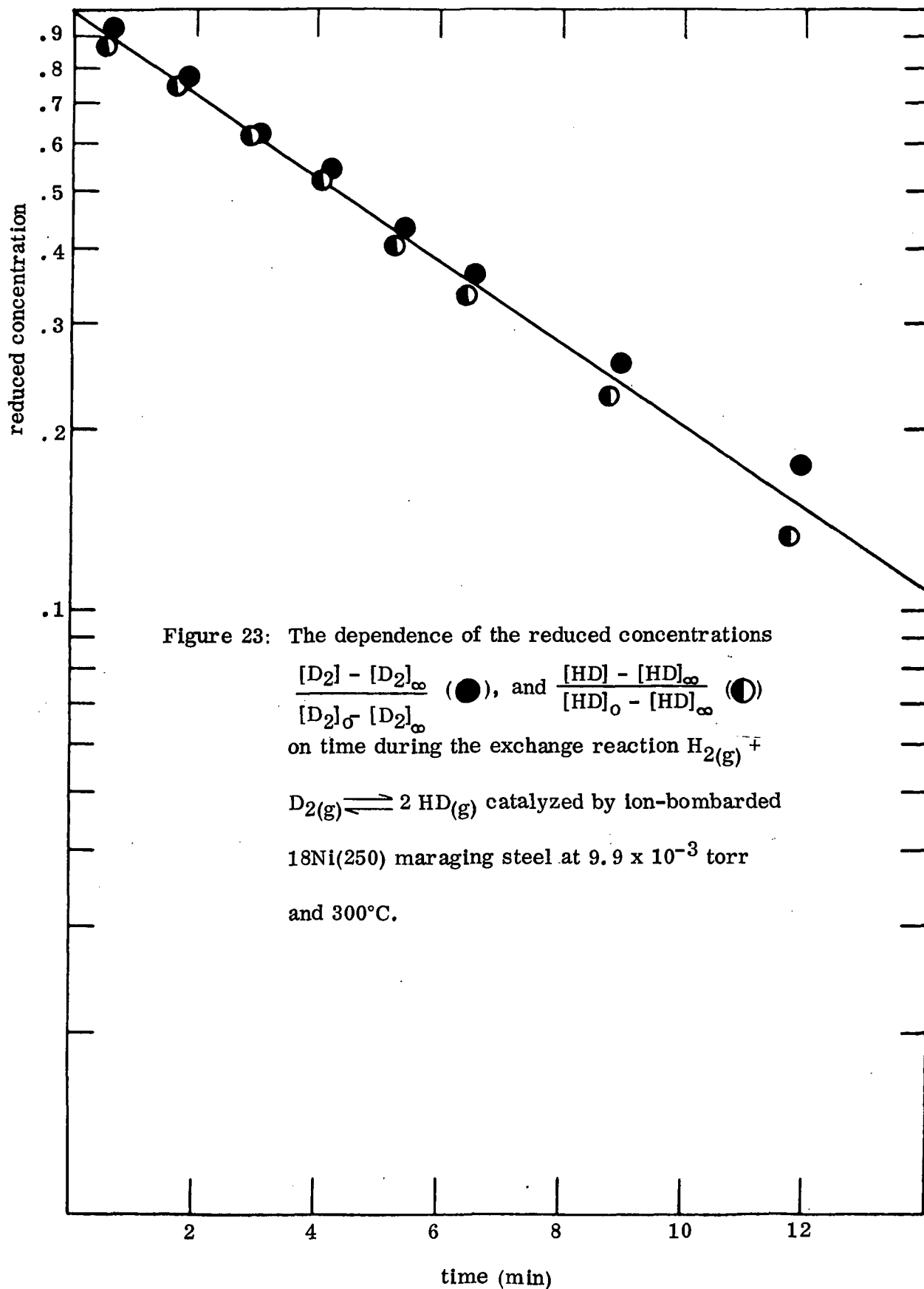


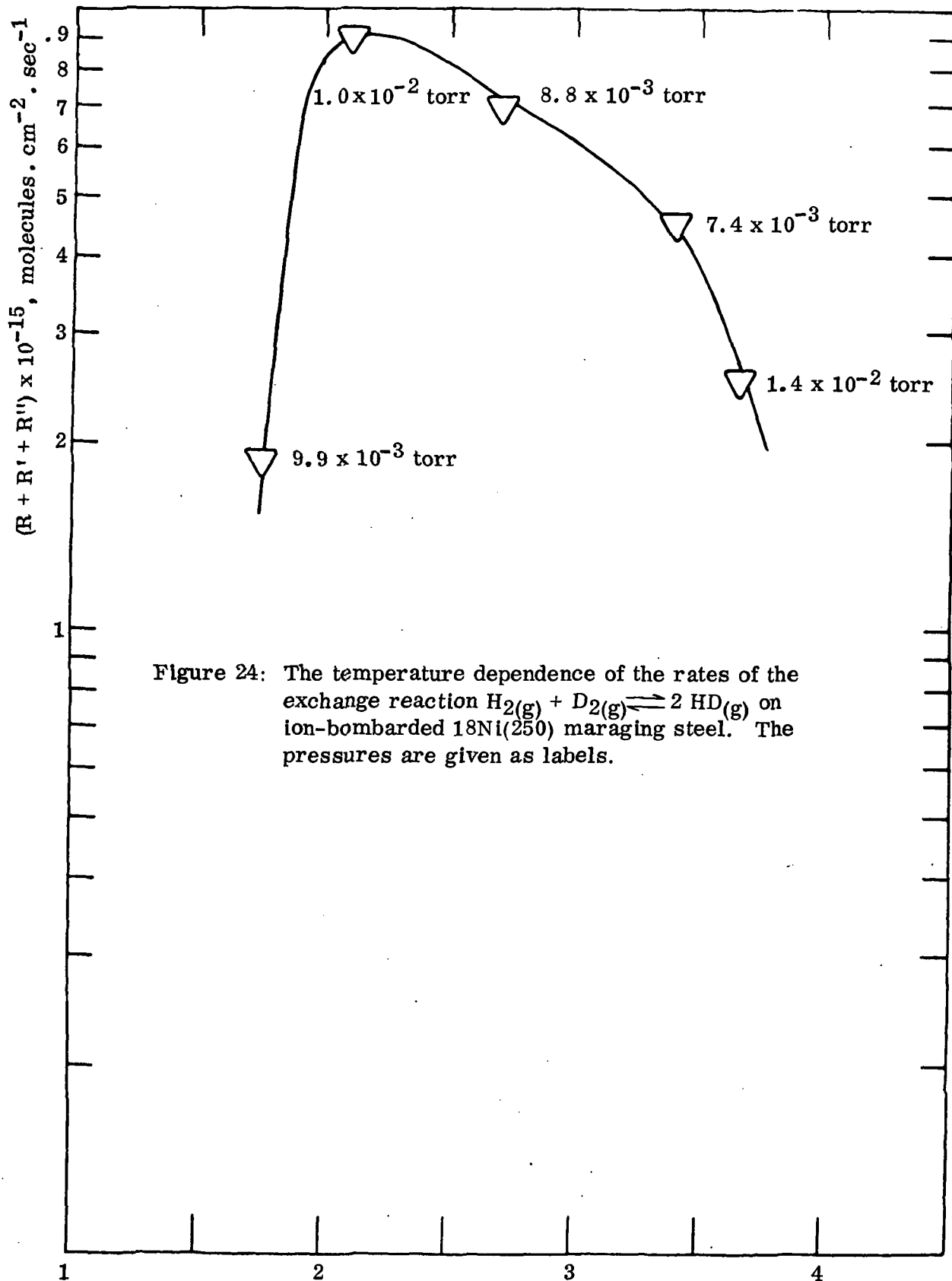


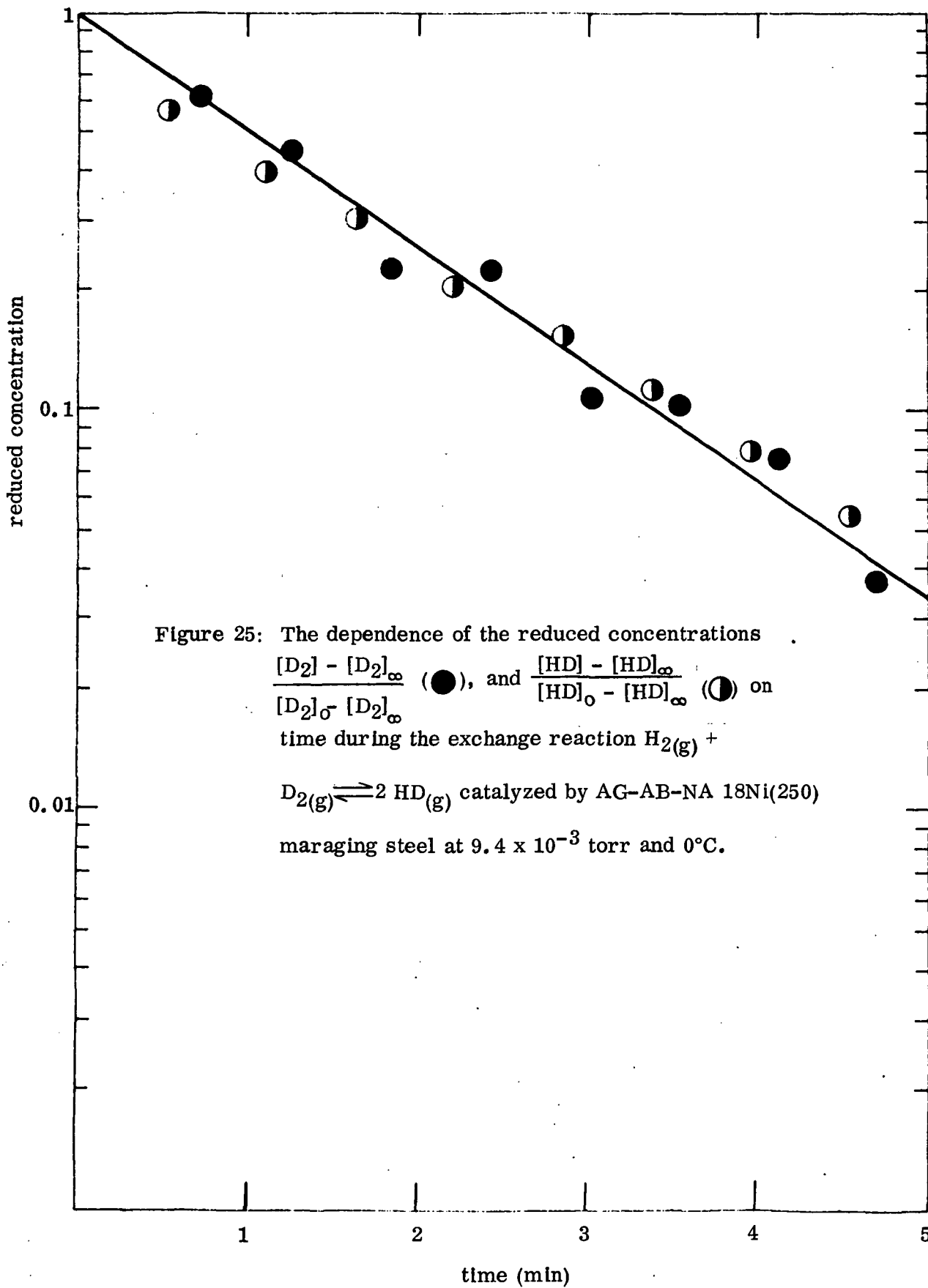


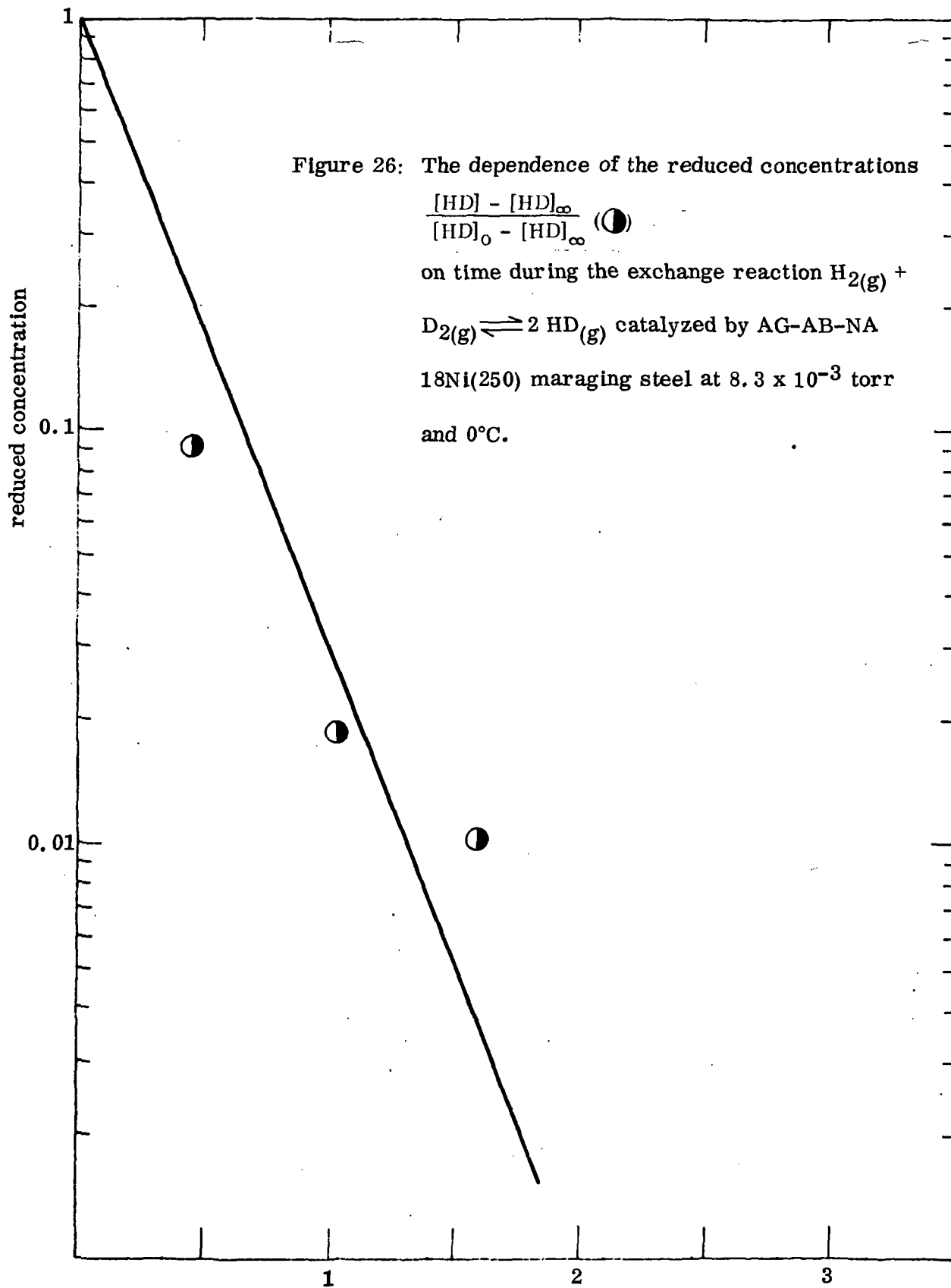


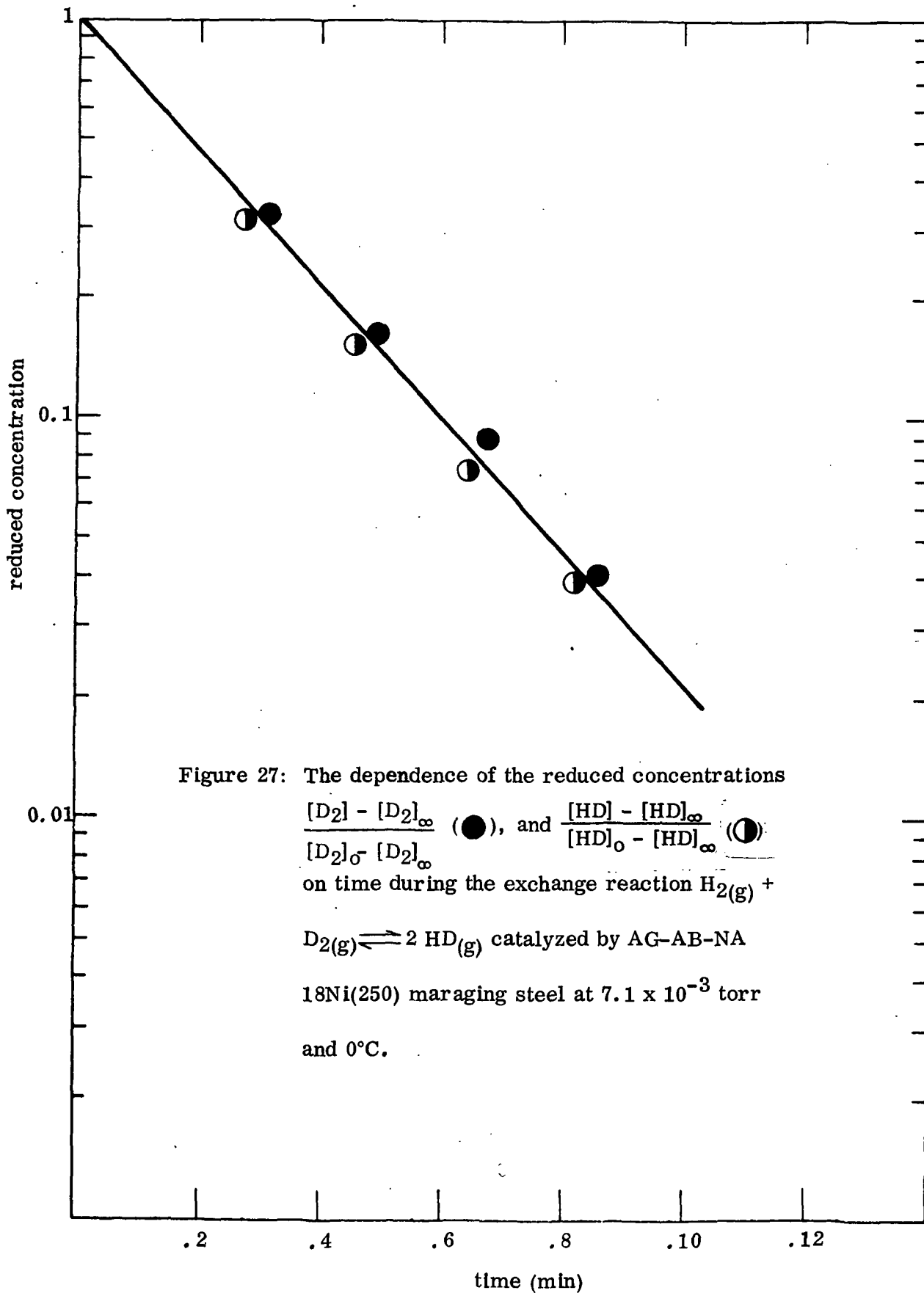


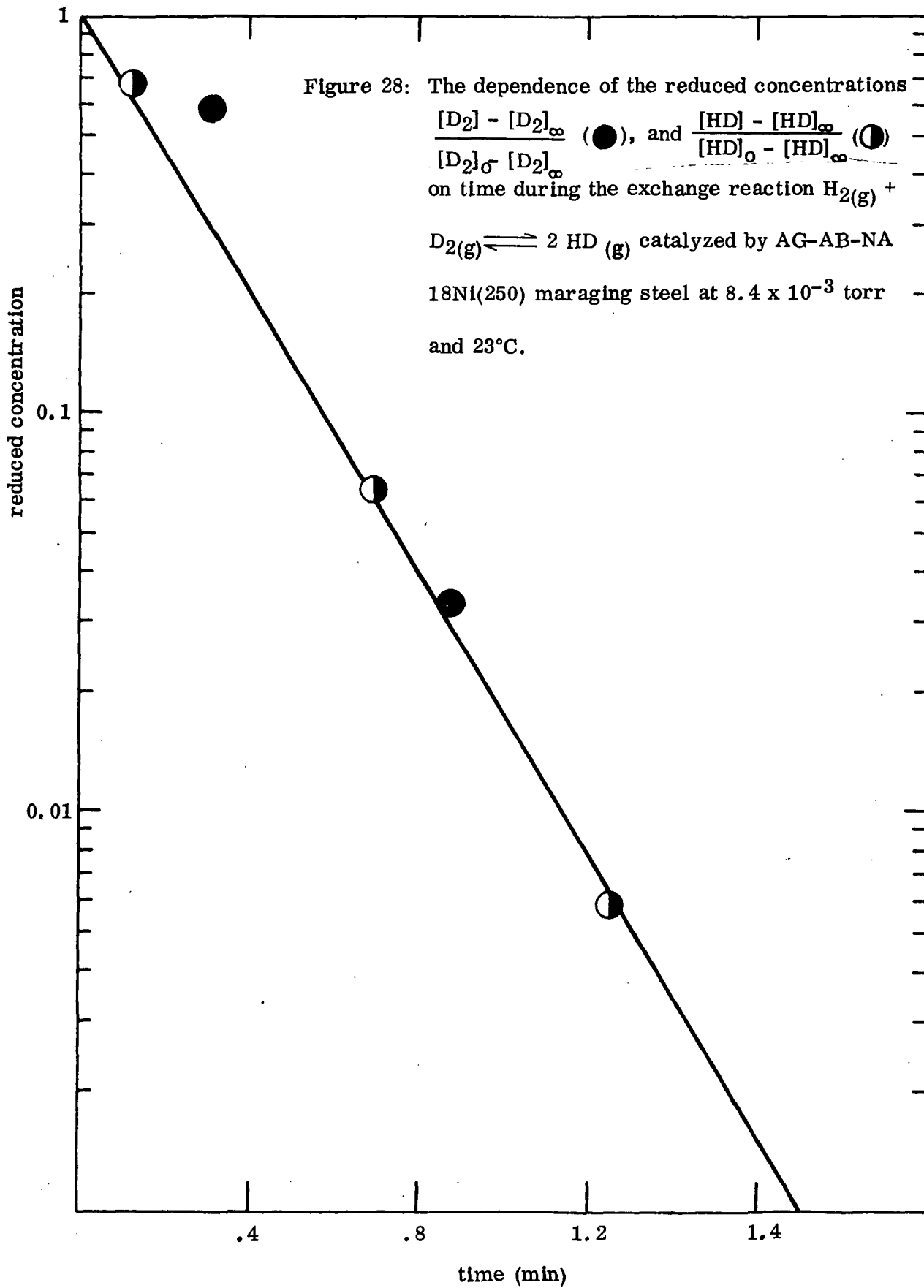


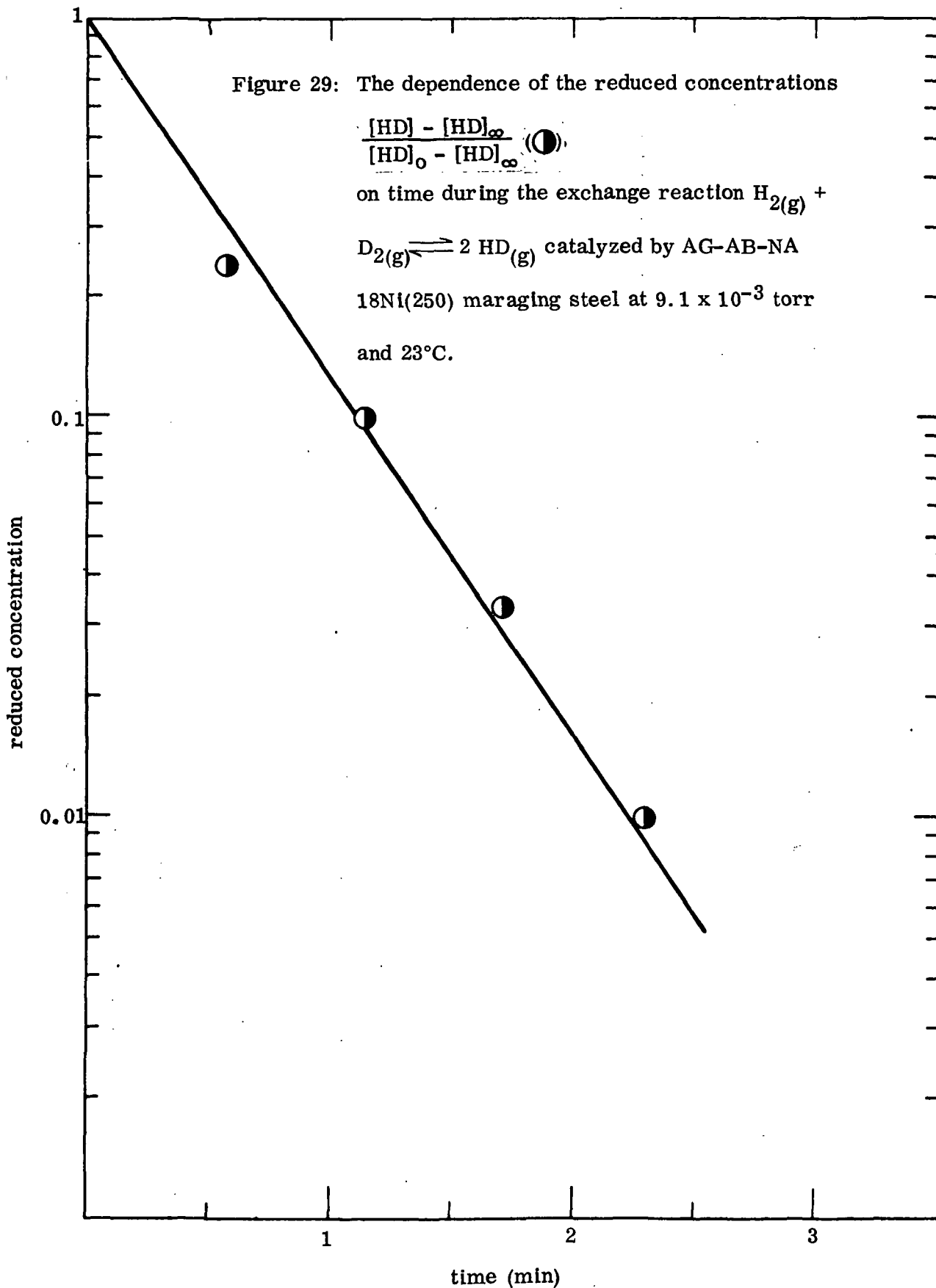


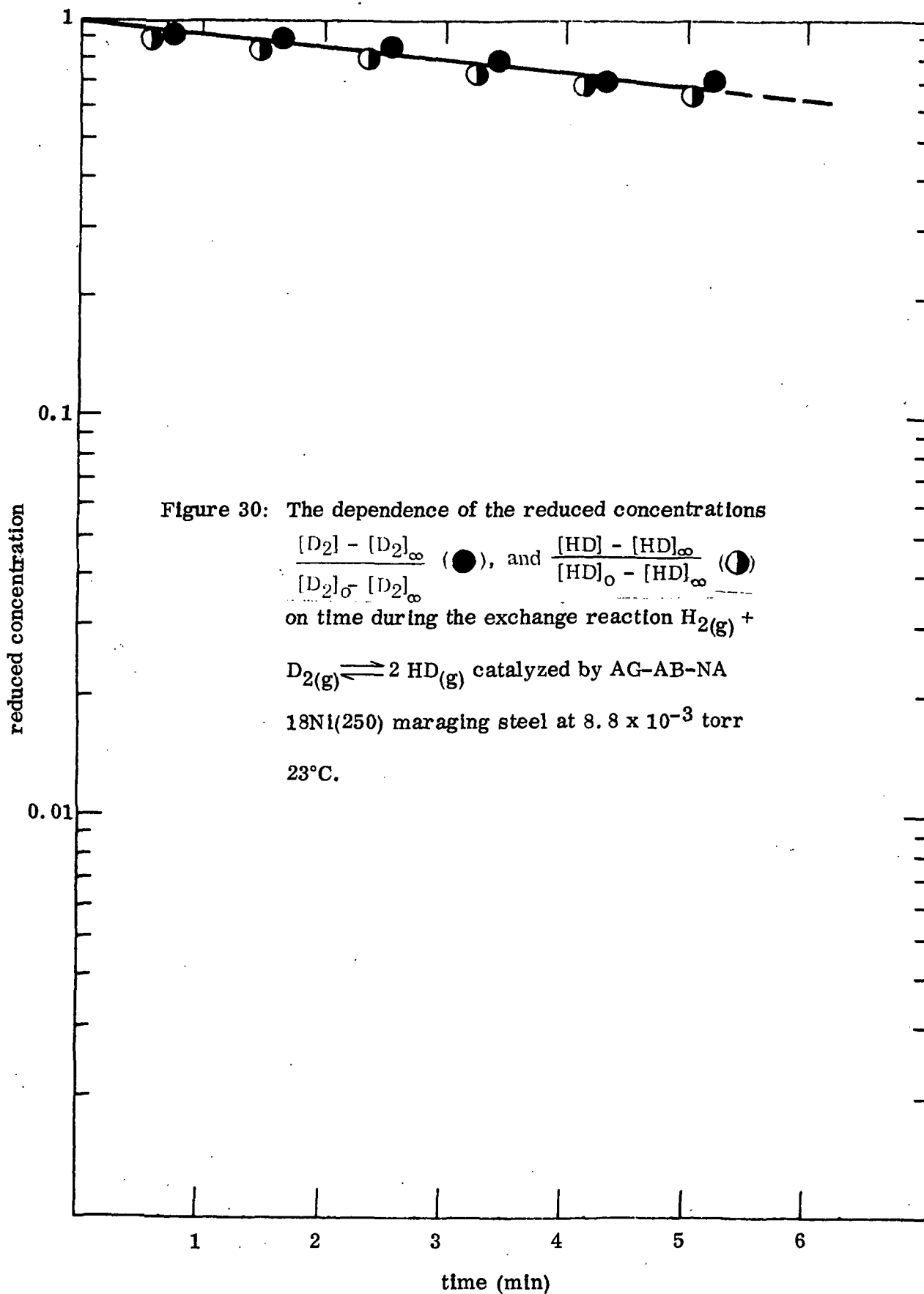


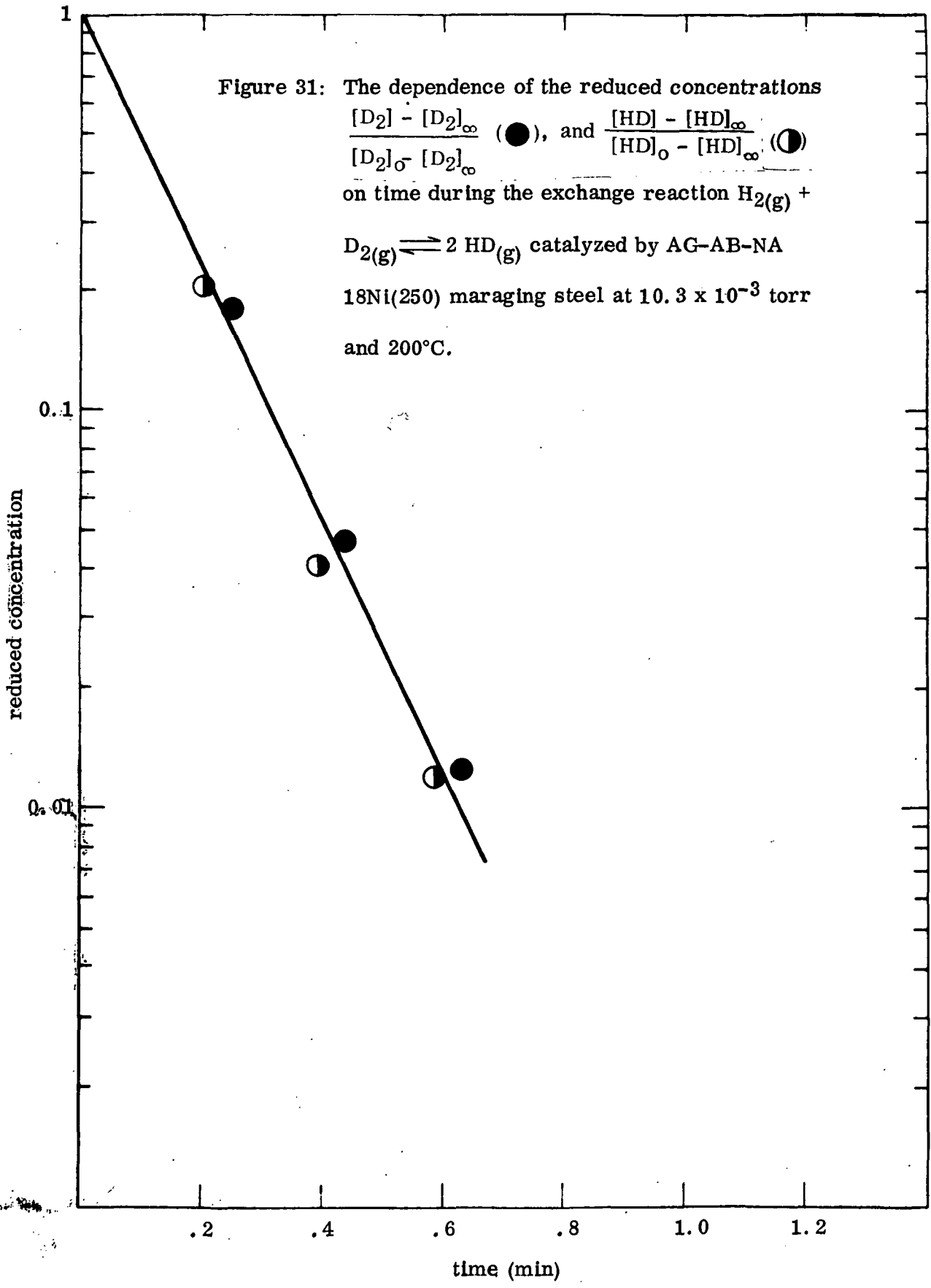


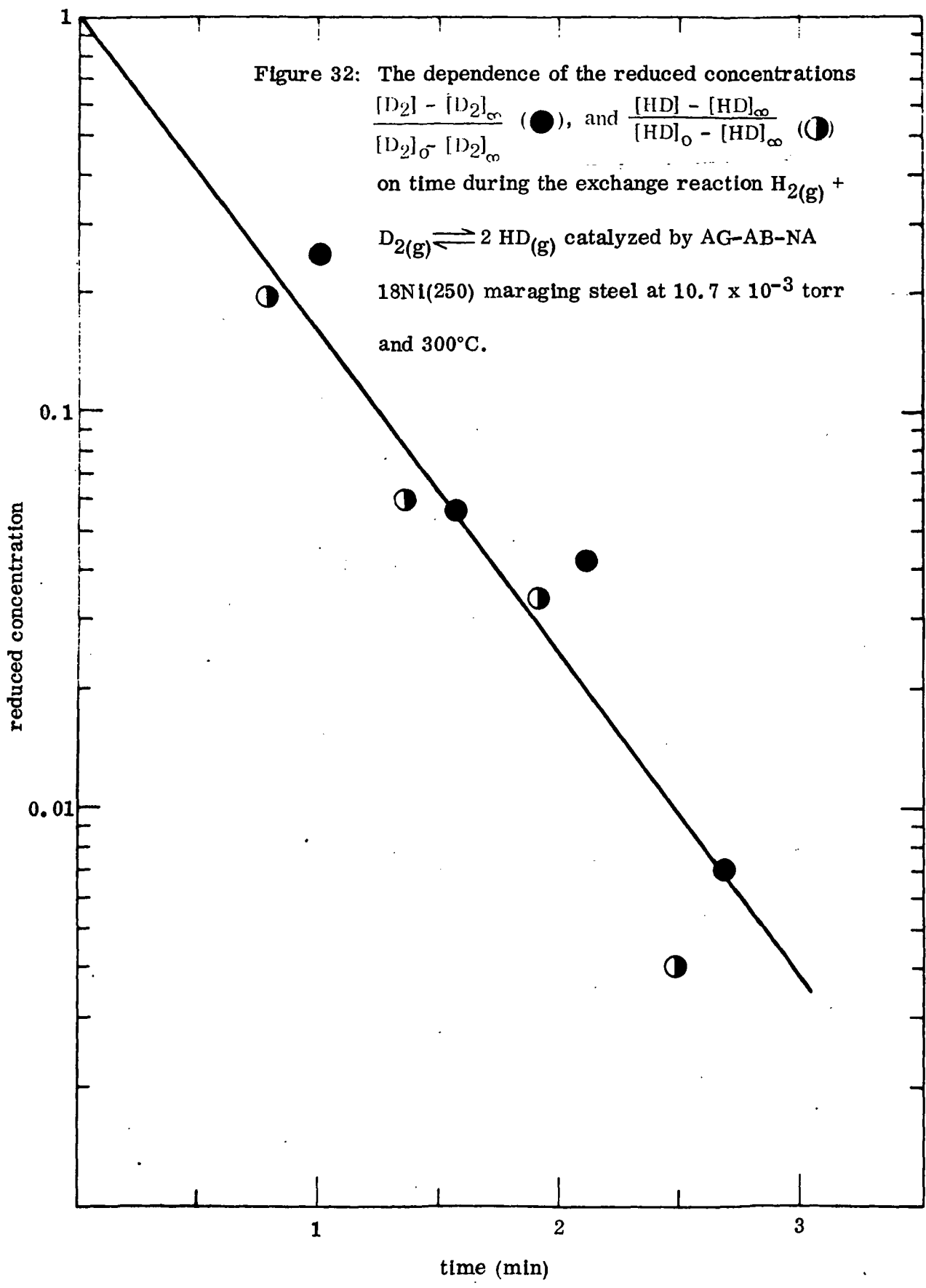


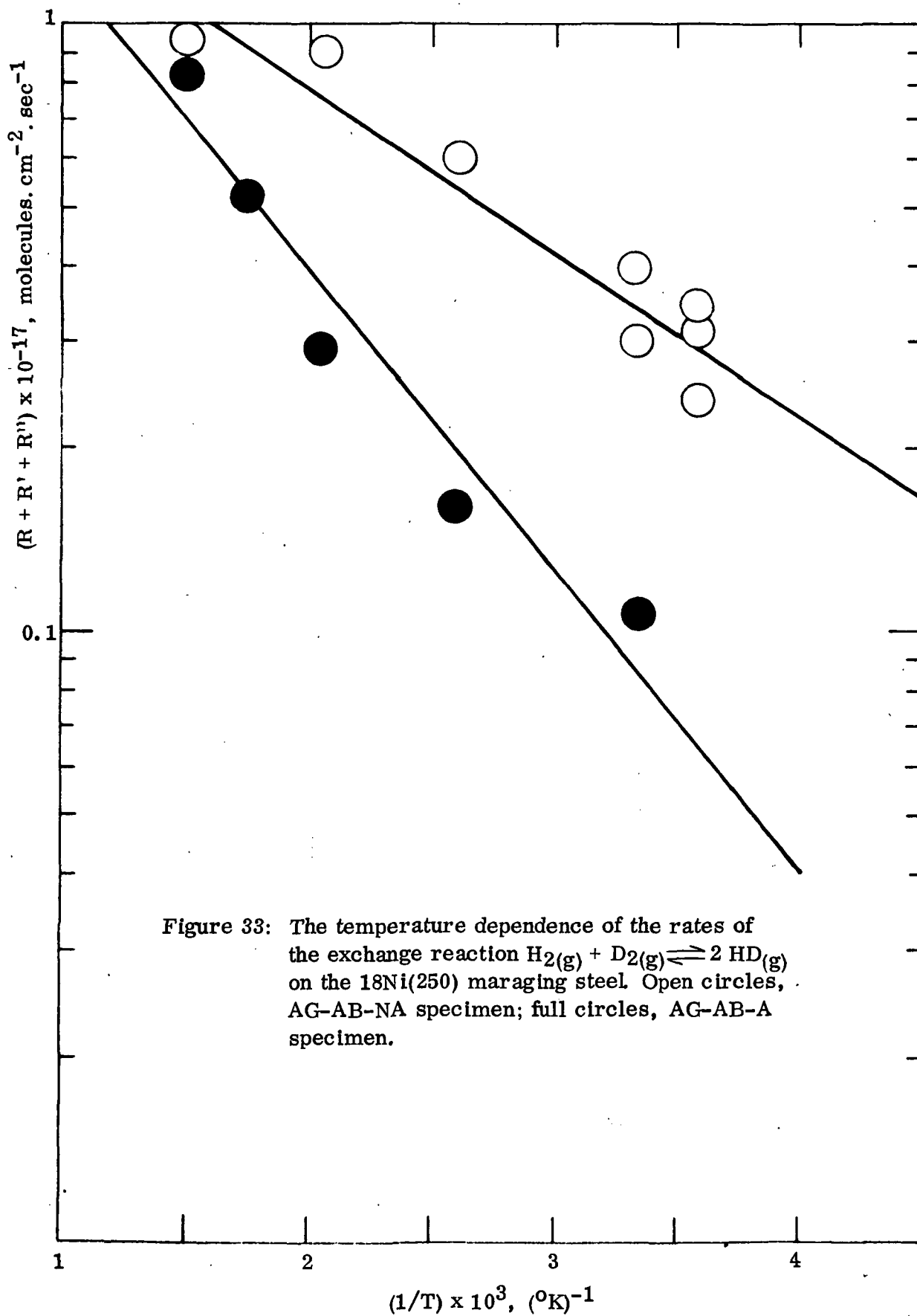


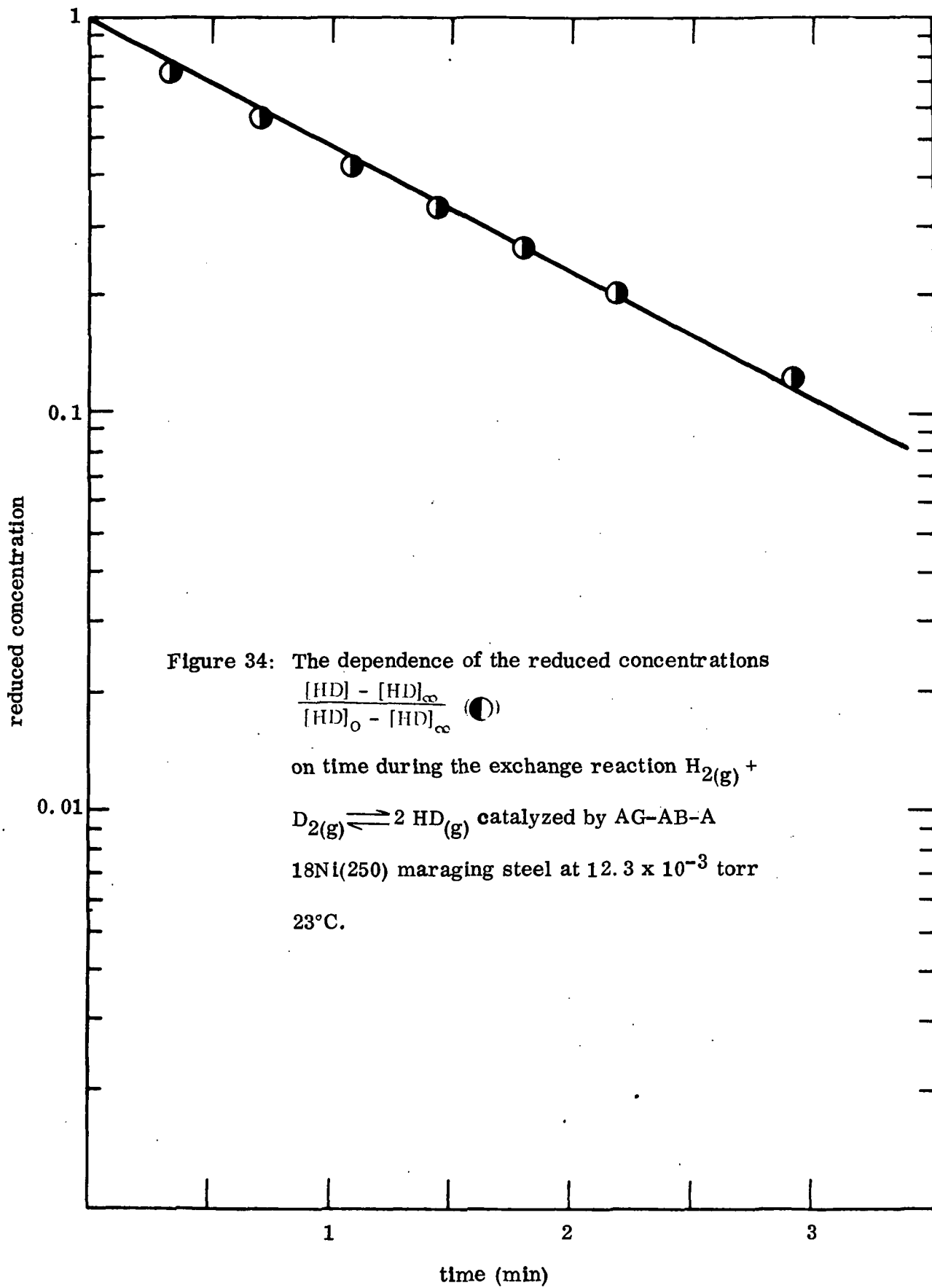


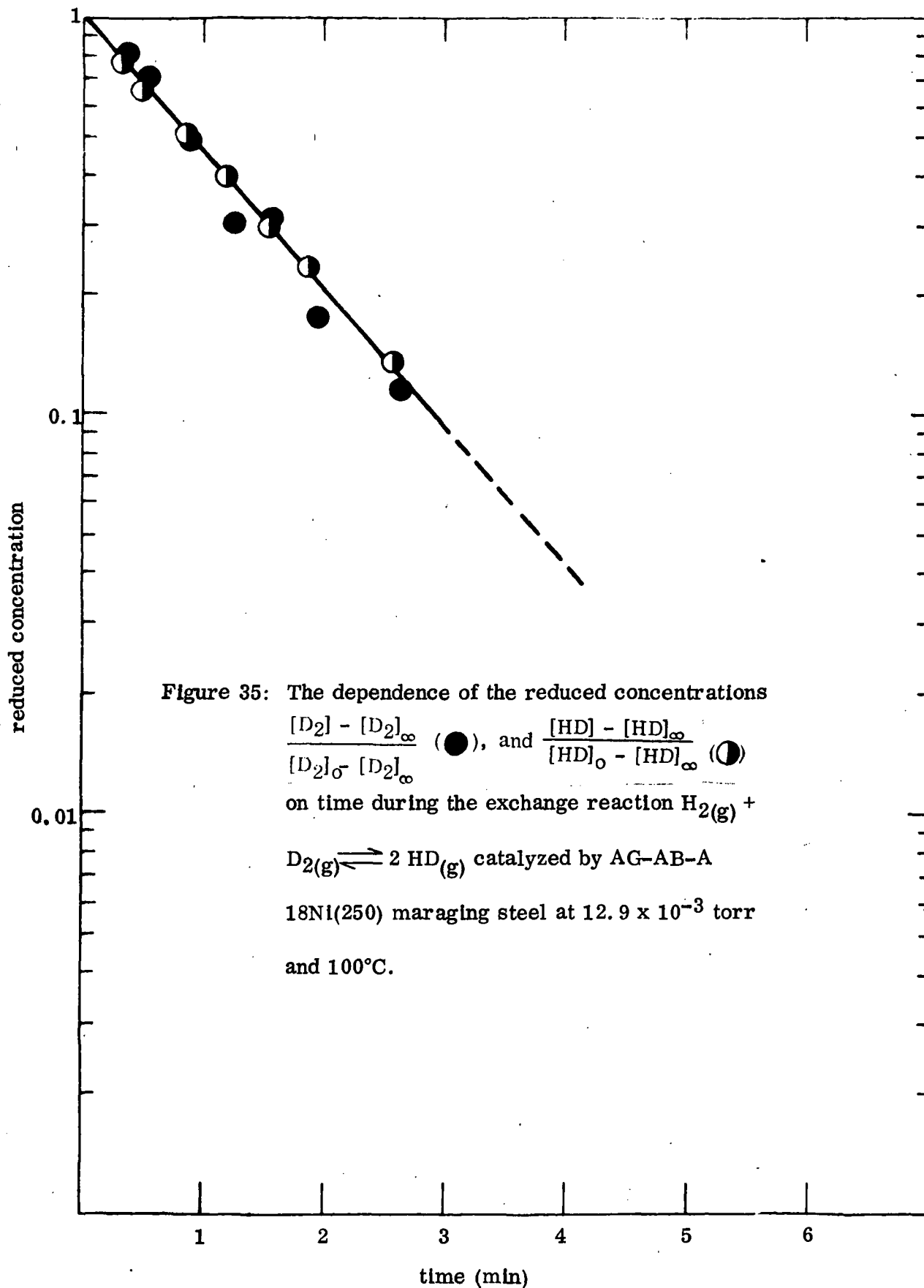


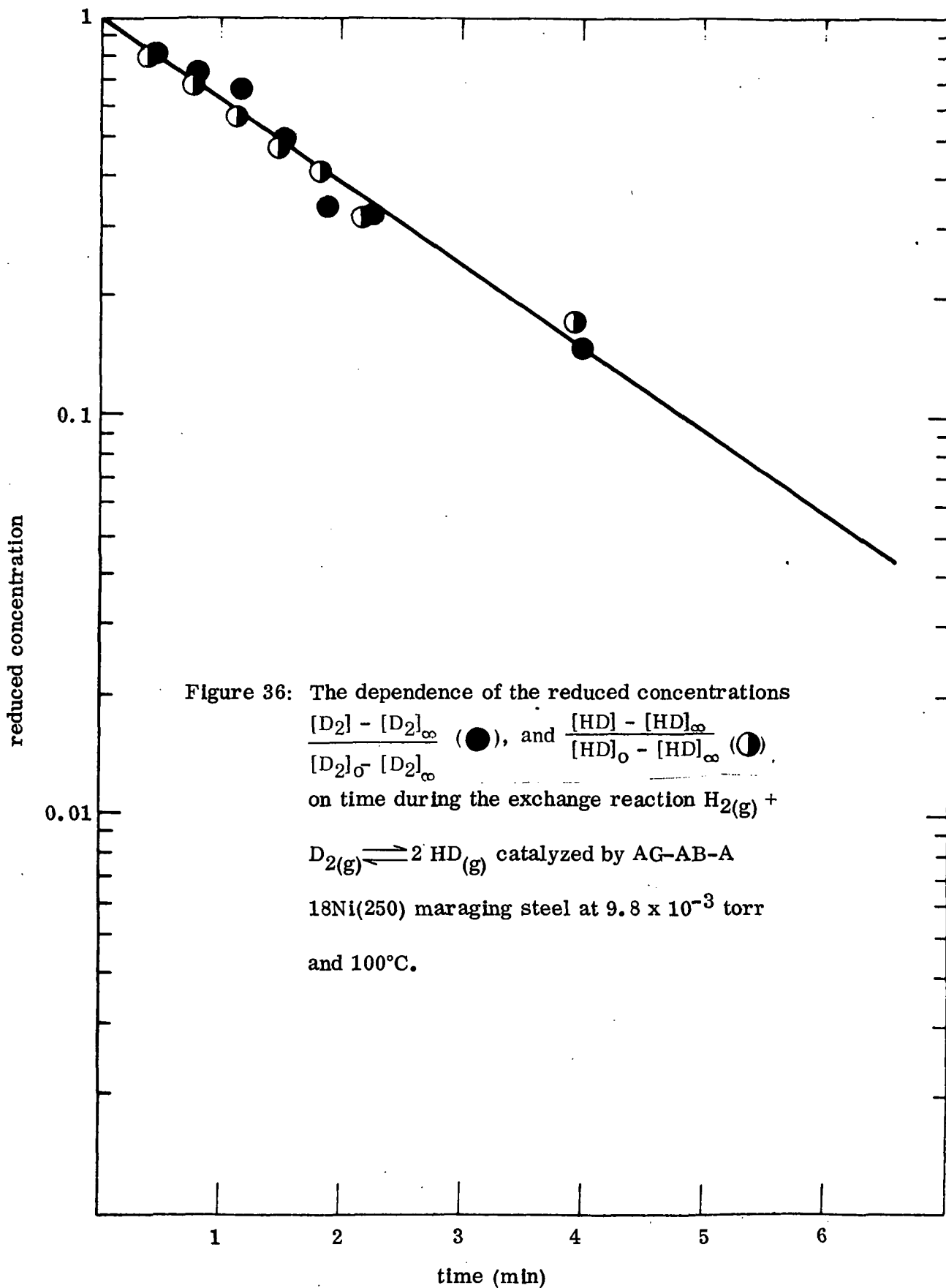


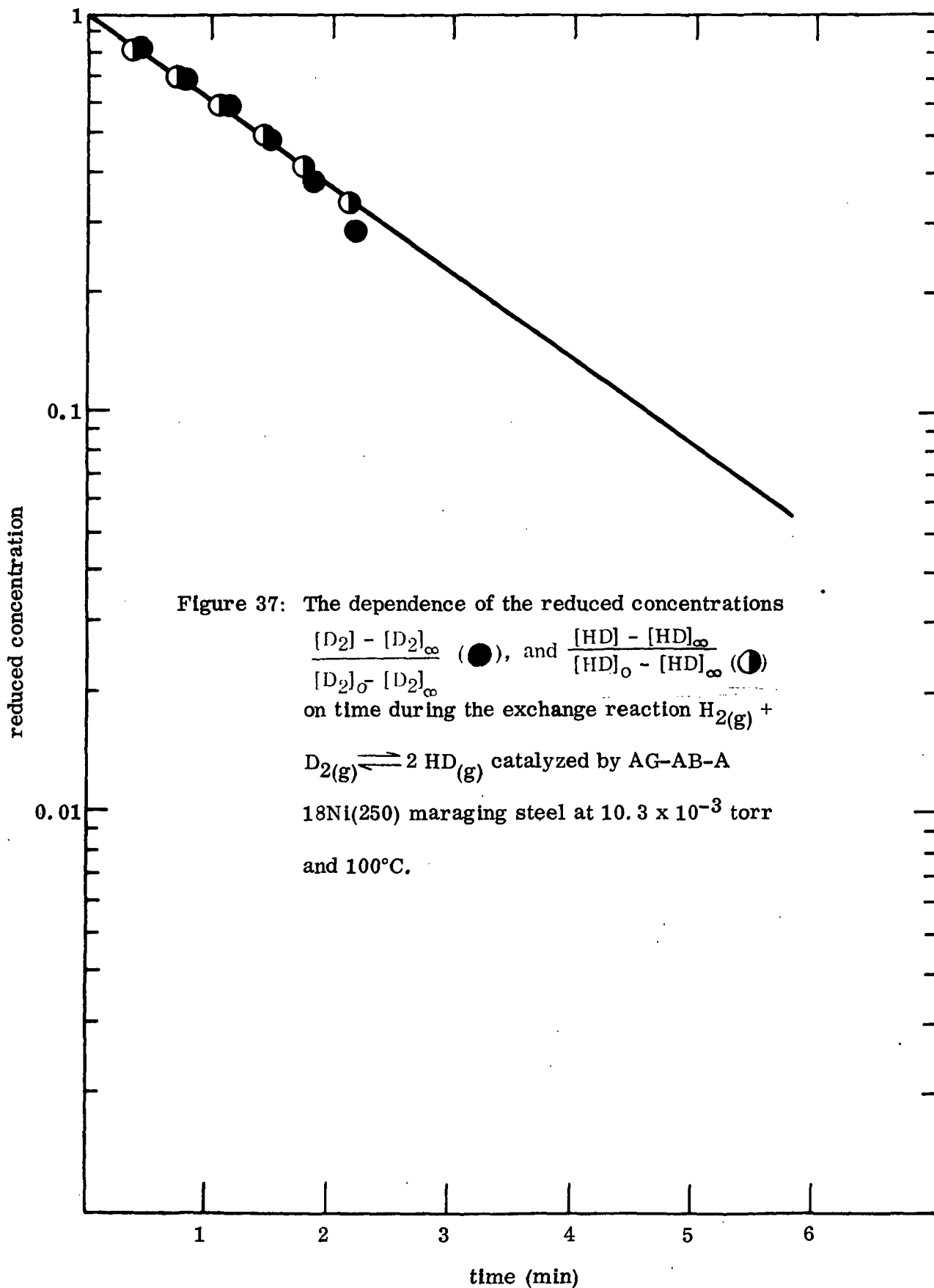


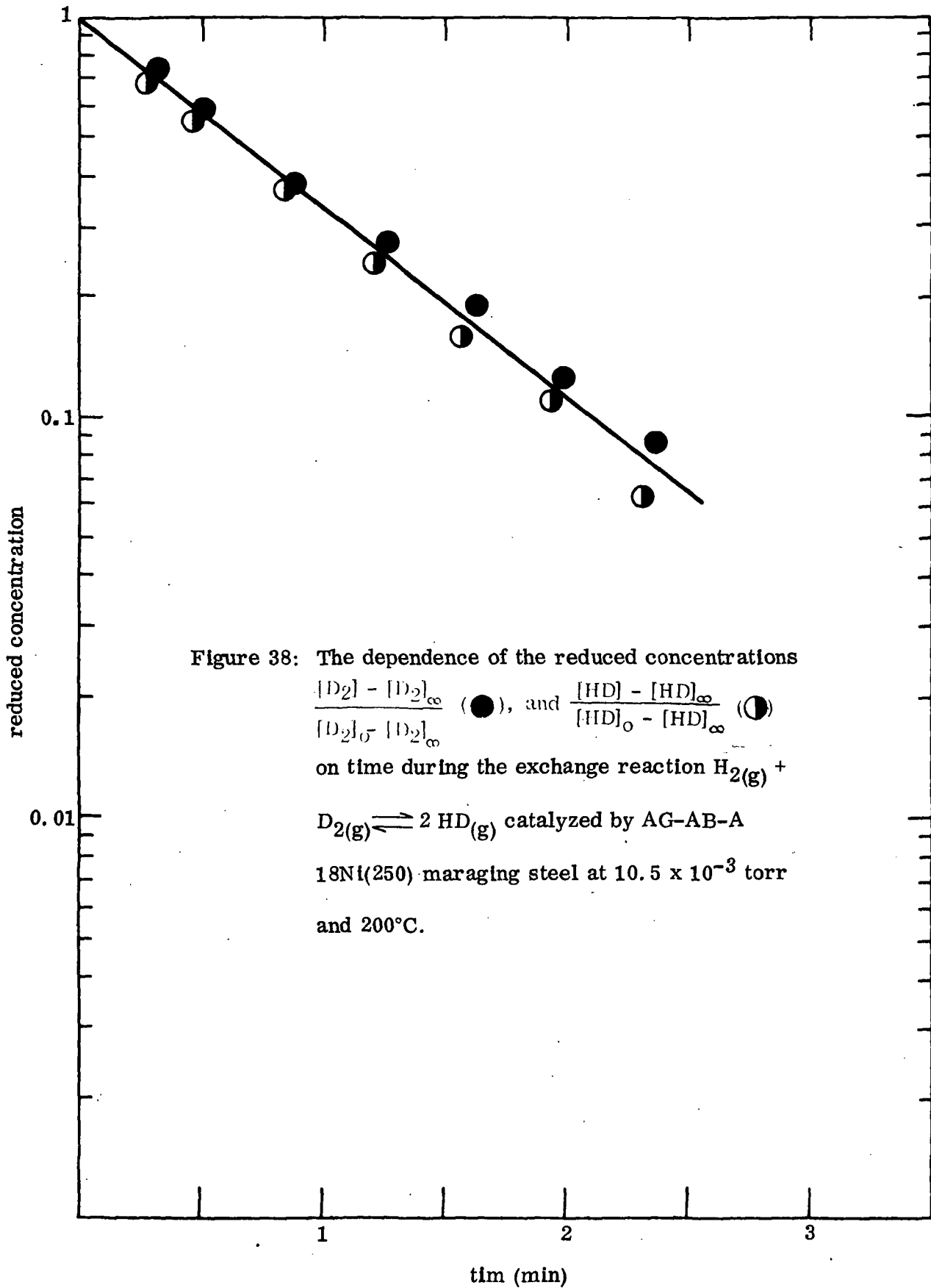


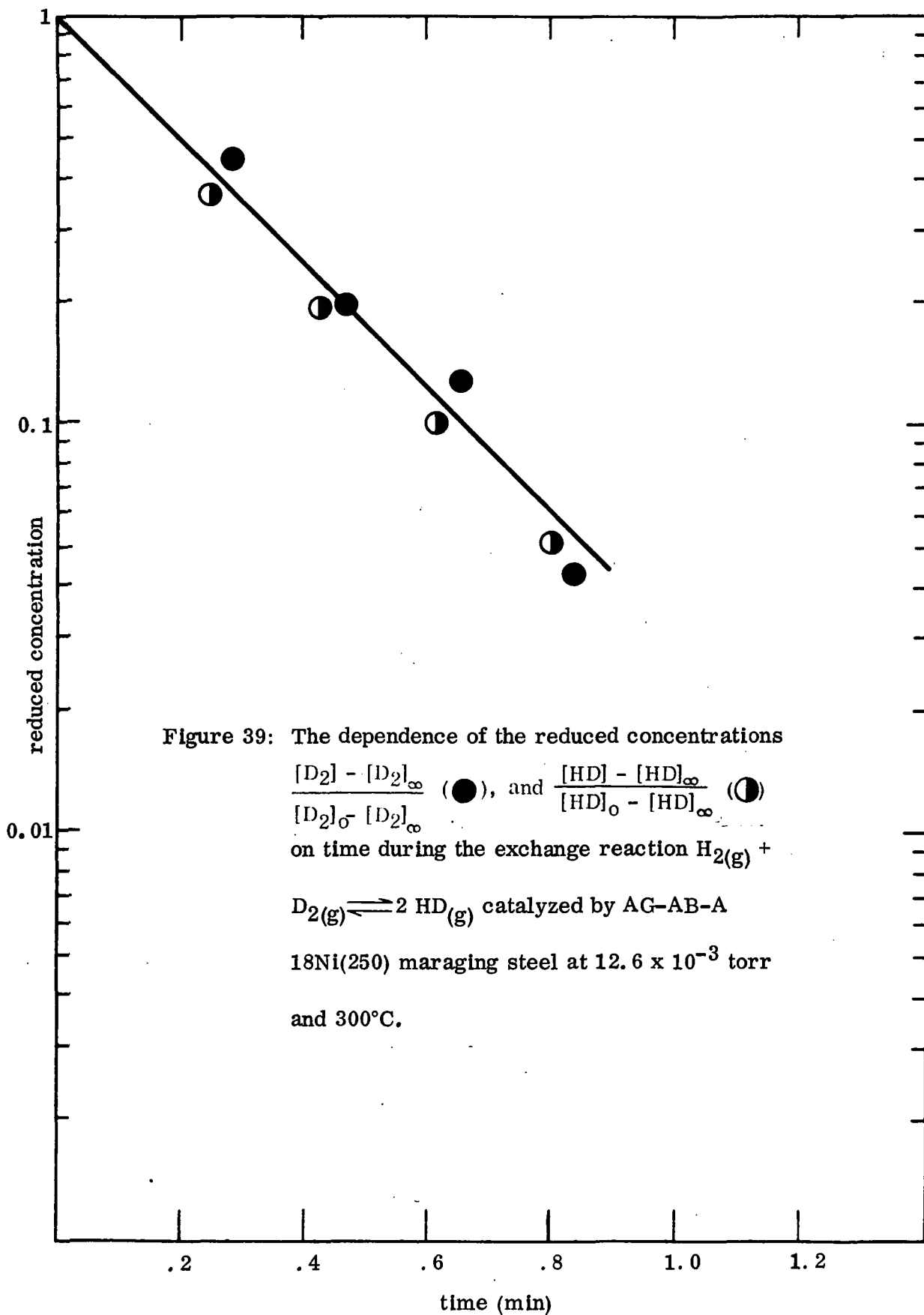


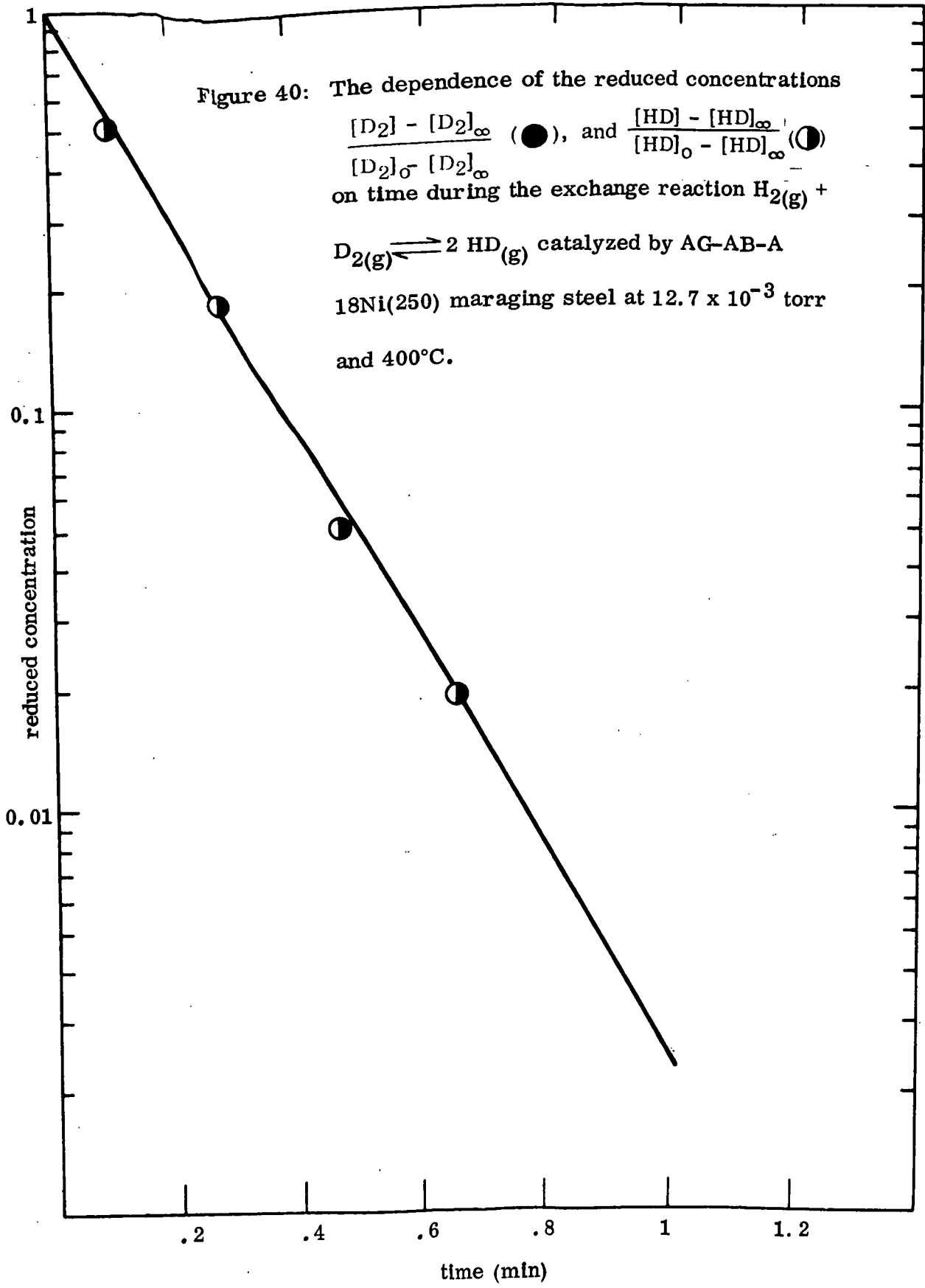


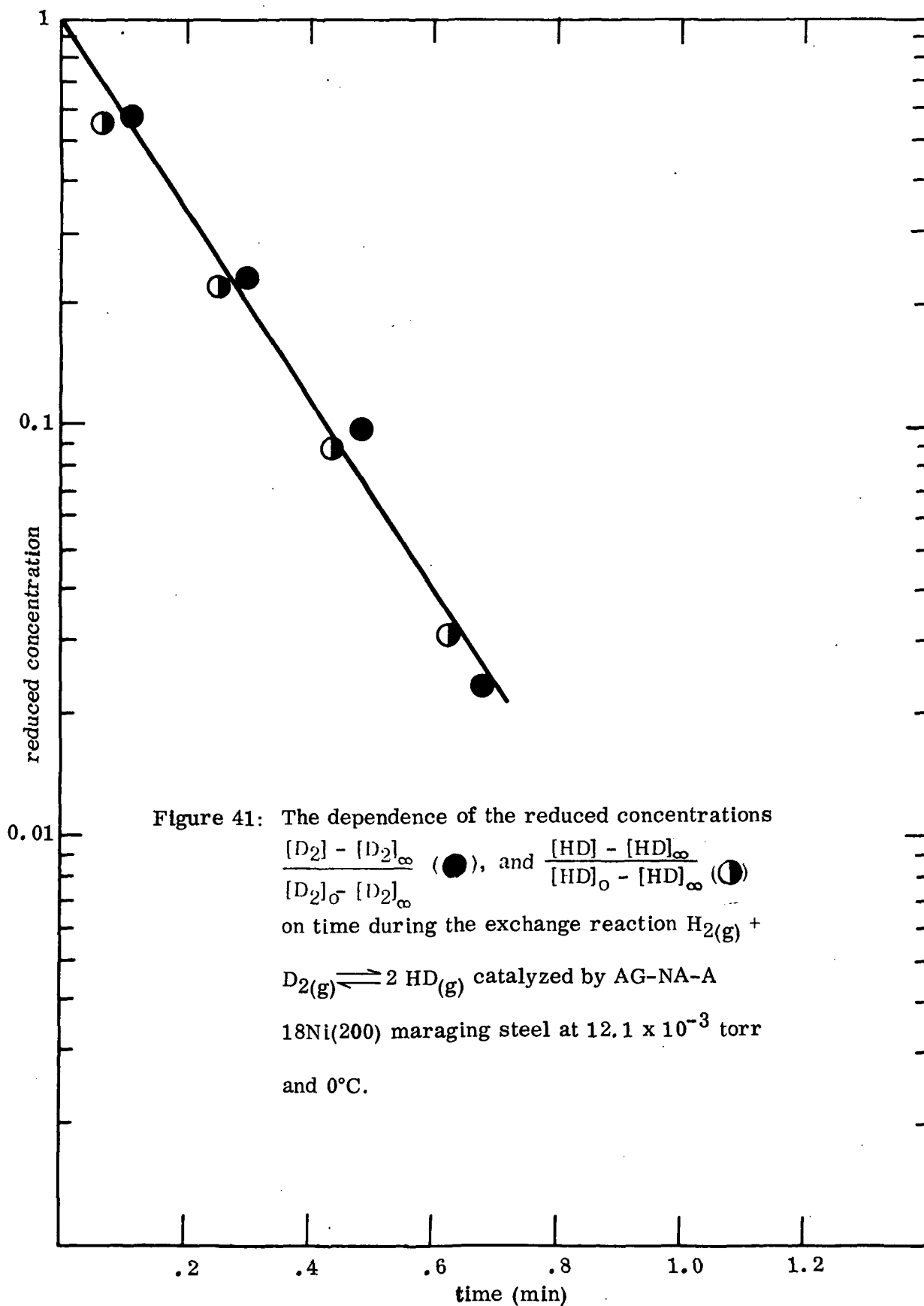


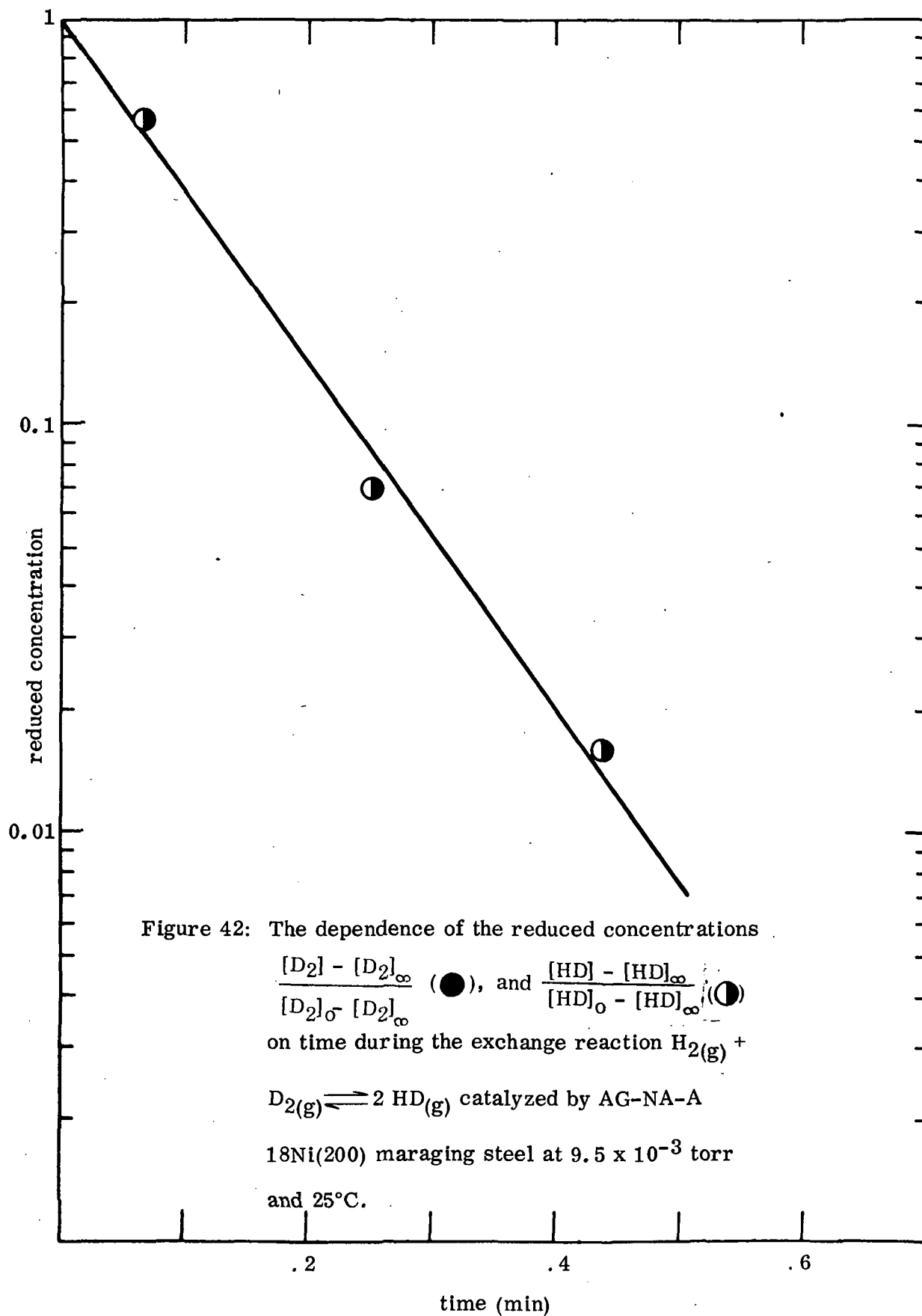


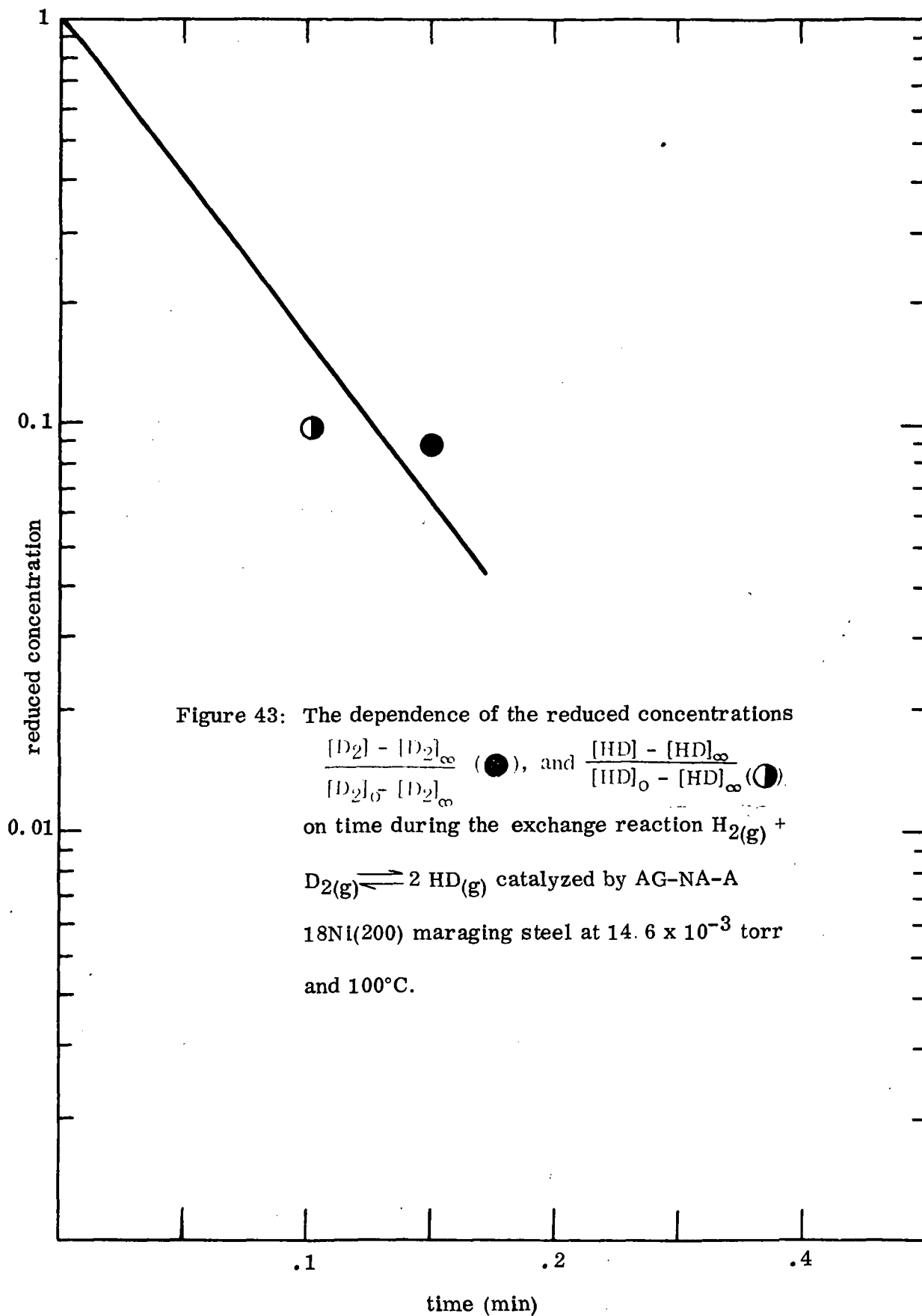


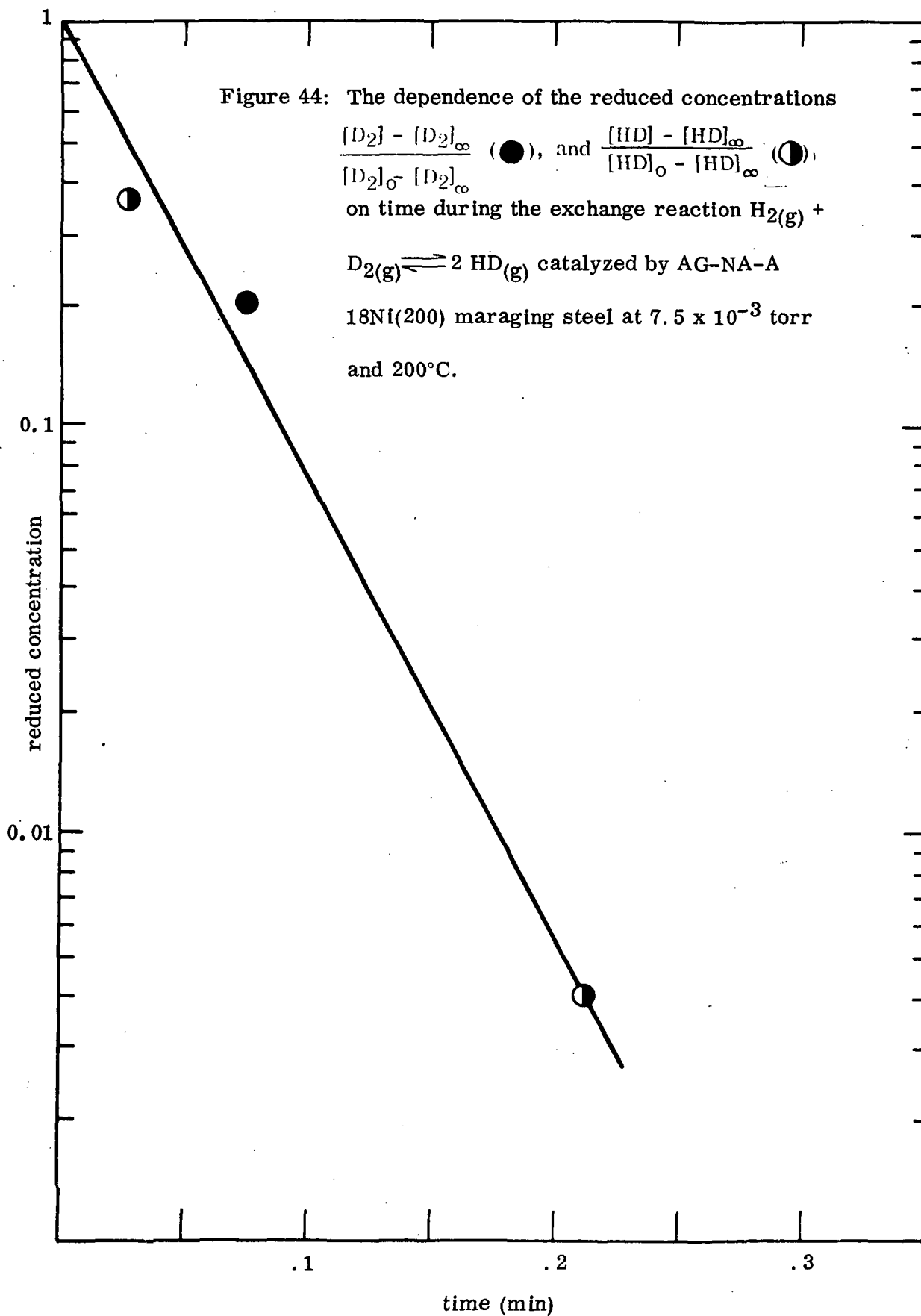


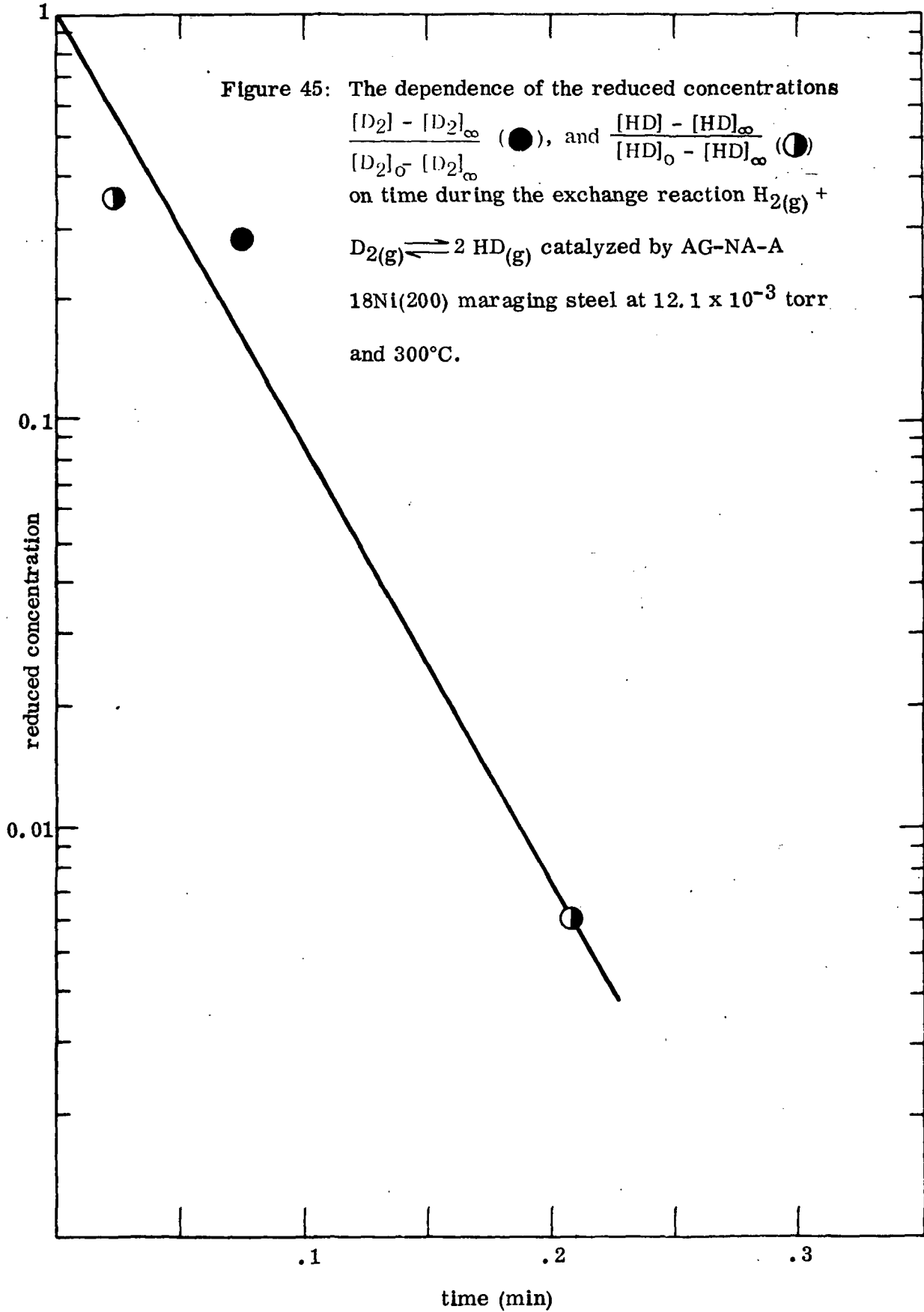


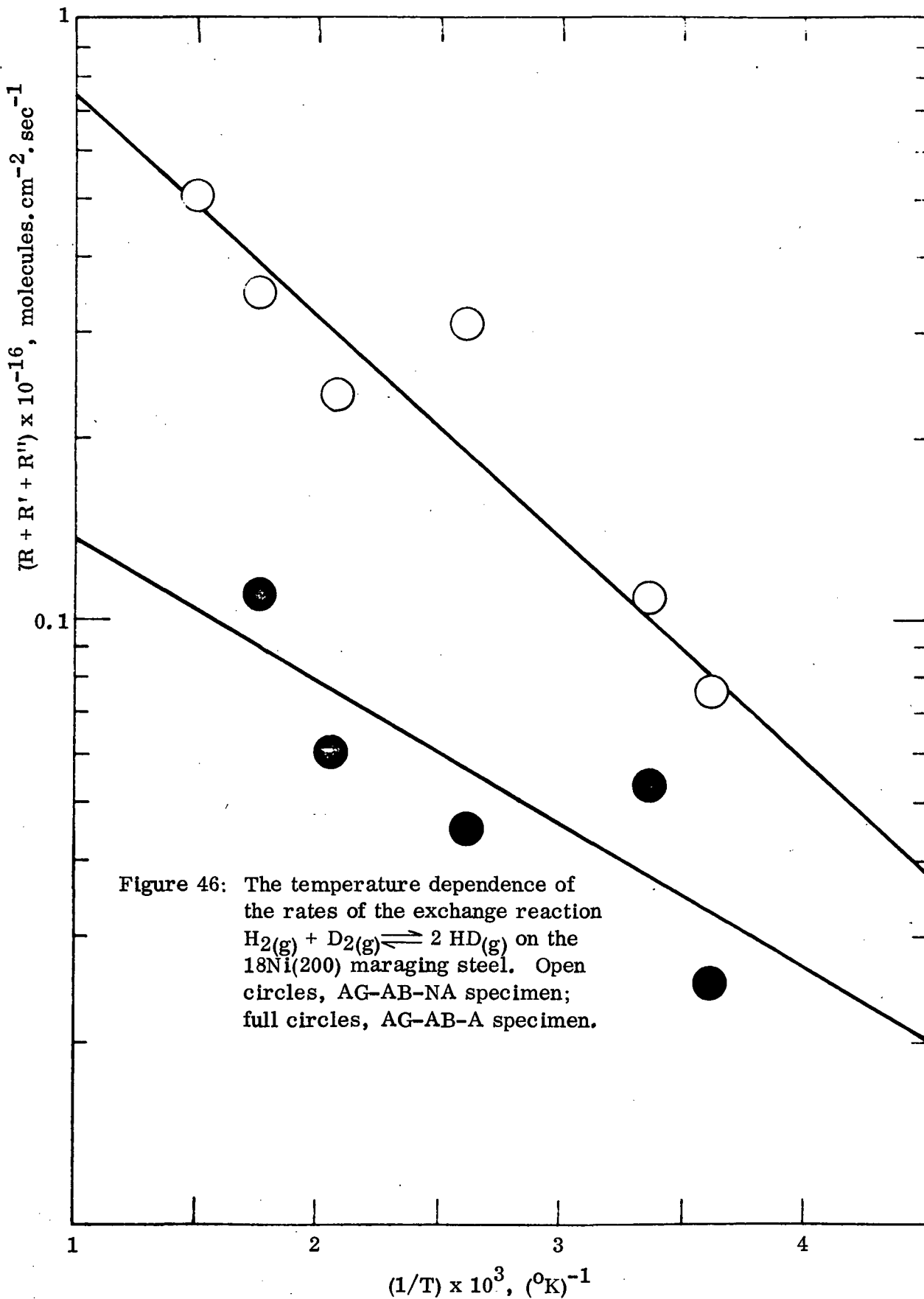


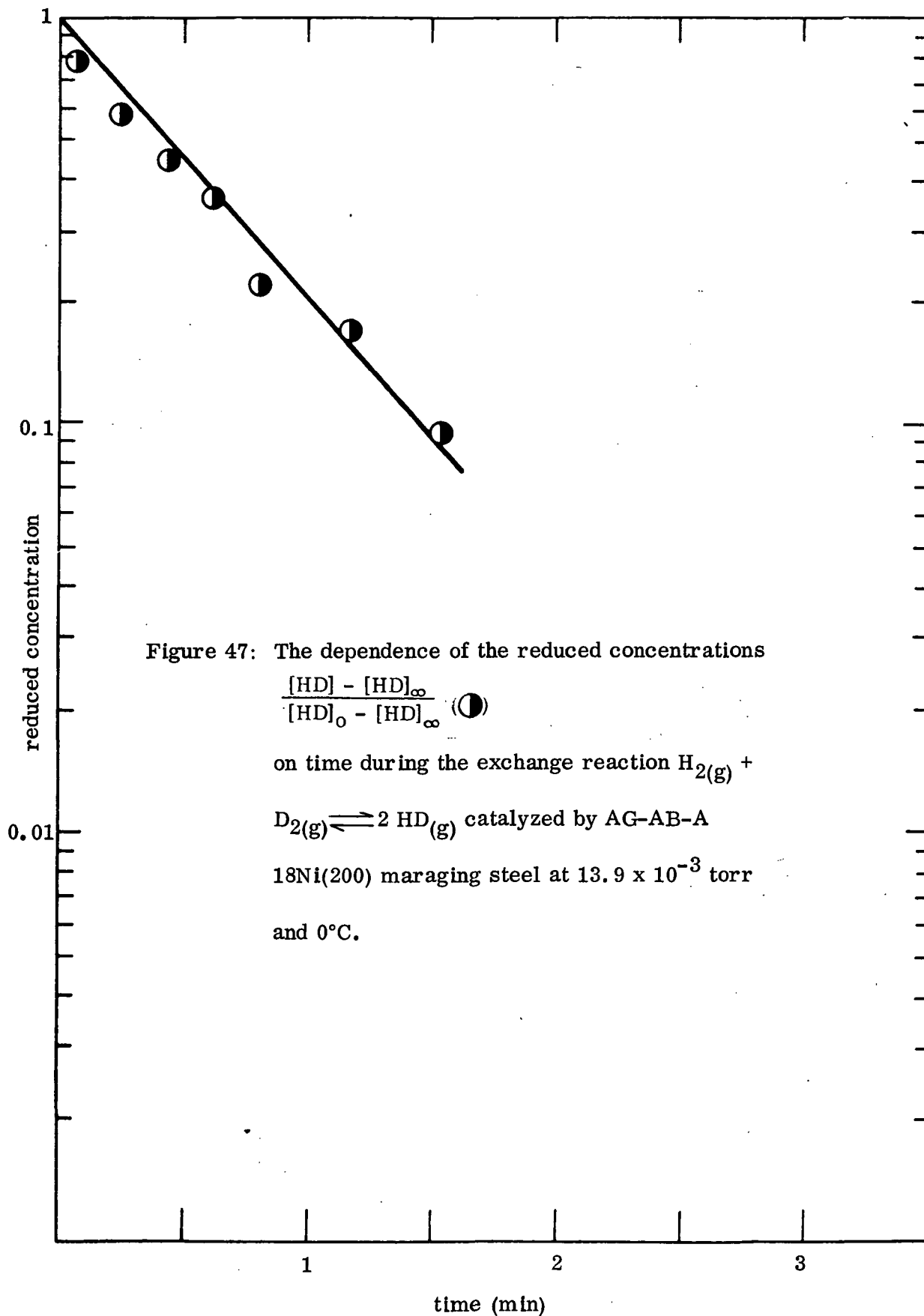


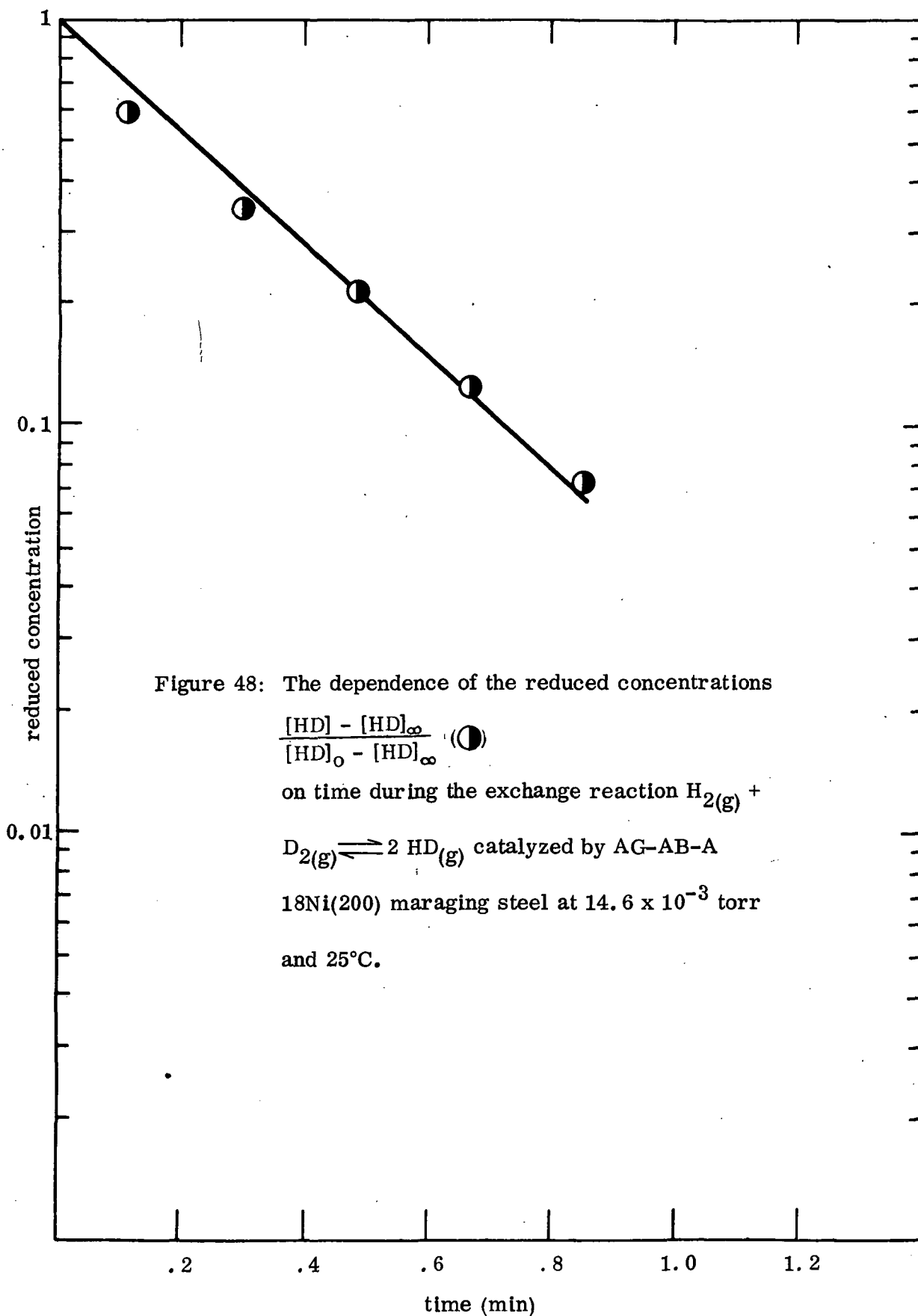












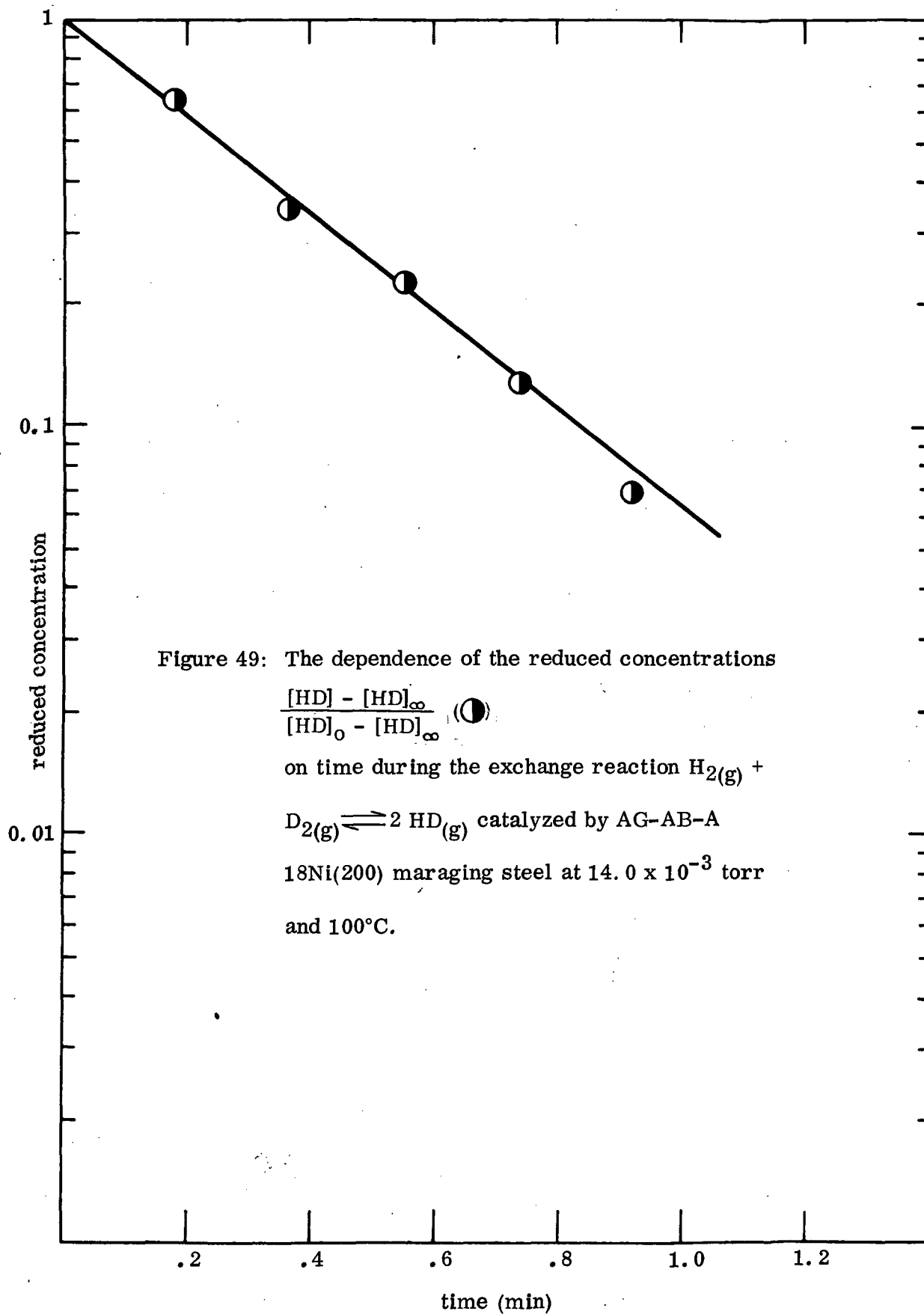
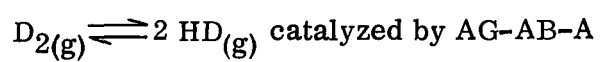


Figure 49: The dependence of the reduced concentrations

$$\frac{[HD] - [HD]_{\infty}}{[HD]_0 - [HD]_{\infty}} \quad (\bullet)$$

on time during the exchange reaction $H_2(g) +$



18Ni(200) maraging steel at 14.0×10^{-3} torr

and $100^{\circ}C$.

